University of Nevada, Reno

Development of a Groundwater Flow Model of Pahrump Valley, Nye County, Nevada and Inyo County, California for Basin-Scale Water Resource Management

A thesis submitted in partial fulfillment of the
Requirements for the degree of Master of Science in
Hydrogeology

By Lise Comartin

Dr. Donald M. Reeves/ Thesis Advisor

December, 2010

University of Nevada, Reno
Statewide • Worldwide

THE GRADUATE SCHOOL

We recommend that the thesis
prepared under our supervision by

LISE M. COMARTIN

entitled

Development of a Groundwater Flow Model of Pahrump Valley, Nye County, Nevada and Inyo County, California for Basin-Scale Water Resource Management

be accepted in partial fulfillment of the
requirements for the degree of

MASTER OF SCIENCE

Donald M. Reeves, Ph.D., Advisor

Greg Pohll, Ph.D., Committee Member

John Louie, Ph.D., Graduate School Representative

Marsha H. Read, Ph. D., Associate Dean, Graduate School

December, 2010

ABSTRACT

Pahrump Valley lies approximately 70 kilometers west of Las Vegas straddling both Nye County, NV and Inyo County, CA. As Nevada's most heavily allocated groundwater basin, Pahrump Valley has seen its population increase exponentially over the past 30 years (pop. ~39,000). The sole source of water within the valley is the underlying basin fill and carbonate aquifers, which provide water for irrigation, domestic, commercial and public uses. Previous studies estimate that the sustainable basin yield of the valley is 64,166 m^3/d (19,000 ac-ft) (Harrill, 1986). Data obtained from the Nevada Division of Water Resources (NVDWR) demonstrate that annual pumping has continuously exceeded this sustainable basin yield estimate for over 50 years. Managing these vital groundwater resources requires determining the future impacts of both current and projected pumping rates.

A three-dimensional, basin-scale groundwater flow model of Pahrump Valley was constructed to serve as a tool for evaluating alternative management scenarios. The model incorporates geologic data from the USGS Death Valley Regional Flow System Model, pumpage inventories from 1913 to 2003 for over 10,000 domestic, irrigation, and public wells, and water levels from 143 monitoring wells. Recharge from the Spring Mountains is based on an estimate of 87, 806 m^3/d (26,000 ac-ft/yr) from Harrill (1986), and was implemented in the model as a constant flux boundary. The model simulates an annual evapotranspiration rate of 42,214 m^3/d (12,500 ac-ft/yr) based on phreatophyte density on the valley floor and plant-specific water use coefficients.

The model was calibrated in transient mode according to water level data from 1946 and 2003. The calibration process consisted of both manual calibration to northeast-

southwest trending transects across the valley and automatic calibration to a global objective function using the inverse parameter estimation program, PEST (Doherty, 2004). Calibration of the model involved varying hydraulic parameters until an acceptable match between simulated head and observed head levels was achieved.

Improving the accuracy of the model required simplifying the geology within the model domain, creating specified hydraulic conductivity (*K*) zones in the underlying carbonate aquifer, incorporating hydraulic conductivity decay with depth, optimizing recharge contributions of watersheds in the Spring Mountains, and using a pilot points method to further optimize simulated head levels in the basin fill. The calibrated model adequately simulates head measurements (RMSE= 9.7 m, relative error of 5%), and is precise at estimating drawdown at most locations. Suggested future work includes converting the model to an unconfined flow solution to enhance the reliability of simulated drawdown predictions. Once this is accomplished, the model can be used to predict future impacts from current and future pumping scenarios, optimize well placement and extraction rates within the valley, and serve as a numerical framework for determining future land subsidence.

ACKNOWLEDGEMENTS

This research was supported through funding from Nye County and the U.S Department of Energy. Special thanks to the late Tom Buqo, for his enthusiasm and commitment to the project. Without him, this project would not have been initiated.

Eternal gratitude to my advisor, Matt Reeves, for all of the time he put into the project, his direction and his patience. His dedication went above and beyond his role as an advisor and he kept the project moving even when the model followed Murphy's Law. Special thanks to Greg Pohll for his insight on the project, computer help and for taking the time to be on my committee. I would also like to thank Justin Huntington for his assistance and for providing unique expertise on the project. Thanks to Rick Felling, Levi Kryder and Darrell Lacy for their help and suggestions. Also, thank you to my third committee member, John Louie for his time and input.

I would like to thank the Hydrologic Science Graduate Program at UNR. Special thanks to the DRI community for their support throughout my degree. Many thanks to the hydro people of the second pod of the CVRB for their encouragement, acting as sounding boards and for creating a great work environment. Special thanks to David McGraw, Jamie Trammell, Alex Lutz, Anna Knust and Conny Barth for their help throughout the project.

Lastly, a big thank you to my friends and family near and far for their unbounded love and for making me smile when the going got tough. I am grateful to have had so many wonderful people support me throughout this journey, especially the ones who picked up the phone on the east coast at 11 pm P.S.T. Thanks to Alena Yancey and the Battleborn Crossfit family for constantly challenging me outside of school and for

making Reno feel like home. “Merci bucket” to the Culp family for always bringing the sunshine and to the Henderson clan for the non-stop laughs. Mom, Dad and Donna, thank you for all your love and support, I could not have done this without you. This thesis is dedicated to both Mémé and Grammy.

TABLE OF CONTENTS

LIST OF FIGURES

LIST OF TABLES

1.0 INTRODUCTION

Pahrump Valley is located approximately 70 kilometers west of Las Vegas within both Nye County, Nevada and Inyo County, California. The primary source of water for the valley originates from infiltration of precipitation in the Spring Mountains, located between the Pahrump and Las Vegas valleys. Springs provided most of the water used in Pahrump until around 1940, with only a few wells – the first of which drilled around 1910 – used to provide small quantities of water for domestic uses. Between 1937 and 1946, 13 wells were drilled for large yield irrigation (Malmberg, 1967). In 1959, a cotton gin was constructed in the valley to process the cotton grown within Pahrump (Malmberg, 1967). Cotton is a water intensive crop with an average rate of use of 1.15-1.2 m (3.77 – 3.93 ft) (Allen et al., 1998). This helped propel Pahrump to become one of the most productive farming areas – primarily of cotton and alfalfa – in southern Nevada during the 1960s. Total irrigated acreage increased eight fold from four square kilometers (1,000 acres) in the early 1940s to 33 square kilometers (8,100 acres) in 1968 at the peak of cultivation (Moreo et al., 2003). In 1968, estimated annual groundwater withdrawals were as high as 162,103 m^3/d (48,000 ac-ft/yr). Aside from a small dairy herd near Manse Ranch, little livestock was raised in the valley due to the scarcity of vegetation (Malmberg, 1967).

Over the past few decades, Pahrump (population ~39,000) has experienced exponential population growth. The vast majority of the population growth has been in Nye County, Nevada with the portion of the valley in California remaining sparsely populated. During this time, water usage has shifted from predominately agricultural uses

towards domestic uses. Pahrump Valley currently has the highest density of domestic wells (~10,000) in Nevada, and consequently, is the most over-allocated groundwater basin in the state. The majority of domestic wells are drilled at an interval between 42 to 49 meters (140-160 feet) below land surface (Buqo, 2006) and are vulnerable to substantial water table declines. Although extraction rates have steadily decreased since the late 1960s, current pumping rates of approximately 84,429 m^3/d (24,000 ac-ft/yr) still significantly exceed the sustainable basin yield estimate of 64,166 m^3/d (19,000 ac-ft/yr) by Harrill (1986). Annual withdrawals continuously surpassed 101,315 m^3/d (30,000 ac-ft/yr) between 1960 and 1980. If the population increases to the projected 50,000 residents by 2050 (Buqo, 2006), the depletion of Pahrump Valley water resources will continue. The strain placed on the Pahrump Valley groundwater system through unsustainable extraction rates threatens the future viability of the basin fill aquifer resource.

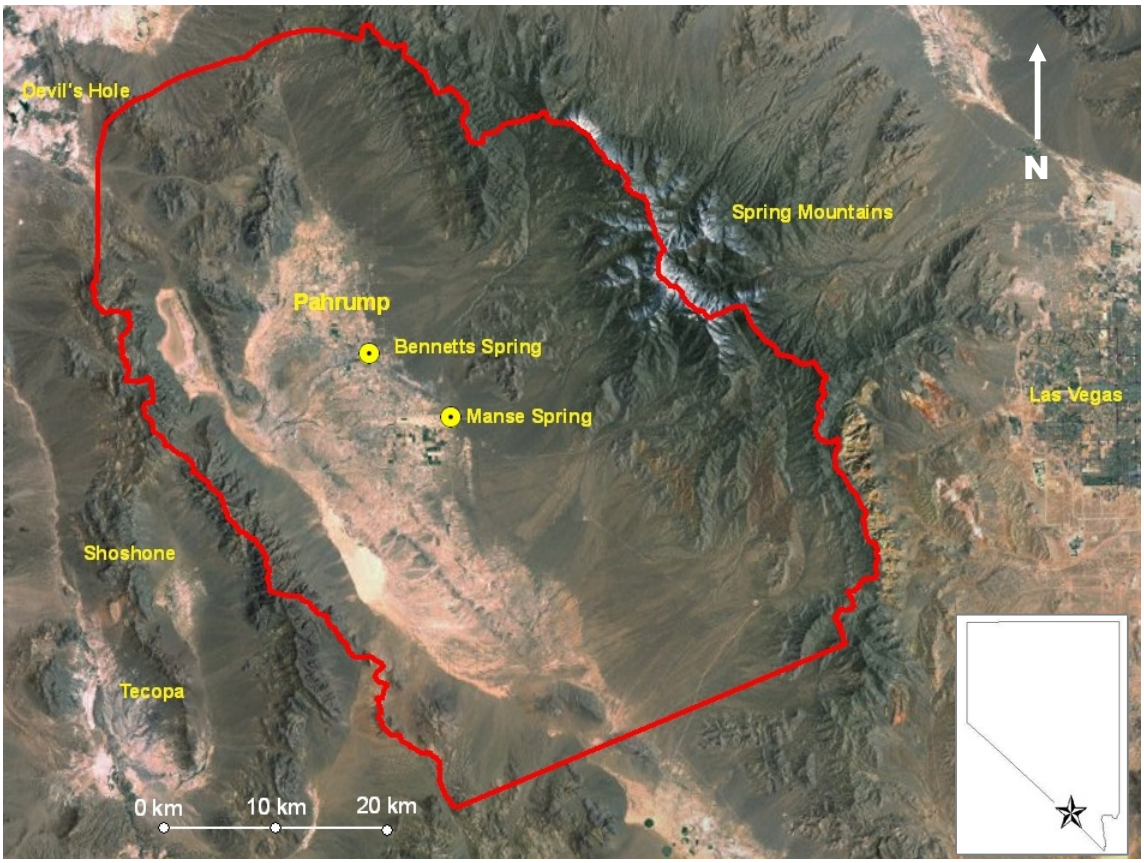

Figure 1. Aerial photograph of the Pahrump Valley basin and surrounding area. The model boundary is highlighted in red.

Hydrographs compiled by Buqo (2006) shown in Figure 2 display the general groundwater water decline within the valley over the last 60 years. All hydrographs demonstrate a negative trend until about 1980. After 1980, some wells near the alluvial fan show signs of recovery. Water level recovery in these wells may be related to a decline in pumpage caused by a shift from agricultural to domestic water uses. Although some wells have shown signs of recovery, groundwater withdrawals have continued to exceed the estimated 64,166 m^3/d (19,000 ac-ft/yr) sustainable basin yield since the 1950s and annual withdrawals continuously exceeded 101,315 m^3/d (30,000 ac-ft/yr) between 1960 and 1980. Future projections of depth to groundwater formulated by Buqo (2006) are shown in Figure 3. Note that depth to water increases away from the center of

the valley because of the increasing land surface elevation, even though the majority of the water level decline has occurred in the central portions of the valley.

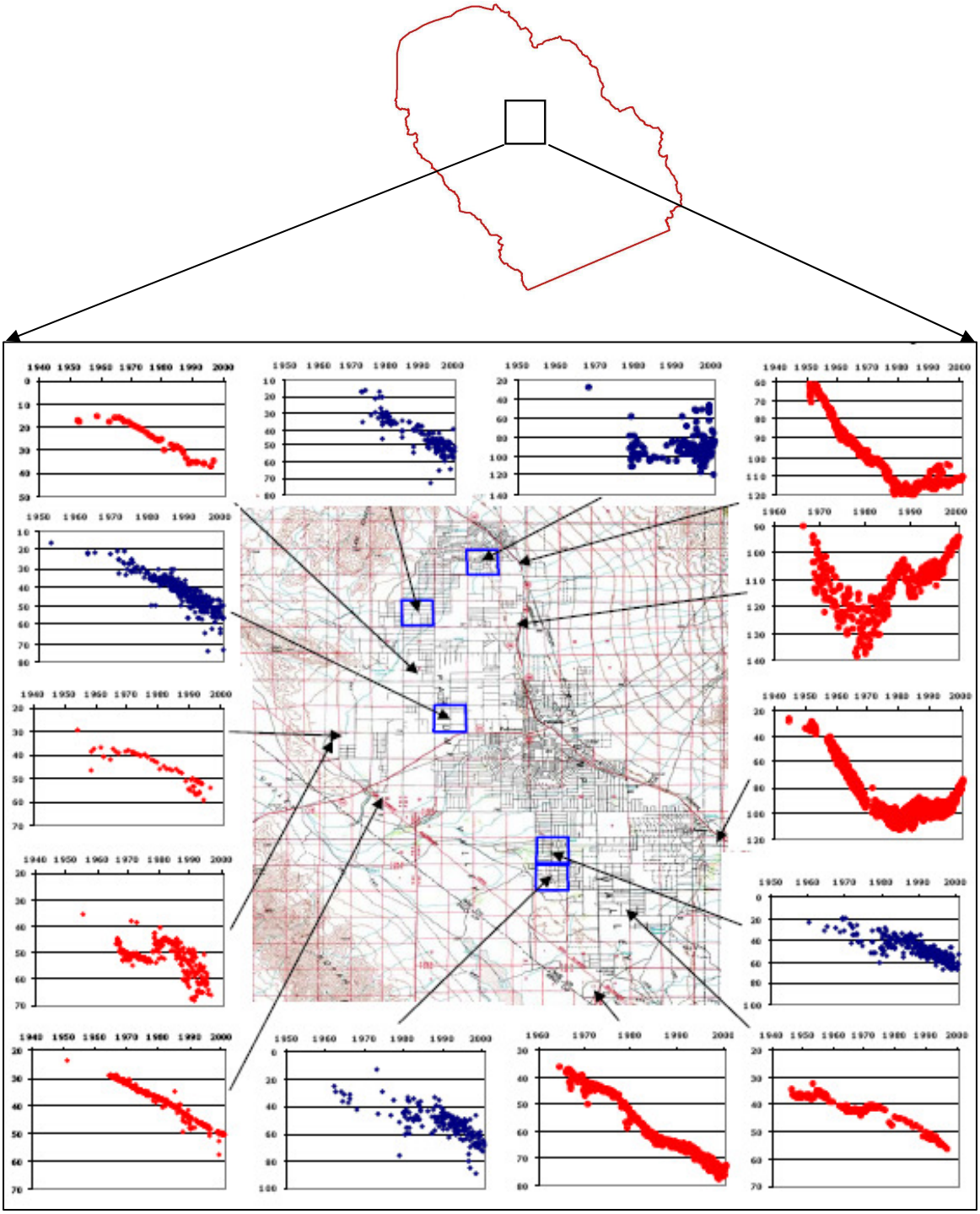

Figure 2. Hydrographs from the Nye County Water Resources Plan (Buqo, 2004). X-axis displays year, y-axis displays depth to groundwater in feet. Note the general decline in groundwater levels until approximately 1980. Hydrographs closer to the mountain block (right side of figure) show signs of recovery; wells in the valley (left side of figure) do not show signs of recovery. Modified from Buqo, 2004.

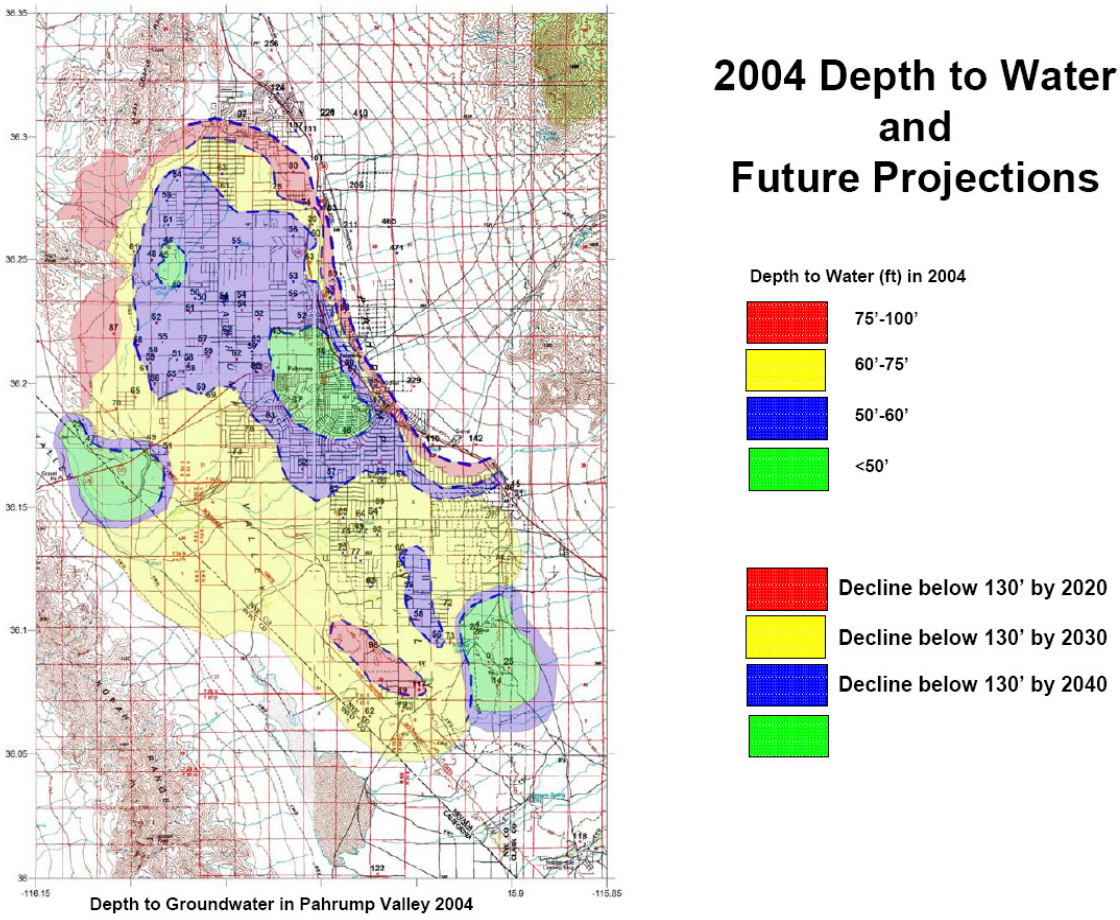

Figure 3. Future depth to water projections prepared by Buqo (2006). Note that all values are in units of feet. Future depth to water projections were computed by looking at pumpage rates and depth to water and projecting it into the future. The first legend displays the depth to water in 2004. The second legend displays the future depth to water projections.

This Thesis details the construction of a basin-scale numerical groundwater flow model of Pahrump Valley for water resource management. This groundwater flow model expands upon previous studies through: (1) the utilization of a refined grid, guided by the spatial resolution of the Division of Water Resources (DWR) well inventory, (2) the incorporation of pumpage inventories from 1913 to 2003, (3) calibration to water level observations from 1946 to 2003, and (4) thorough evaluation of the relationship between hydraulic parameters for various geologic units and water levels within the basin.

1.1 Study Objectives and Research Questions

The objective of this project is study is to construct a calibrated, basin-scale groundwater flow model of Pahrump Valley, intended to serve as a tool for Nye County to assess the impacts of current and future pumping scenarios on groundwater levels within the valley.

To accomplish this objective, the following research questions were investigated:

- How does newly available data influence conceptual and numerical models of groundwater flow for Pahrump Valley?
- How do various geologic units influence groundwater flow within the Pahrump Valley?
- How to best achieve calibration of the transient model given large periods of time with incomplete water level data and large uncertainty in pumpage magnitudes and location?

1.2 Model Setting

1.2.1 Geology

Pahrump Valley, located within the Basin and Range tectonic province, is a northwest-southeast trending basin formed by regional tectonic extension (Harrill, 1986). The valley is bounded by fault block mountain ranges comprised of Paleozoic and Late Proterozoic carbonate and clastic rocks (Malmberg, 1967). The highest point, Mount Charleston (3,600 m), is located to the northeast in the Spring Mountains. The Spring Mountains are formed from thrust plates comprised of approximately 2,600 meters of

fossiliferous limestone and dolomite overlying 1,300 meters of sandstone, shale and conglomerate (Malmberg, 1967). These thrusts plates are sporadic and are broken by normal faults caused by crustal extension, and therefore, may not be regionally significant (Belcher et al., 2004). The Kingston Range, located in the southwest portion of the basin, contains a large Tertiary granitic pluton and ranges in height between 600-1,800 meters (Sweetkind, 2003).

The basin fill is approximately 600 meters deep and consists of unconsolidated coarse-grained alluvial materials near the periphery of the valley, with fine-grained silt, clay, sand and volcanic tuff in the central parts of the valley (Sweetkind, 2003). The basin fill deposits are of Tertiary and Quaternary age, mainly comprised of detrital sediments, forming an area of approximately 650 square miles (1,700 km^2) (Malmberg, 1967). The coarse-grained deposits are located mainly in alluvial fans; they are older than the fanglomerate of Pliocene and early Pleistocene age. Pahrump and Manse alluvial fans are the result of an accumulation of smaller alluvial fans extending southeast far into the valley and are one of the most distinguished topographic features within the valley (Malmberg, 1967).

A strike-slip fault zone known as the Pahrump Valley Fault Zone (PVFZ) runs parallel to the California-Nevada state line (Blakely, et al., 1998). The PVFZ can be followed southward to the State Line fault and northward to active faults in Ash Meadows. More than 24 kilometers of displacement occurs in this fault system (Hoffard, 1991). The fault zone is comprised of fault-bounded lenses of Late Proterozoic Stirling Quartzite (Belcher et al., 2004). The fault zone forms a buried bedrock ridge separating the valley into two sub-basins, the southwest and northeast. It is estimated the PVFZ has

a rupture length ranging from 50 to 150 kilometers and may pose a significant seismic hazard for the city of Las Vegas and surrounding regions (Shields et al., 1998).

1.2.2 Surface and Groundwater Hydrology

The semi-arid climate of Pahrump Valley is characterized by limited amounts of precipitation on the valley floor (12.3 cm/yr) (Buqo, 2006), low humidity and large variations in daily temperatures. The mean annual air temperature is approximately 18° C (65° F) while the temperature of groundwater in the valley mostly equals or exceeds the mean annual air temperature (Malmberg, 1967). Precipitation occurs mainly in the winter months where it increases in abundance with elevation. The highest frequency and most intense storms occur around Mount Charleston; records indicate precipitation is highest at the crest and east slope of the Spring Mountains (Maxey and Robinson, 1947).

Pahrump Valley is a topographically closed basin that lacks surface outflow (Malmberg, 1967). Infrequent runoff from intense precipitation events discharges into one of two playas within the valley. The larger playa, located in Stewart Valley occupies the northwestern part of the study area at a 749 meters (2,457 ft) elevation (Malmberg, 1967). The smaller playa lies 21 kilometers southeast in the southwestern part of the basin at the base of Resting Spring and Nopah Ranges. At lower elevations on the valley floor, potential evaporation rates are high and can exceed 2.5 meters (8.2 ft) per year. The only surface water features of Pahrump Valley (besides infrequent runoff) are groundwater-fed springs, the largest of which include Bennetts and Manse Springs, located at the terminal ends of alluvial fans originating in the Spring Mountains (Belcher et al., 2004) (Figures 1 and 4). These springs were some of the first sources of water for early travelers and were later used for irrigation (Malmberg, 1967).

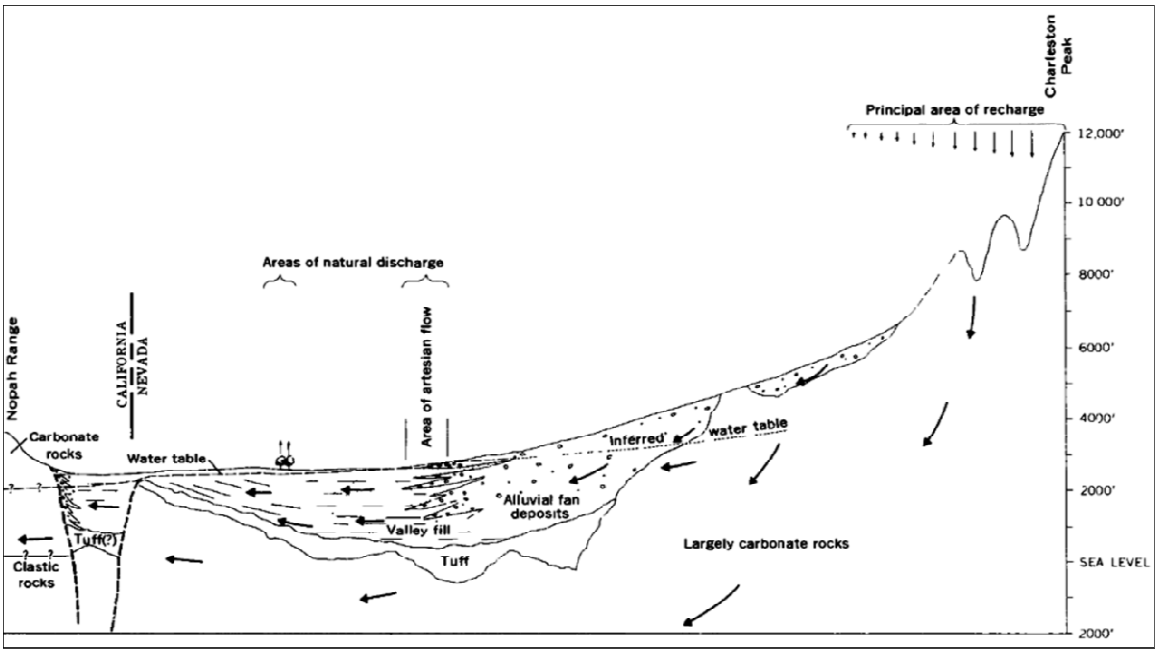

Figure 4. Principal topographic, geologic and hydrogeologic features of Pahrump Valley (Modified from Malmberg, 1967).

Precipitation within the Spring Mountains eventually recharges two distinct groundwater aquifers within the valley: 1) unconsolidated basin fill deposits underlying Pahrump Valley and 2) the consolidated carbonate rocks that form the mountains surrounding Pahrump (Harrill, 1986). The basin fill deposits form an area of about 1,685 square kilometers (350 mi^2), and are composed largely of fine-grained sand, silt, clay and some precipitates (Malmberg, 1967). These fine-grained deposits are also interbedded by tuff of Miocene and Pliocene age, older medial lacustrine deposits of Pleistocene and early Pleistocene age and younger surficial deposits of Pleistocene and Recent age (Malmberg, 1967). Water yielding sediments found in the basin fill include well-sorted gravel and sand. This indicates that water obtained from wells that penetrate a variety of materials and significant quantities of water may be derived from only a few beds of coarse sand and gravel (Harrill, 1986). The majority of water in the basin fill aquifer discharges within the valley through extraction by groundwater wells and phreatophytes,

and to a much lesser extent, springs. The remaining recharge flux from the Spring Mountains is transmitted through the carbonate aquifer which discharges through the Nopah Range towards Tecopa and Shoshone (Malmberg, 1967; Harrill, 1986; Belcher et al., 2004). The Paleozoic carbonate aquifer is heavily fractured and constitutes a major reservoir system in southern Nevada. The stratigraphic thickness of this aquifer is potentially as much as 5,490 meters (Malmberg, 1967) which promotes the formation of groundwater systems in southern Nevada with interbasin flow.

Groundwater flow from the Spring Mountains moves in a southwesterly direction towards Tecopa and Shoshone (Figure 1). Estimates of total groundwater flux through Pahrump basin were computed by Malmberg (1967) and Harrill (1986). Malmberg (1967) estimated that approximately 12,000 ac-ft/yr (40,530 m^3/d) of groundwater leaves Pahrump Valley through the carbonate aquifer toward the Nopah and Resting Ranges which border Pahrump Valley in the southwest. Harrill (1986) suggested the total amount of subsurface flow in the basin ranges between 6,000 - 19,000 ac-ft/yr (20,262 - 30,395 m^3/d). The large range in possible subsurface flow is attributed to the lack of data on the carbonate aquifer, particularly head levels to compute hydraulic gradients and flow directions, and values of hydraulic conductivity. Based on previous studies, there are no available records of wells that penetrate the carbonate aquifers. Additionally, both Malmberg (1967) and Harrill (1986) noted that a small portion of groundwater may move northwesterly through a small section of carbonate rocks. This northwestern groundwater movement potentially contributes to spring discharge in Ash Meadows such as Last Chance, Bole, Big and Jack Rabbit Springs (Winograd and Thordarson, 1975).

Notable changes to the groundwater flow system of Pahrump Valley have occurred since the early 1900s. Early development of the groundwater resources of Pahrump focused on capturing spring discharge. When pumping within the valley fill began in 1913, artesian pressure declined dramatically and significantly decreased spring discharge. Bennetts Spring to ceased to flow in 1959 (Malmberg, 1967), and discharge in Manse Spring continuously declined until the point of no flow in 1979 (Buqo, 2004). The impacted areas of the valley where water levels are more severely impacted are primarily in the north-central part of the valley where the majority of the population resides. The vast amount of pumping in the northern and central parts of the valley has had little effect on water levels in the western part of the valley.

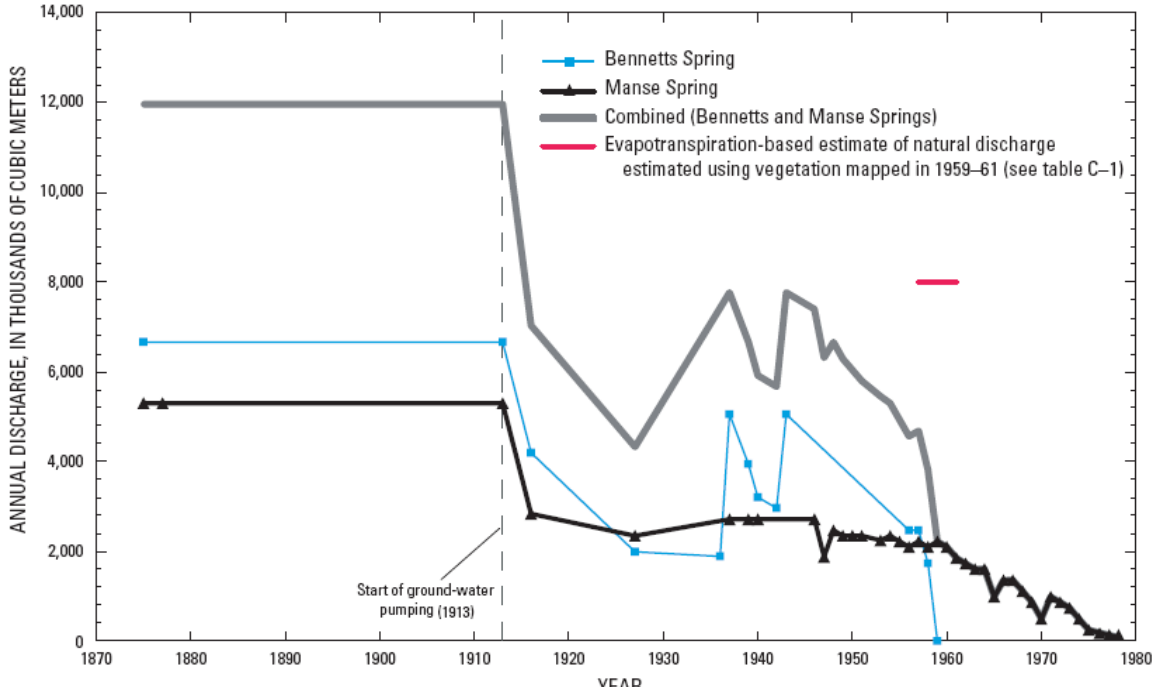

Figure 5. Annual discharge from Bennetts and Manse Springs, 1875-1978. From Belcher et al. (2004).

1.3 Previous Studies and Models of Groundwater Flow

Numerous studies have been conducted over the past century to better understand the Pahrump Valley groundwater flow system. One of the first investigations of the water resources in the area was completed by Mendenhall (1909) who explored the water resources of southern Nevada and southeastern California. Waring (1921) continued this research, studying water resources in Pahrump and collecting data on the quantity and quality of the groundwater from wells and springs. In 1944, Maxey and Jameson published a study which summarized the early history and development of groundwater along with its quality and occurrence in the area. General overviews of the most recent and applicable studies of Pahrump Valley to this project are provided below.

1.3.1 Hydrology of the Valley-Fill and Carbonate-Rock Reservoirs, Pahrump Valley, Nevada-California, Malmberg (1967).

This study was motivated by residents of Pahrump who noticed dramatic declines in water levels and decreases in spring discharge. Most water users were concerned with the rapid decline of groundwater levels as the economy of the valley at that time relied almost wholly on irrigated agriculture. The purpose of the research was to describe the groundwater hydrology, estimate perennial yield of the basin and determine the level of overdraft. This report provides the first comprehensive hydrogeological survey of the entire valley, focusing on both the valley fill and carbonate-rock layers.

From the mid-1940s through 1962, annual pumpage in the valley increased from approximately 10,000 ac-ft/yr (33,771 m^3/d) to 28,000 ac-ft/yr (94,560 m^3/d) as farming became more widespread. Malmberg estimated that during the study period (1959-1962), pumping caused a storage depletion of 25,000 ac-ft (84, 429 m^3/d) with an annual

recharge rate of 22,000 ac-ft/yr (74, 297 m^3/d). During that short time, water levels in the southern part of the valley dropped by four feet (1.2 m). Malmberg predicted large withdrawals would lessen the amount of groundwater outflow from the valley fill to the carbonate-rock reservoir by as much as 50 percent. It was suggested that long-term pumping may also have reduced subsurface outflow from the carbonate-rock reservoirs to adjacent valleys.

Evapotranspiration (ET) rates were calculated from delineated phreatophyte zones on the valley floor distinguishing areas of mesquite, saltgrass, saltbush, saltcedar and cottonwood. For each phreatophyte species, Malmberg estimated the annual rate of use and multiplied it by the phreatophyte areas to determine evapotranspiration rates. This method produced an annual ET rate of 10,000 ac-ft/yr (33, 771 m^3/d).

1.3.2 Ground-Water Storage Depletion in Pahrump Valley, Nevada-California, 1962-75, Harrill (1986).

Harrill (1986) continued and expanded upon the work from Malmberg (1967) by building a model that included additional water level data from 1962-1975. Groundwater withdrawals from springs and wells were estimated to be 29,000 ac-ft/yr (97,937 m^3/d) in 1962 to 48,000 ac-ft/yr (162,103 m^3/d) in 1968, and then reduced to 41,000 ac-ft/yr (138,463 m^3/d) in 1975. The general decline in water use between 1968 and 1975 was the result of a transition in water usage from agricultural to domestic uses. During this 13-year period, approximately 219,000 ac-ft (739, 598 m^3/d) of groundwater was extracted from the groundwater flow system resulting in considerable water level declines. Areas surrounding the town of Pahrump and along the Manse fans experienced the greatest groundwater declines due to the high density of pumping wells in the area, as pumping in

Pahrump Valley was originally positioned to capture the discharge of Bennetts and Manse Springs.

The northeast boundary of the model simulated recharge from the Spring Mountains by placing injection wells along the northeast boundary and injecting water into the model at a constant rate. No flow boundaries were prescribed to the north and south of the basin due to the low permeability bedrock present in those areas. The western boundary was assumed to be the discharge area of the flow system. This southwest border was simulated by a series of constant head nodes. The head levels were set to elevations representative of the potentiometric surface near the Amargosa River. The upper surface of the model was specified as a general head boundary while the bottom surface was the model was specified as a no-flow boundary.

The model suggested a sustainable basin yield of 19,000 ac-ft/yr (64,166 m^3/d). This number represents an increase from the sustainable basin yield estimate of 12,000 ac-ft/yr (40,525 m^3/d) proposed by Malmberg (1967). These differences in sustainable basin yield estimates may be attributed to the fact that Malmberg (1967) estimated the total recharge in the Spring Mountains at 22,000 ac-ft/yr (74,297 m^3/d), with approximately 12,000 ac-ft/yr (40,525 m^3/d) leaving the basin via subsurface flow. Malmberg estimated the perennial yield would be limited to 12,000 ac-ft/yr (40,525 m^3/d) if a recharge estimate of 22,000 ac-ft/yr (74,297 m^3/d) was used. This is because pumping within the valley fill would only salvage 6,754 m^3/d (2,000 ac-ft/yr). Recharge estimates from Harrill ranged from 22,000-26,000 ac-ft/yr (74,297 – 87,806 m^3/d). There is significant uncertainty in estimates that attempt to quantify a groundwater budget for

Pahrump Valley; nonetheless, all estimates specify a considerable overdraft from the aquifer caused by high rates of groundwater extraction.

1.3.3 Three-dimensional model of Paleozoic basement beneath Amargosa Desert and Pahrump Valley, California and Nevada: Implications for tectonic evolution and water resources, Blakely (1998).

This report provided geophysical data acquired through gravity surveys to delineate the contact between basin fill sediments and underlying Paleozoic carbonates. The study area, centering on Pahrump Valley and Amargosa Desert, also included the towns of Beatty, Amargosa Valley, Furnace Creek, Death Valley Junction and Shoshone. Blakely studied the carbonate rocks that compose most of the basement underneath Amargosa Desert and Pahrump Valley. This study noted the importance of carbonate aquifers in the region in promoting interbasin groundwater flow.

Within Pahrump Valley, the carbonate surface contains two deep basins in the northeast and southwest portions of the valley (Figure 6 and the northern half of Figure 7). The deep basins are separated by gravity ridges a few kilometers north and parallel to the Nevada-California state line. These gravity ridges were interpreted from gravity anomalies, and represent compressional features in the pre-Cenozoic basement as either anticlinal fold or horsts bounded by reverse faults (Figures 6 and 7). Overall, it is estimated that the basement surface has greater than seven kilometers of total relief ranging from the summit of the Nopah Range to the bottom of the northeastern Pahrump Valley sub-basin (Figure 7).

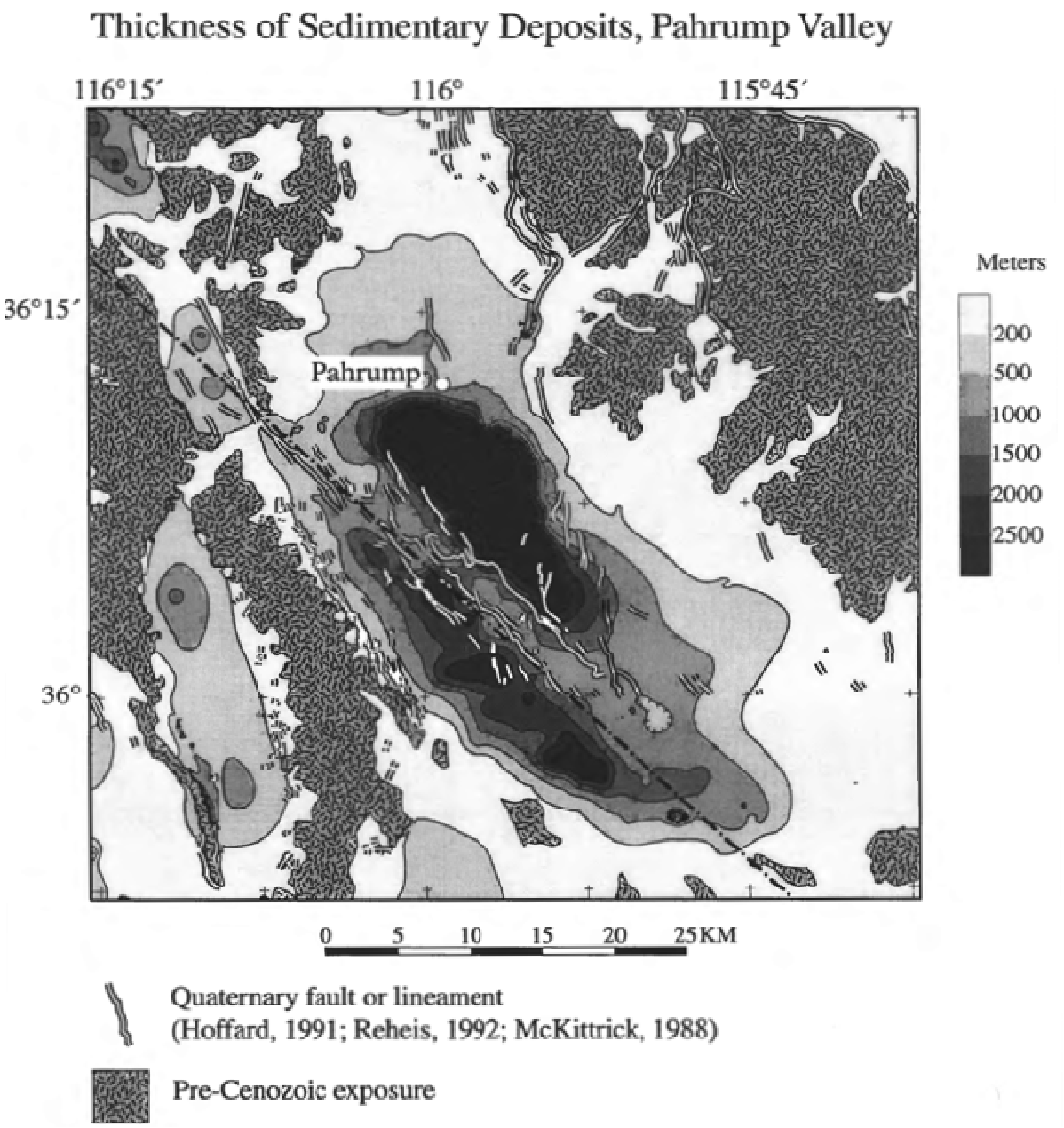

Figure 6. Image displays thickness of basin fill deposits in Pahrump Valley contrasted by contour intervals. Pre-Cenozoic rocks are exposed primarily in mountains that surround Pahrump, as indicated by the stipple pattern. From Blakely (1998).

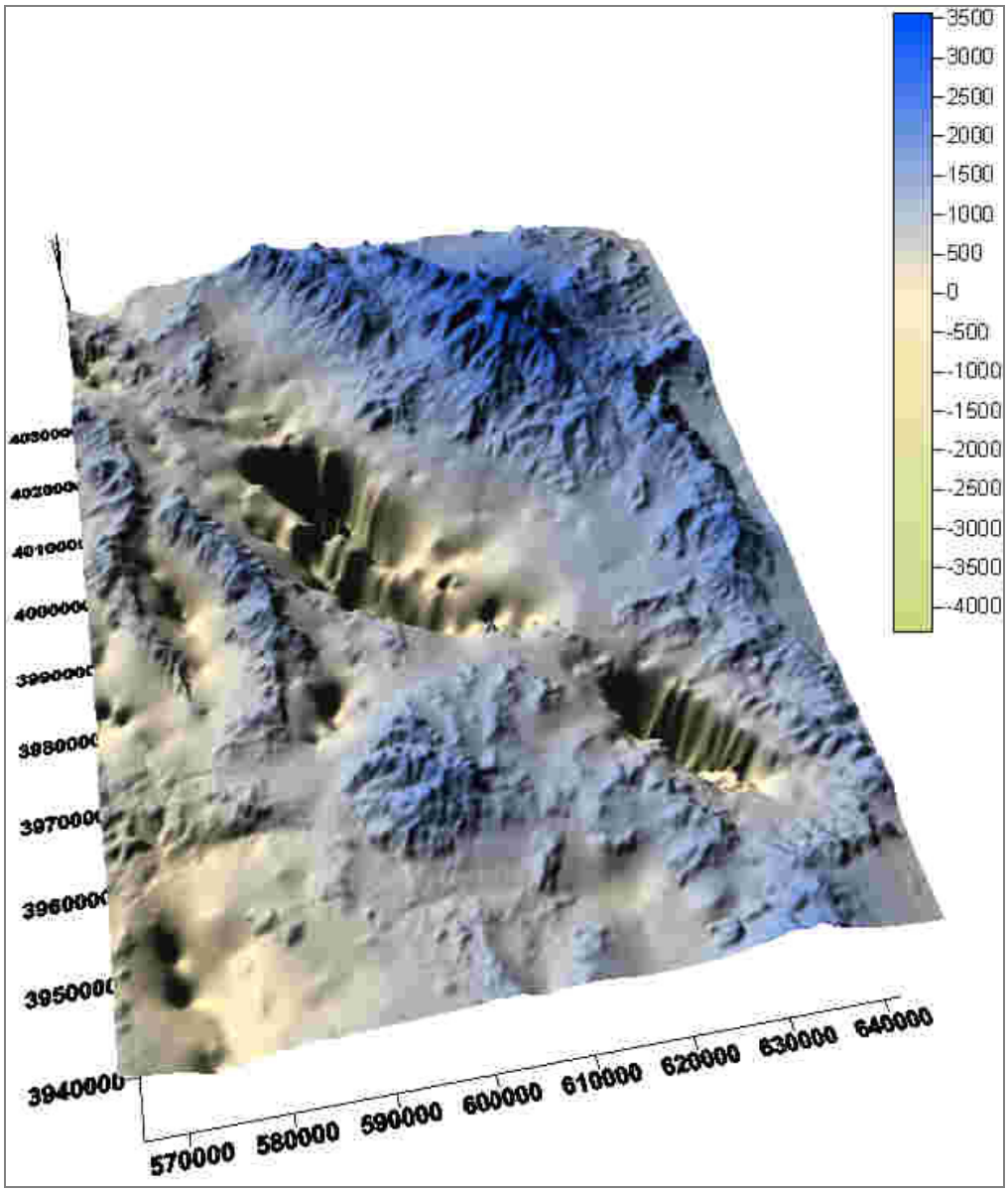

Figure 7. Pre-tertiary surface constructed from Blakely, 1998. This survey was also used to determine the entire surface of the DVRFS model. All values are in meters.

1.3.4 Stratigraphic inferences derived from borehole data of Tertiary basin-filling rocks of the Pahrump Valley basin, Nevada and California, Sweetkind (2003).

Sweetkind (2003) collected and then analyzed lithologic data (boreholes) from 266 drillers' logs within the central-northern part of Pahrump Valley (where the majority of groundwater wells are located). Boreholes were chosen to provide an extensive spatial distribution, and the deepest boreholes in the Valley were used to enhance the vertical

resolution of the analysis. Boreholes penetrating the basin fill vary from tens of meters to more than 300 meters below land surface. Spatial variability within the upper basin fill was captured by grouping borehole stratigraphy into 14 lithologic categories, and interpolating between locations of known stratigraphy (Figures 8 and 9). Alluvial fans containing coarse-grained deposits from the Spring Mountains are present in the northeast portion of the basin, while fine grained sediments are present along the valley axis.

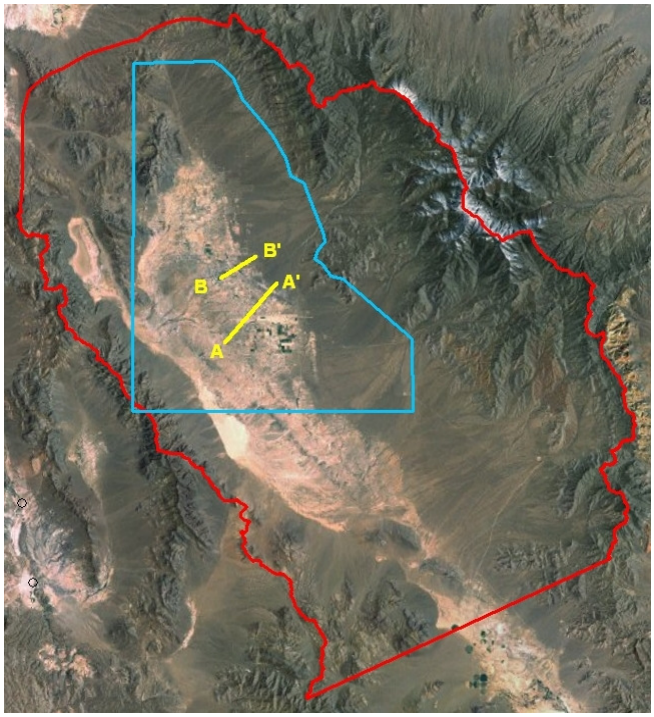

Figure 8. Aerial view of Pahrump Valley featuring the study area boundary (blue) of Sweetkind (2003) along with the locations of the example stratigraphic sections found in Figure 9.

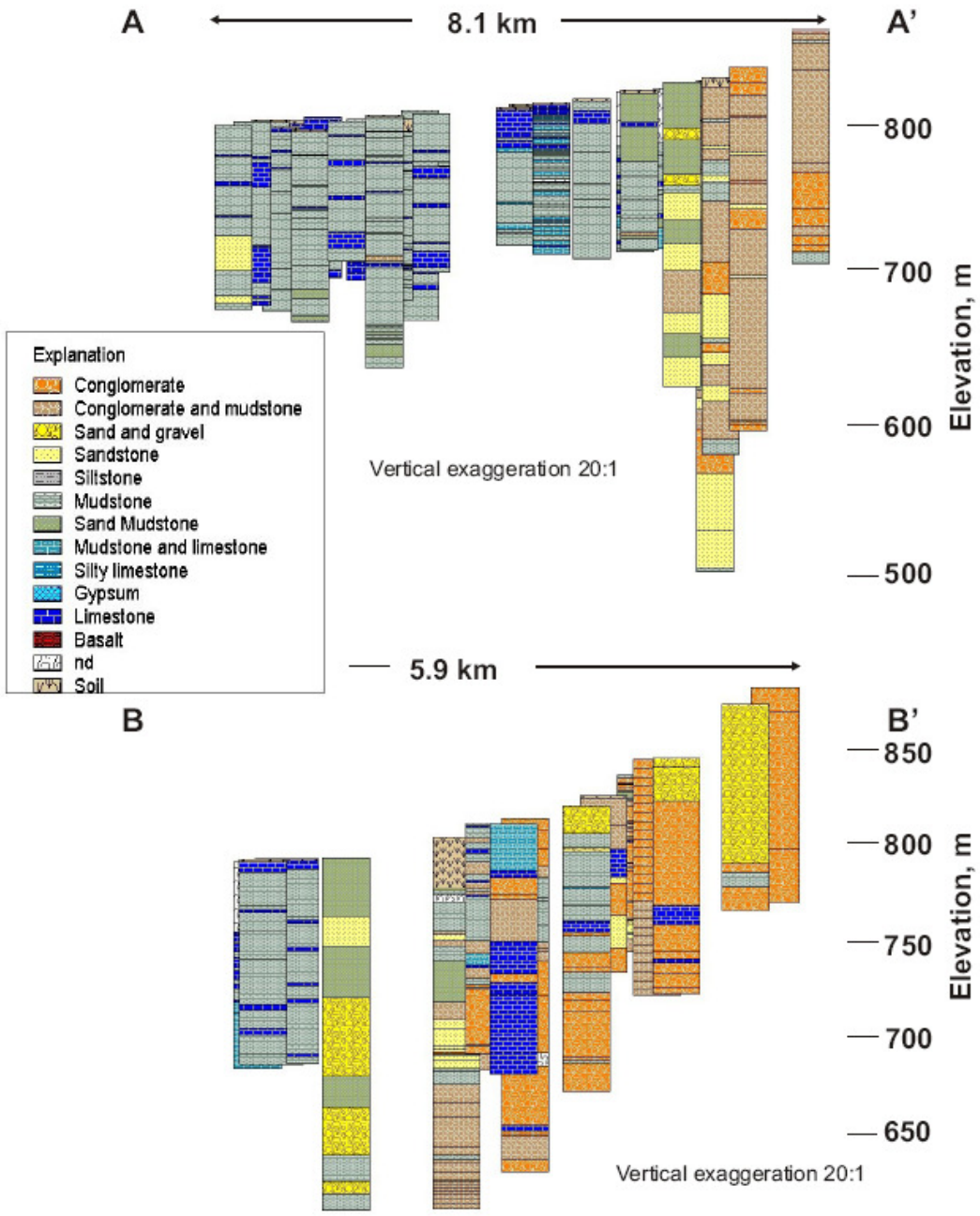

Figure 9. Example stratigraphic sections found in the central part of the study area. From Sweetkind, 2003.

1.3.5 Death Valley Regional Ground-Water Flow System, Nevada and California—Hydrogeologic Framework and Transient Ground-Water Flow Model, Belcher et al., (2004).

This study was the result of a five-year project by the USGS in cooperation with the U.S. Department of Energy (DOE) to develop a groundwater flow model of the Death Valley Regional Flow System (DVRFS). The main objectives of this model were to (1) characterize the flow paths and time associated with movement of radionuclides in groundwater from the Nevada Test Site (NTS); (2) geologically delineate the vicinity of the proposed high-level radioactive waste repository at Yucca Mountain; and (3) determine the effects of groundwater movement on areas south of the NTS and Yucca Mountain, including agricultural regions. The entire DVRFS model encompasses and area of approximately 100,000 square kilometers in both Nevada and California.

The DVRFS model grid consists of 194 columns, 160 rows, cells 1500 meters by 1500 meters in the x-y plane, with 16 vertical layers. The model has variable layer thicknesses and extends from land surface to -4000 meters amsl. The model incorporates updated data and modeling tools while also integrating results from two previous numerical models that were completed in the 1990s. This groundwater model includes the reassessment of groundwater discharge via evapotranspiration, accounts for groundwater pumping between 1913 and 1998, incorporates depth decay in relation to hydraulic conductivity and assesses model inflows and outflows of Pahrump Valley according to regional flow constraints. It also reassesses recharge through the development of a watershed process model that computes net-infiltration.

The DVRFS domain includes a combination of reverse, normal and strike-slip faults resulting in an intricate distribution of rocks. Subsurface conditions vary strikingly within the model domain and are composed of varied rock types, ages and deformational structures. The consolidated rocks and unconsolidated sediments found within the DVRFS were segmented into 27 hydrogeologic units (HGUs) including two thrust units. Of these HGUS, only a few are particularly significant to Pahrump Valley: the lower and upper volcanic and sedimentary-rock unit known as the basin fill (upper and lower VSU), the lower carbonate-rock aquifer (LCA), the lower classic-rock confining unit (LCCU) and lastly, the crystalline-rock confining unit (XCU). The LCA is the regional aquifer and carries most of the water from the north and east to the Death Valley discharge region. Specific storage values for the HGUs within the model domain were obtained from aquifer tests and previous modeling studies. The model was confined with the application of specific yield values for the top layer, and specific storage values for all other layers. Hydraulic properties were harmonically averaged when a model cell enclosed more than one hydrogeologic unit.

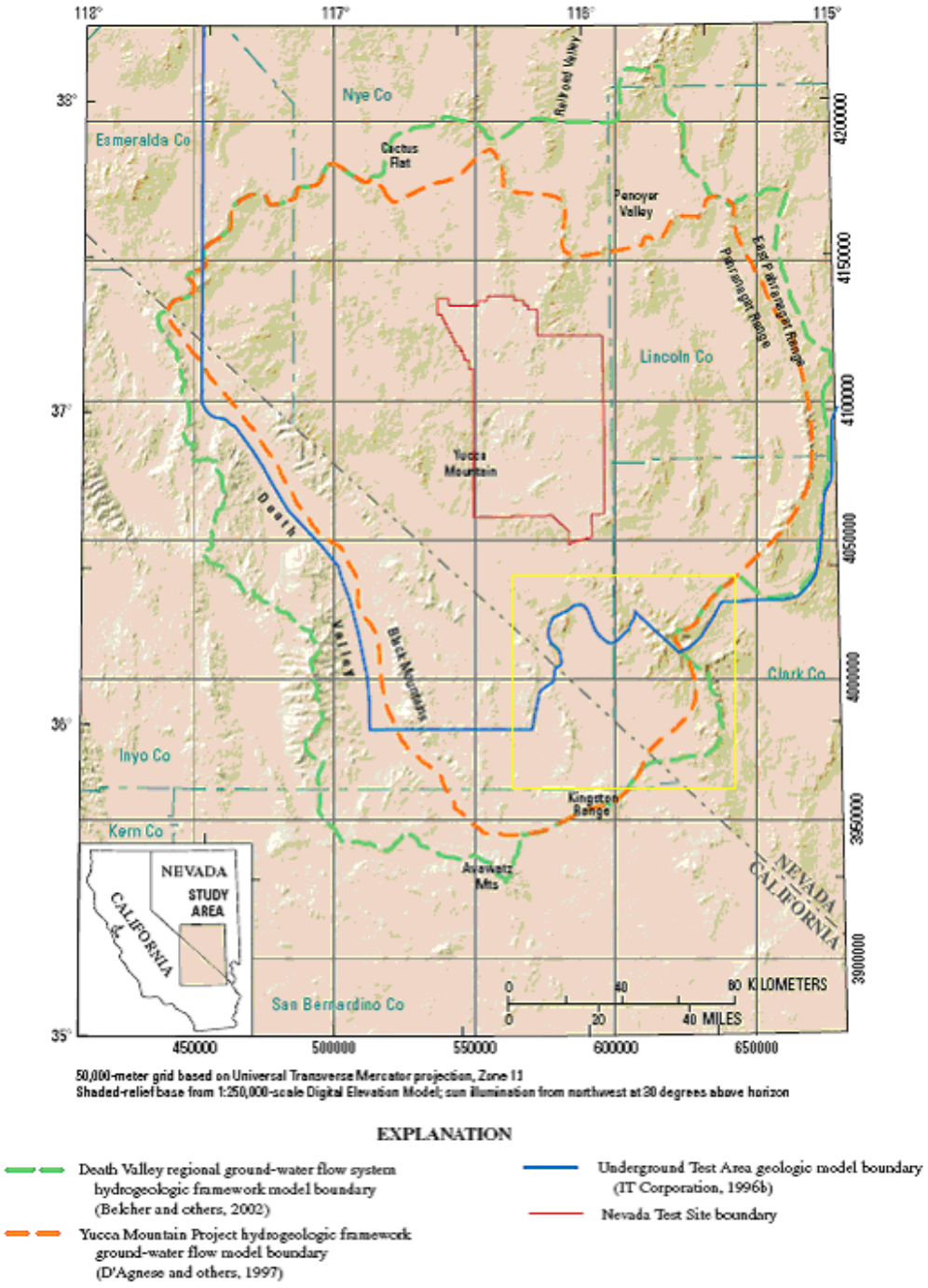

Figure 10. Delineation of the hydrogeologic framework models of previous DVRFS models. Yellow box outlines Pahrump Valley. Figure modified from Belcher et al. (2004).

The DVRFS model estimated annual recharge from the Spring Mountains at 27,017 m^3/d (8,000 ac-ft/yr). Mean annual groundwater discharge from major ET-dominated areas was calculated throughout the DVRFS model. The approach assumed that most of the groundwater issuing from springs and seeps transpires locally within the DVRFS model domain and is accounted for in ET estimates. The majority of the discharge data for the entire DVRFS model were based on previous estimates of ET from earlier studies. For Pahrump Valley, D'Agnese and others (2002) provided an estimate of ET that was based on the phreatophyte map delineated by Malmberg (1967) based on data from 1959-1961. Pahrump Valley phreatophytes had an estimated rate of use of 2.16×10^{-3} m^3/d (2.59 ft/yr), while Stewart Valley was assigned a rate of use of 5.5×10^{-4} m^3/d (0.66 ft/yr). Using these coefficients the estimated ET in Pahrump Valley is 22,127 m^3/d (6,552 ac-ft/yr) and Stewart Valley had an ET discharge rate of 3,380 m^3/d (1,000 ac-ft/yr), totaling 25,497 m^3/d (7,552 ac-ft/yr) of ET for both valleys. Natural discharge from Manse and Bennetts Springs were estimated at 32,400 m^3/d (9,594 ac-ft/yr) prior to groundwater pumping in 1913. In general, the DVRFS model simulates trends, heads and drawdown on a regional scale, but lacks the ability to simulate spikes in data due to the complexity of the basin fill.

2.0 METHODS

2.1 Conceptual Model

The conceptual model of groundwater flow for Pahrump Valley in this study is that all aquifer recharge originates as the infiltration of precipitation in the Spring Mountains, the recharge water percolates vertically downward in the mountain block, and

then discharges as groundwater into the basin fill and carbonate aquifers (Figure 4). The groundwater then flows horizontally in a southwesterly direction through the Valley, and exits the basin through carbonate rocks in the Nopah Range and flows towards Tecopa and Shoshone (Figures 4 and 11). This conceptual model is based on all available data and is consistent with the initial conceptual model of groundwater flow proposed by Malmberg (1967) and further refined by Harrill (1986).

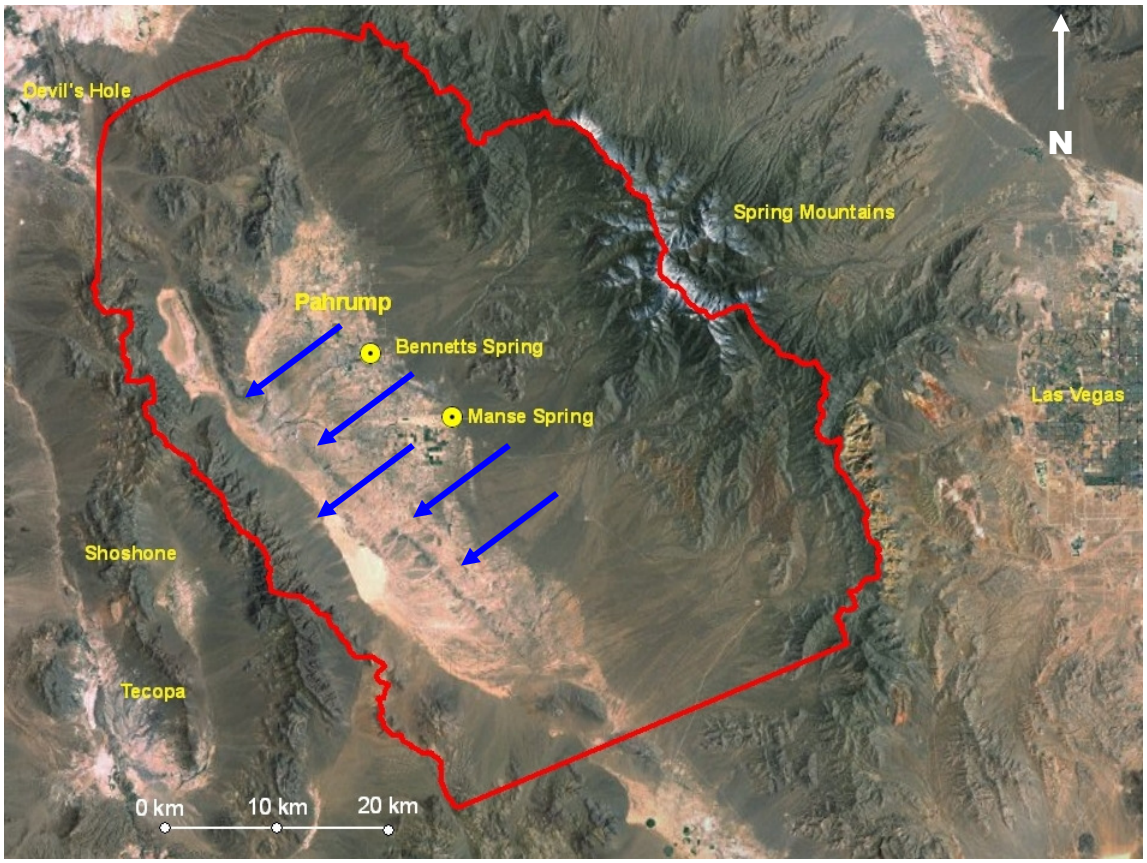

Figure 11. Aerial view of model domain. The model domain is selected from the topographic outline of the basin. It includes regions with significant precipitation, evapotranspiration, groundwater flow and pumping. The southern boundary is considered a natural cut-off that separates Pahrump and Sandy Valleys. The northern boundary is extended to the northwest to encompass all of the surrounding mountains and runs perpendicular to the head contours in the DVRFS model. Blue arrows display direction of groundwater flow off the Spring Mountains towards Tecopa and Shoshone.

The conceptual model of groundwater flow is incorporated into the numerical model through the selection of the model domain, and assignment of boundary conditions that honor observed groundwater flow directions and total recharge estimates. Water balance components of the Pahrump groundwater flow system are estimated using established methods and by assessing current land and groundwater usage. A water balance formulation for Pahrump Valley is:

$$\Delta S = R - ET - Q_O - Q_S - Q_P \quad (1)$$

where ΔS is the change in storage of the aquifer system, R is recharge from precipitation, ET is evapotranspiration, Q_O is interbasin outflow, Q_S is spring discharge,, and Q_P is groundwater pumping from wells. Springs are included in the water balance equation, although they are not implemented in the study – a justification for this is presented in Section 2.2.5. The model was developed using study-specific Fortran 90 codes to create input files for MODFLOW-2000 (Harbaugh et al., 2000). The implementation of sources and sinks, boundary conditions and monitoring wells is shown in Figure 12.

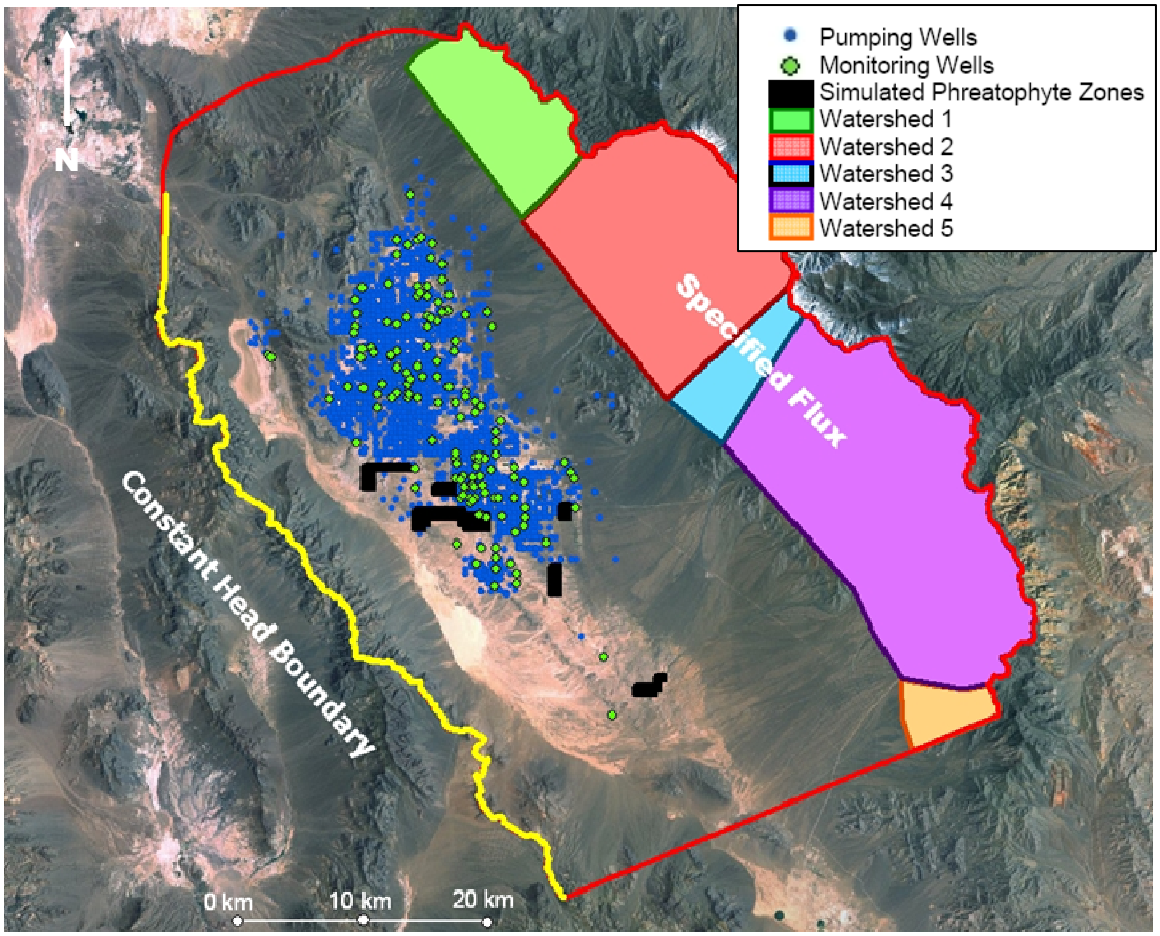

Figure 12. Implementation of boundary conditions and sources and sinks of the groundwater flow model. The configuration of the model boundaries honor the southwesterly groundwater flow movement. Note the pumping wells are concentrated at the northern end of the valley, whereas the phreatophyte zones are located at the central and southern ends of the valley.

2.2 Model Design

2.2.1 Model Domain and Boundary Conditions

The model domain is based on the topographic outline of the basin as shown in Figures 11 and 12. The southern model boundary is located at the divide between Pahrump and Sandy Valleys. The northern boundary extends to the northwest to encompass all of the surrounding mountains. No-flow conditions are assigned to the northern and southern model boundaries to reflect the absence of groundwater flow

across these boundaries, as suggested by previous studies (Malmberg, 1967; Harrill, 1986) and head contours produced by the DVRFS model (Belcher et al., 2004). A constant flux condition is applied to watersheds in the Spring Mountains to simulate groundwater recharge (inflow), and a constant head boundary is used to simulate groundwater outflow from the carbonate aquifer towards Tecopa and Shoshone. The implementation and configuration of these model boundaries honors both the estimated recharge rates and southwesterly groundwater flow direction.

The model grid is consistent with the quarter-quarter resolution of the Nevada Department of Water Resources (NVDWR) well inventory database by having a constant 400 meter by 400 meter spacing in the horizontal direction. The lower left origin of the model grid in Universal Traverse Mercator (UTM) Zone 11 North is x = 565515 m and y = 3955520 m and is co-aligned with the township and range grid to ensure that pumping and monitoring wells are located properly. The model domain extends in the vertical direction from land surface, the highest point of which is 3,600 meters (Mount Charleston) amsl, to a constant -4000 meters amsl. A 400 meter by 400 meter digital elevation map (DEM) is used to assign land surface elevations to the top model layer. A three-dimensional view of the model grid and domain is shown in Figure 13. The vertical layers are configured to have a finer resolution for the shallow basin fill, where groundwater pumping occurs, and coarsen with depth (Table 1). The bottom elevations of cells in Layer 1 were set to a saturated thickness of 300 m based on a planar projection of the water table. Layers 2 through 9 have constant thickness (Table 1), with Layer 10 consisting of the remaining vertical distance between -4000 m amsl and the bottom

elevation of cells in Layer 9. The model grid contains 183 columns, 205 rows, and 10 vertical layers resulting in a total of 375,150 cells.

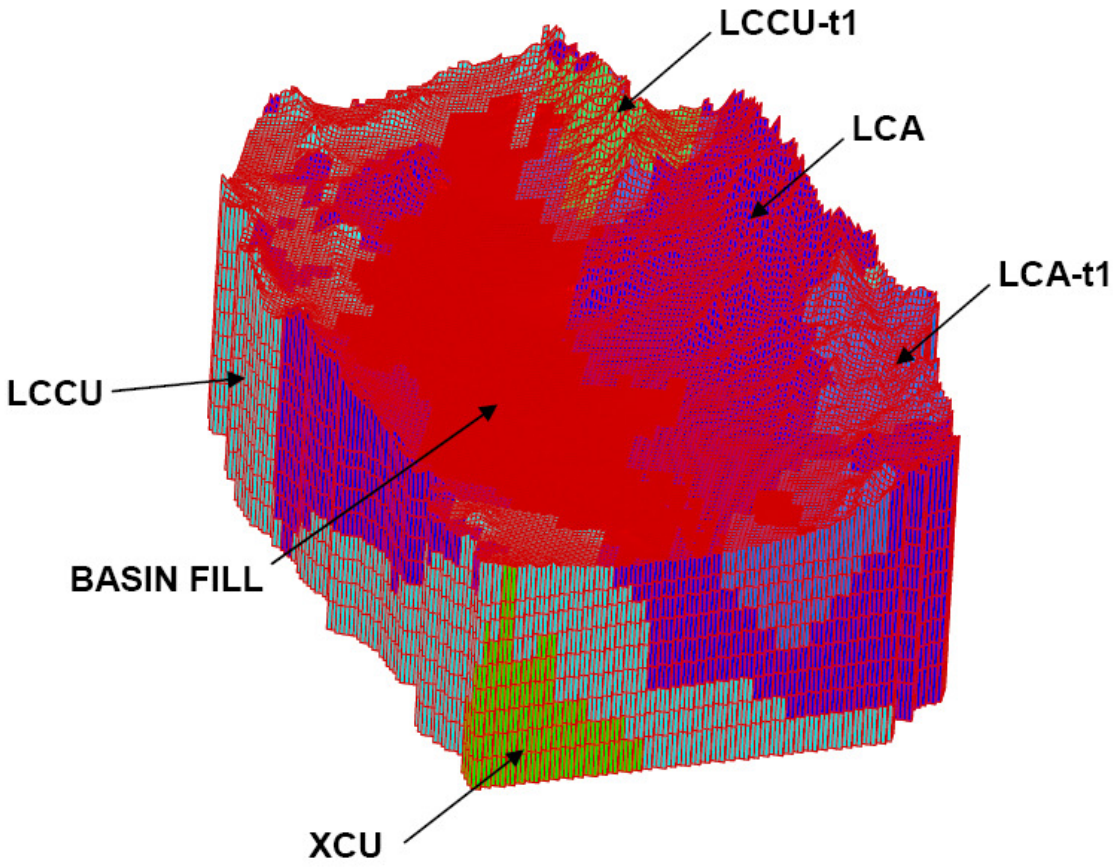

Figure 13. Model grid has 183 columns, 205 rows and 10 layers ranging from land surface to -4000 meters amsl. Hydrogeologic units are highlighted and discussed in Section 2.2.2.

Table 1. Thickness of each layer in the model in meters. The bottom elevations of cells in Layer 1 were set to a saturated thickness of 300 m based on a planar projection of the water table Layer 10 has a thickness of 500 m or greater since it encompasses the remainder of the model to -4000 m amsl.

Vertical Layer	Layer Thickness (m)
1	~300
2	300
3	400
4	500
5	500
6	500
7	500
8	500
9	500
10	500+

2.2.2 Hydrostratigraphy

The hydrostratigraphy of the Pahrump groundwater flow model is based on the DVRFS model hydrogeologic unit (HGU) configuration. HGUs from the DVRFS model were mapped onto the refined grid via a study-specific code. A total of 15 HGUs from the DVRFS model are located in the Pahrump Valley. Of this total, only 7 HGUs cover a large volumetric extent, as the other HGUs comprise a very small volume of the model domain (Table 2). HGUs were consolidated to 7 major groups by eliminating HGUs that comprise less than one percent of the geology of the model. The mapping code was tested extensively against Hufprint (Anderman and LeFrancois, 2003) transects (Figure 14). A generic basin fill unit is assigned to the model in all areas where the pre-Tertiary surface elevation is below land surface. Note that the LCA and LCA-t1, LCCU and LCCU-t1 and VSU upper and lower are combined as single units in the model, respectively.

Table 2. Table of HGUs used in the DVRFS Hydrogeologic Framework Model. HGUs highlighted in bold were implemented in this model.

HGUs Used in the DVRFS Hydrogeologic Framework model found in Pahrump Valley	
ICU	**VSU (lower)**
LCA	**VSU (upper)**
LCA-t1	WVU
LCCU	**XCU**
LCCU-t1	YAA
OAA	YACU
SCU	YVU
UCA	

Table 3. Descriptions of the HGUs obtained from the DVRFS model. Information modified from Belcher et al., 2004.

Hydrogeologic Unit	Description
LCA (Lower Carbonate-Rock Aquifer)	The LCA consists of a Middle Cambrian through middle Devonian carbonate-dominated succession that includes dolomite, interbedded limestone, shale, quartzite and calcareous clastic units. LCA carbonates have a collective thickness of 8,000 m and are considered the most permeable rocks in the region. Higher hydraulic conductivity values result from of fractures, faults and solution channels.
LCCU (Lower Clastic-Rock Confining Unit)	The LCCU consists of Middle Proterozoic to Cambrian siliciclastic rocks. These rocks are exposed in the northwestern part of the Spring Mountains and Nopah Range and are approximately 3,000 m thick. LCCU may have been deposited in a fault-controlled rift basin setting based on the facies changes and blunt stratigraphic pinch-outs. These rocks have very low permeability overall, but local areas may have increased permeability because of regional extension faulting.
XCU (Crystalline-Rock Confining Unit)	The XCU is composed of Early Proterozoic schist, gneiss, granitic intrusive rocks and metamorphosed Middle and Later Proterozoic sedimentary rocks. Groundwater is found heavily only locally where the XCU is fractured. Since these fractures are generally poorly connected, these rocks generally act as barriers to groundwater flow.
VSU (Consolidated Cenozoic Basin Fill Deposits- Volcanic and Sedimentary Rock Unit)	Basin fill deposits within the DVRFS model range from late Eocene to Pliocene and consist of a plethora of volcanic and sedimentary rocks. Rock types include: lavas, welded and non-welded tuffs, and alluvial, fluvial, colluvial, eolian, paludal and lacustrine sediments.

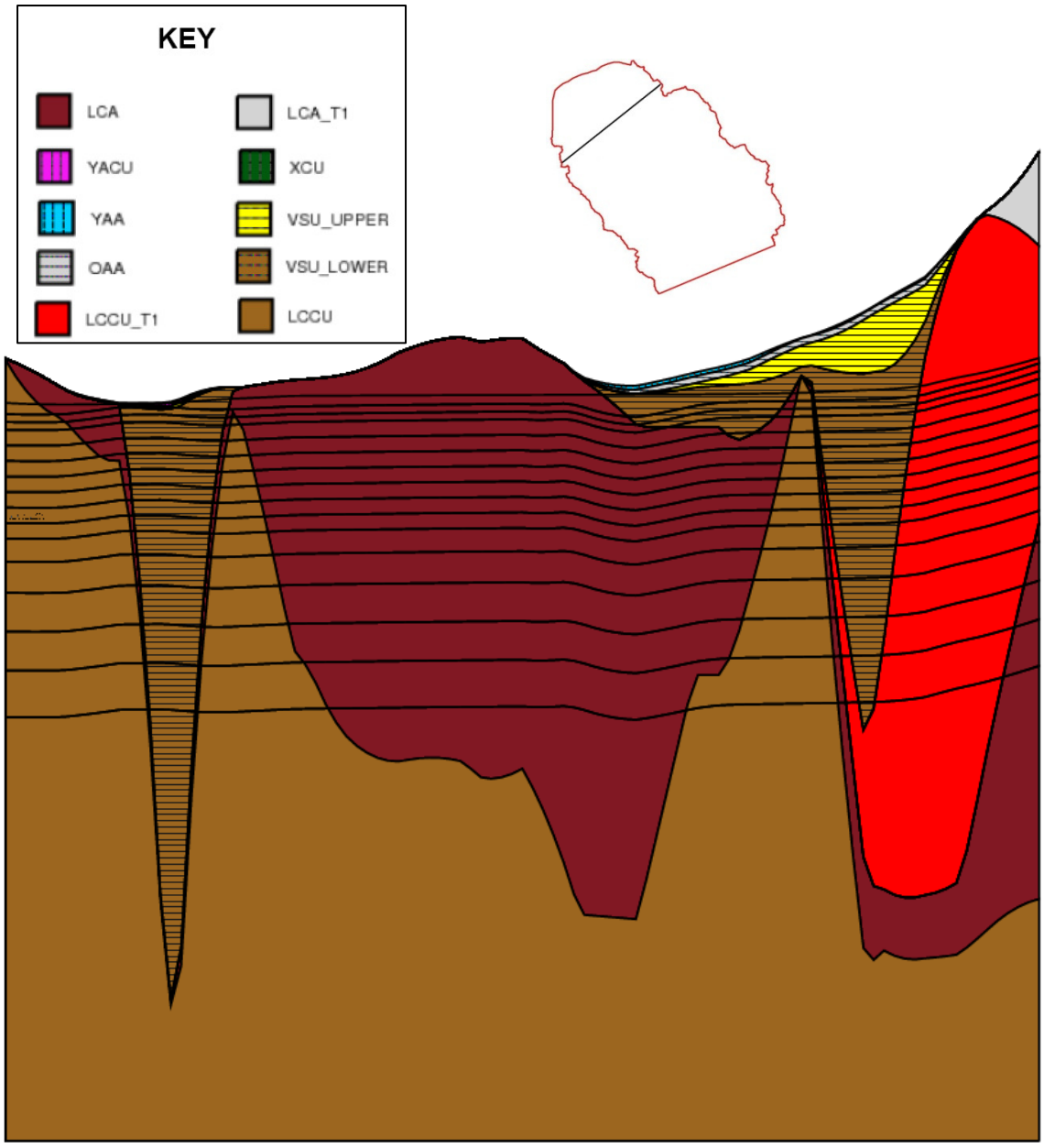

Figure 14. Geologic cross-section of Pahrump Valley with present HGUs listed in the key. This figure demonstrates how little volume YACU, YAA and OAA occupy within the model domain. Note this transect is in the northern portion of the valley where the majority of the population resides and a significant amount of groundwater pumping occurs. The figure has a 20:1 vertical exaggeration.

Although the geology of the basin fill from Sweetkind (2003) is available, the vertical dimension of the first layer (300 meters) exceeds the vertical extent of Sweetkind's data. Consequently, the basin fill is implemented as a single geologic unit (Figure 15).

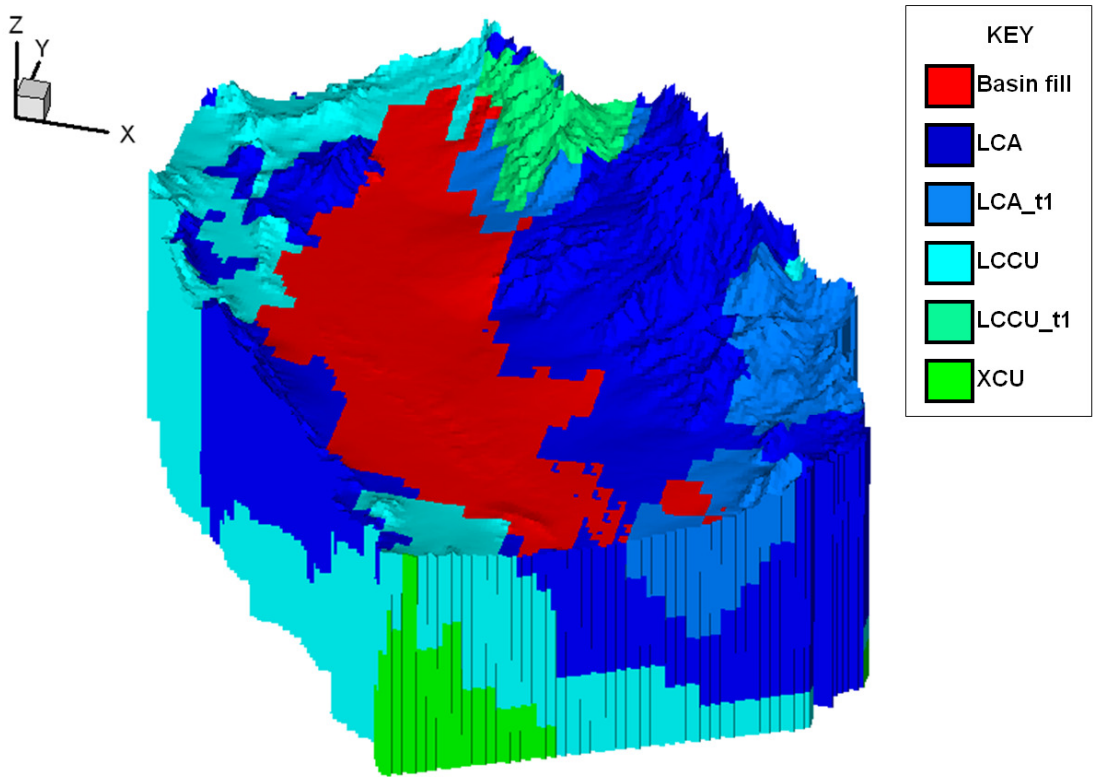

Figure 15. The Pahrump model grid showing the dominant HGUs. The figure has a 5:1 vertical exaggeration.

2.2.3 Potentiometric Surface

The potentiometric surface declines 182 meters across the valley floor. This head drop necessitates that the bottom elevations of cells in Layer 1 slope in a manner consistent with the potentiometric surface. Specifically, the elevation of the bottom of all cells in Layer 1 is equal to 300 meters below a best-fit plane representative of the

potentiometric surface across the Valley. The thickness of 300 meters was arbitrarily selected to ensure that the cells in Layer 1 are saturated and that MODFLOW wet-dry cell problems are avoided during transient simulation, given the large contrast in pumping rates throughout the years. Note that *K* values in the HFM assigned to Layer 1 were based on the geologic units located within the saturated zone, and that hydraulic properties of the geologic units located above the saturated zone are ignored.

A least-squares planar regression was performed on head measurements in Pahrump Valley based on data from 2004 to represent the groundwater potentiometric surface as a plane:

$$z = Ax + By + C \tag{2}$$

where *A*, *B*, and *C* are planar coefficients and *x*, *y*, and *z* represent UTM easting, northing, and elevation, respectively. The planar regression is based on a total of 19 data points: 15 points were selected from potentiometric contours in Figure 16, and the remaining 4 points represent head levels from monitoring wells (Table 4, Figure 16). Assuming that UTM Northing and Easting locations are exact with no error, and all error of the plane is associated with head, the following relationship is used to define a best-fit plane:

$$\beta = \left(X^T X\right)^{-1} X^T H \tag{3}$$

where β is a planar coefficient matrix, *X* contains individual location measurements, i.e., *X*=(UTM Easting, UTM Northing, 1), and *H* is a matrix of head values. The incorporation of data from Table 1 results in: $\beta^T = \left(7.86\times10^{-3} \quad 3.73\times10^{-3} \quad -1.88\times10^{4}\right)$, where $\beta^T = (A \;\; B \;\; C)$. The best-fit plane in relation to the data points are shown in Figure 17.

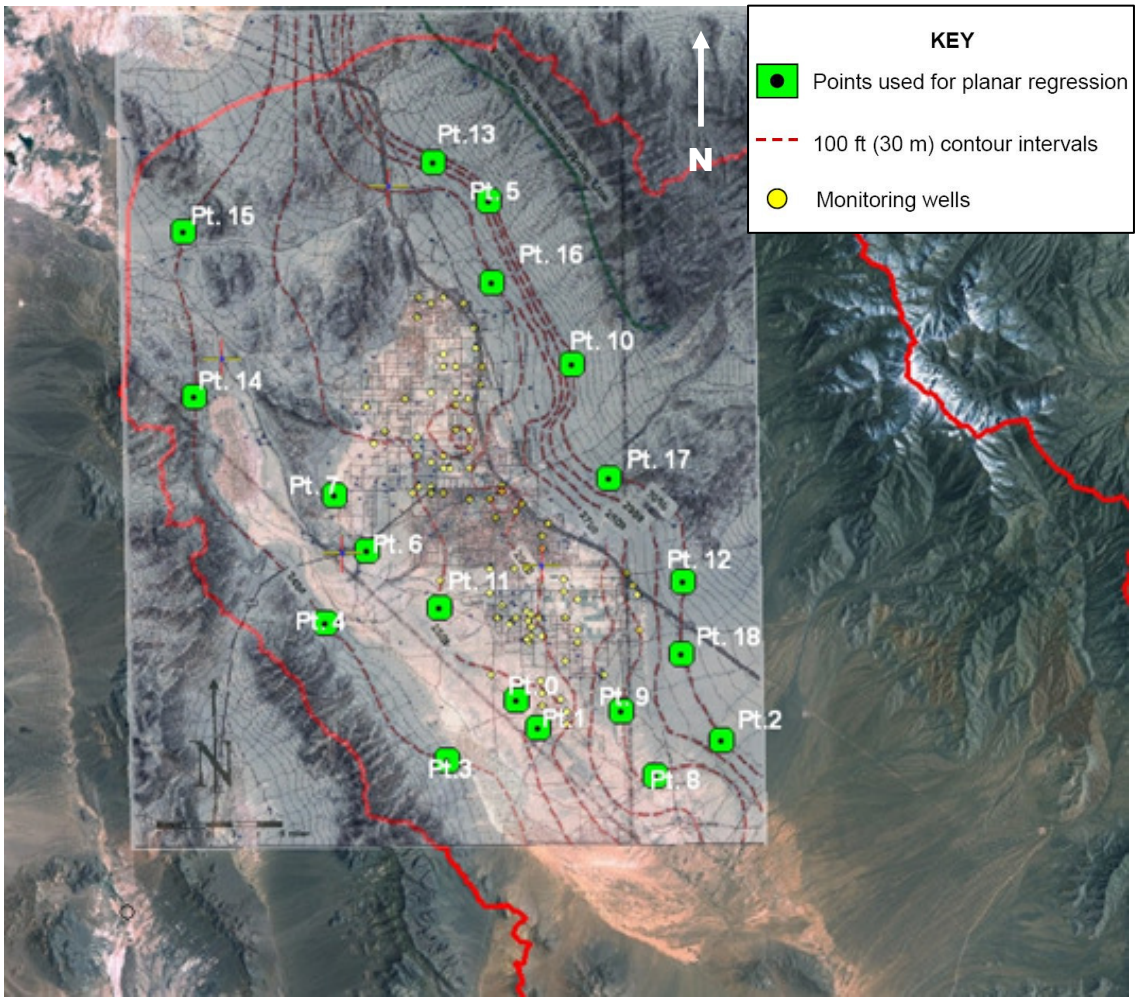

Figure 16. Pahrump model domain (red outline) along with head contours (map overlay) from Figure 7 in Buqo (2006). Water level data was used from 2004. The green dots represent the points used for the planar regression. Note contours are in 100 ft (30m) increments.

Table 4. Table of data points used to represent potentiometric surface as a plane with points 1-14 extracted from the potentiometric map from Buqo (2006), and points 15-18 are recent head levels from monitoring wells.

Point	UTM Easting (m)	UTM Northing (m)	Head (m)
1	592132.974	3993641.002	14.716
2	593602.006	3991804.006	52.488
3	605311.895	3991053.993	22.242
4	587680.226	3989813.111	61.946
5	579902.073	3998622.611	56.701
6	590405.137	4025739.890	208.078
7	582609.997	4003186.001	16.654
8	580456.003	4006775.999	9.565
9	601099.148	3988785.071	12.467
10	598922.956	3992969.429	4.099
11	595694.286	4015166.275	161.864
12	587271.001	3999599.995	20.409
13	602833.319	4001300.626	122.598
14	586784.157	4028122.274	158.697
15	571505.013	4013128.513	51.312
16	570755.200	4023712.635	38.512
17	590597.090	4020494.662	144.499
18	598104.715	4007927.801	124.767
19	602798.686	3996553.271	33.435

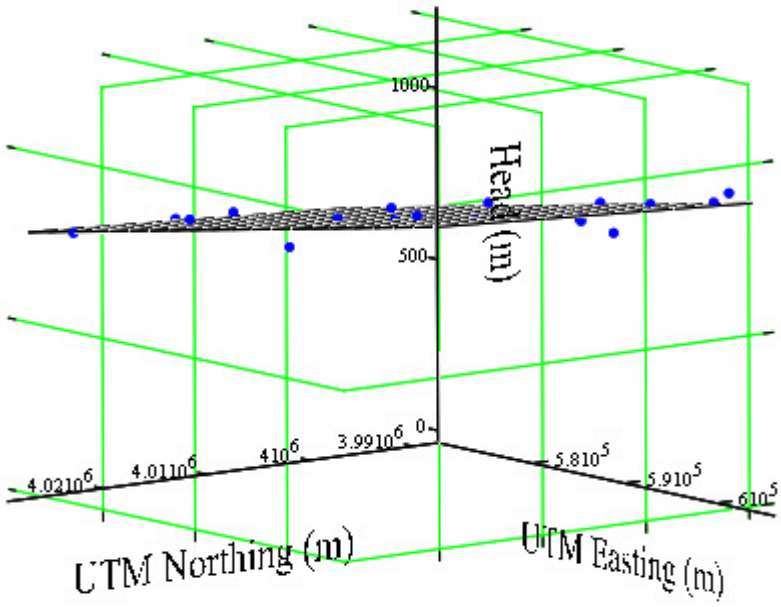

Figure 17. Data points from 2004 (blue dots) compared to best-fit potentiometric surface plane used to assign the bottom elevation of the top model layer.

The Pahrump Valley Fault Zone (PVFZ) is located within the model domain parallel to the Nevada-California state line. The potential influence of the PVFZ on the potentiometric surface was explored using recent data from Nye County. Monitoring well data in the southwest portion of the basin, in Pahrump and Stewart Valley were used to determine the water level gradient between monitoring wells (Figure 18, Table 5). The Stewart Valley Vacant and Stewart Valley South wells are located directly on the fault. Gradients were determined from the 2004 map by Buqo (2006). Low gradients of 1.23 x 10^{-3} m and 1.81 x 10^{-3} m are compared to the overall gradient of the valley, 8.3 x 10^{-3} m. The hydraulic gradients computed from these wells suggest that the hydraulic function of the fault is inconclusive, although the lower hydraulic gradients may suggest that the fault may act as a weak barrier to flow in the transverse direction. Additional monitoring wells

are needed on either side of the PVFZ to further investigate the impacts of the fault on groundwater flow.

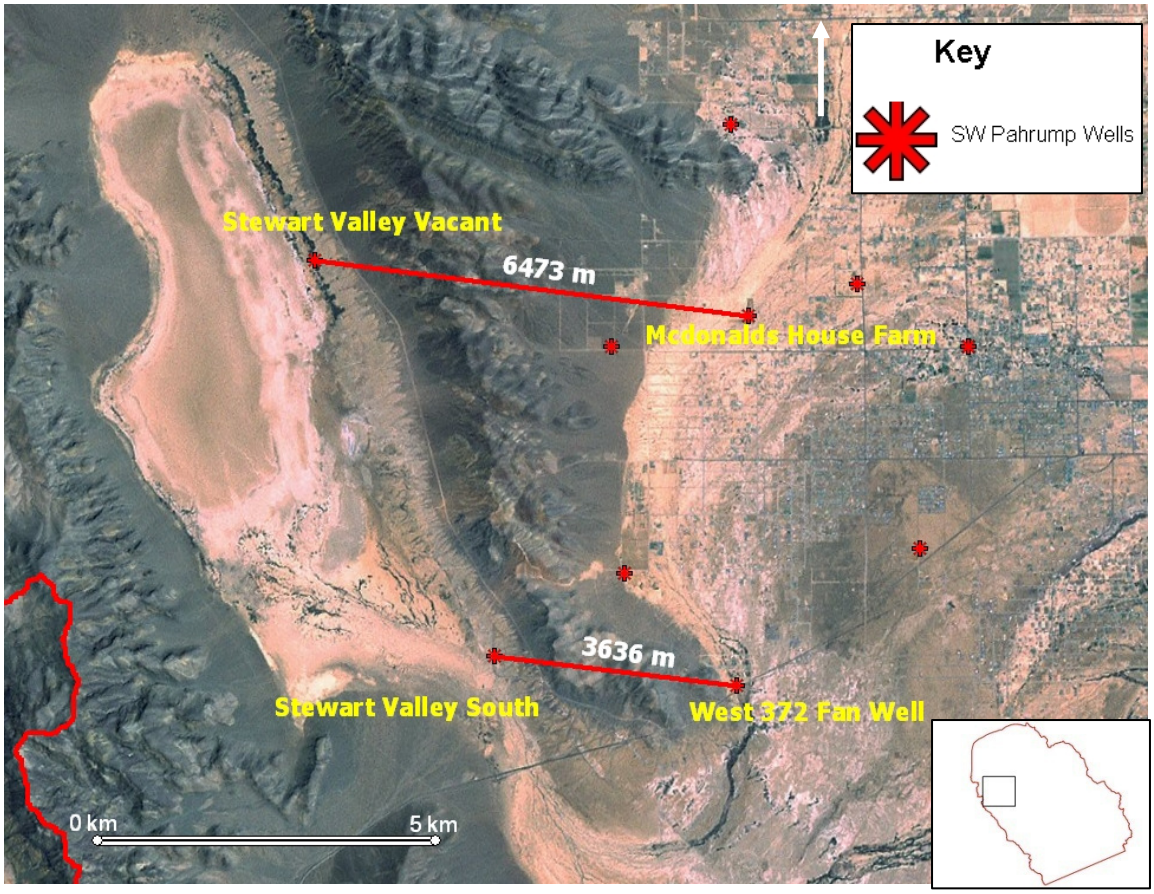

Figure 18. Location of monitoring wells in the southwest portion of basin along with distances between the wells in meters.

Table 5. Table of water levels, distances between wells and calculated gradient. Locations of wells are found in Figure 18. The average gradient across the valley is approximately 8.3×10^{-3} m.

McDonalds House Farm Water Level (m)	**Stewart Valley Vacant Water Level (m)**	**Distance Between Wells (m)**	**Gradient (m)**
755	747	6473	0.00123
West 372 Well Water Level (m)	**Stewart Valley South Water Level (m)**	**Distance Between Wells (m)**	**Gradient (m)**
751	745	3636	0.00181

2.2.4 Recharge

Recharge to the groundwater system of Pahrump Valley occurs through infiltration of precipitation from high elevation watersheds within the Spring Mountains that receive significantly more precipitation than the valley floor. Annual precipitation on the valley floor (12.3 cm/yr) (Buqo, 2006) is very low, and any precipitation that makes it past the root zone and becomes available as recharge to the groundwater flow system is considered negligible. The amount of recharge from the Spring Mountains is uncertain; consequently, several estimates – based on the Maxey-Eakin and Nichols empirical methods that relate mean annual precipitation to recharge – are used to provide a range of likely recharge rates.

Previous studies by Malmberg (1967) and Harrill (1986) provided recharge estimates for Pahrump Valley to be approximately 74,297-87,806 m^3/d (22,000-26,000 ac-ft/yr) using the Maxey-Eakin method. The Maxey-Eakin method relies on the Hardman precipitation map (Epstein, 2004), and assumes that a fixed percentage of precipitation recharges the groundwater system (Harrill, 1986). The difference between the two estimates is attributed to Harrill using higher precipitation estimates that were developed in the 1960s and 1970s and tested throughout Nevada. Precipitation data from Malmberg (1967) was altered by assuming above 2,438 m (8,000 ft) elevation, a rate of 0.53 m (1.75 ft) and 20 percent and 0.61 m (2 ft) and 25 percent (Harrill, 1986). Harrill applied these estimates to data obtained from Malmberg (1967); the revised recharge was 87,806 m^3/d (26,000 ac-ft/yr). Harrill (1986) stated there was insufficient data to determine which dataset assigned the precipitation values best, so he applied a range depending on the set of assumptions.

The Nichols method is used in this study to provide an additional recharge estimate based on the updated Parameter-elevation Regressions on Independent Slopes Model (PRISM) precipitation map (Daly et al., 2007). The Nichols method, similar to the Maxey-Eakin method, estimates recharge based on coefficients assigned to each precipitation zone:

$$Y = b_0 + \sum_{i=1}^{6} b_i X_i + \varepsilon_i \quad (4)$$

where Y is the estimated recharge, b_0 is the y-intercept in ac-ft, b_i are the dimensionless recharge coefficients found in Table 6, X_i are precipitation volumes in ac-ft for each of the six precipitation zones and ε_i is the error in ac-ft in the estimated discharge.

To compute recharge from precipitation according to the Nichols method, a DEM is used to delineate watersheds within the basin using ArcGIS 9.3. A PRISM map of 400 meter by 400 meter sized cells for the years 1971 through 2000 is placed over the DEM (Figure 19). The Nichols' method estimates recharge in Pahrump Valley at 104,692 m^3/d (31,000 ac-ft/yr).

In general when applied to semi-arid basins in Nevada, the Nichols method most often produces recharge rates at the higher end of the range of estimates, while the Maxey-Eakin method produces recharges rates at the lower end of the estimates (Epstein, 2004). A comparison of recharge coefficients for the Maxey-Eakin and Nichols methods is presented in Table 6. This implies that the "true" recharge rate is contained somewhere in between these two estimates. For this reason, the central recharge estimate of 87,806 m^3/d (26,000 ac-ft/yr) is implemented in the final model.

Table 6. Precipitation intervals and associated translation coefficients developed by Maxey-Eakin (1949) and Nichols (2000). The empirically-derived coefficients are multipliers which correlate precipitation to recharge. Note that the Nichols' method generally has higher coefficients, particularly for precipitation zones greater or equal to 34 inches.

Maxey-Eakin Method	
Precipitation Zone (inches per year)	**Coefficient**
Less than 8	0
8 to less than 12	0.03
12 to less than 15	0.07
15 to less than 20	0.15
Equal or greater than 20	0.25
Nichols' Method	
Precipitation Zone (inches per year)	**Coefficient**
Less than 8	0
8 to less than 12	0.008
12 to less than 16	0.13
16 to less than 20	0.144
20 to less than 34	0.158
Equal or greater than 34	0.626

Table 7. Recharge estimates for Pahrump Valley using each recharge approximation method. A recharge estimate of 87, 806 m^3/d (26,000 ac-ft/yr) was used for this model.

Recharge Estimate	**Method**	**Source**
74,298 m^3/d (22,000 ac-ft/yr)	Maxey-Eakin	Malmberg, 1967
74,298 m^3/d - 87,806 m^3/d (22,000 - 26,000 ac-ft/yr)	Maxey-Eakin and Modified Maxey-Eakin	Harrill, 1986
104,692 m^3/d (31,000 ac-ft/yr)	Nichols	This Thesis

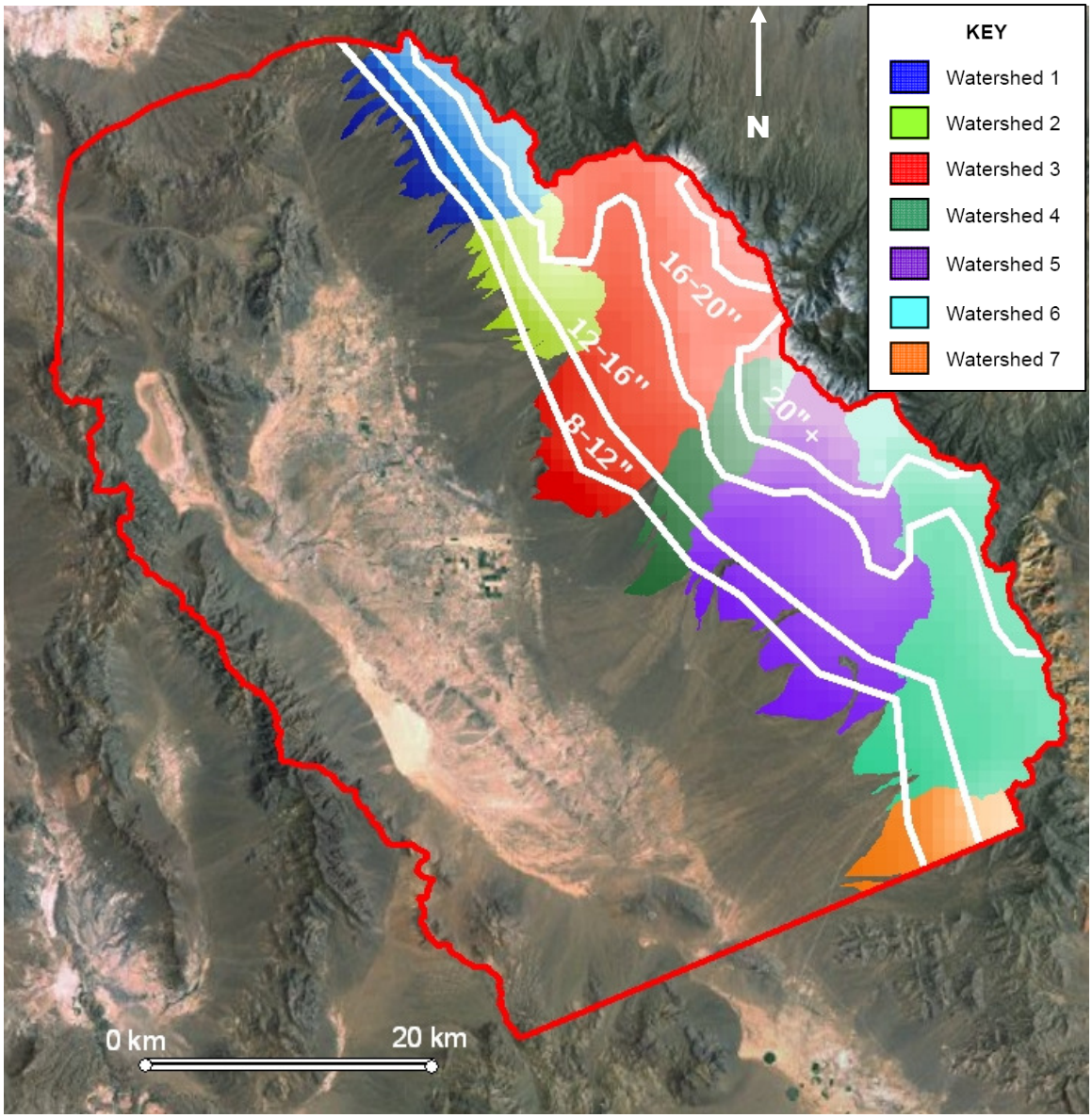

Figure 19. Delineated watersheds in the Spring Mountains with corresponding Nichols' precipitation zones in inches.

Several attempts were made to spatially represent recharge from the Spring Mountains. Initially, a single row of cells was implemented as injection wells along the northeastern portion of the boundary. This application of recharge lead to erroneously high head values for low-permeability cells, irregular flow patterns, and numerous dry cells. To remedy this situation, recharge zones were created by combining mountain

block watersheds and extending them southwesterly towards to the valley floor (Figure 20). The total recharge rate of 87,806 m^3/d (26,000 ac-ft/yr) was then distributed across the mountain block based on the contribution (as a percent) of each recharge zone. Recharge applied to each cell within the mountain block watersheds is weighted according to hydraulic conductivity and cell thickness (transmissivity weighted).

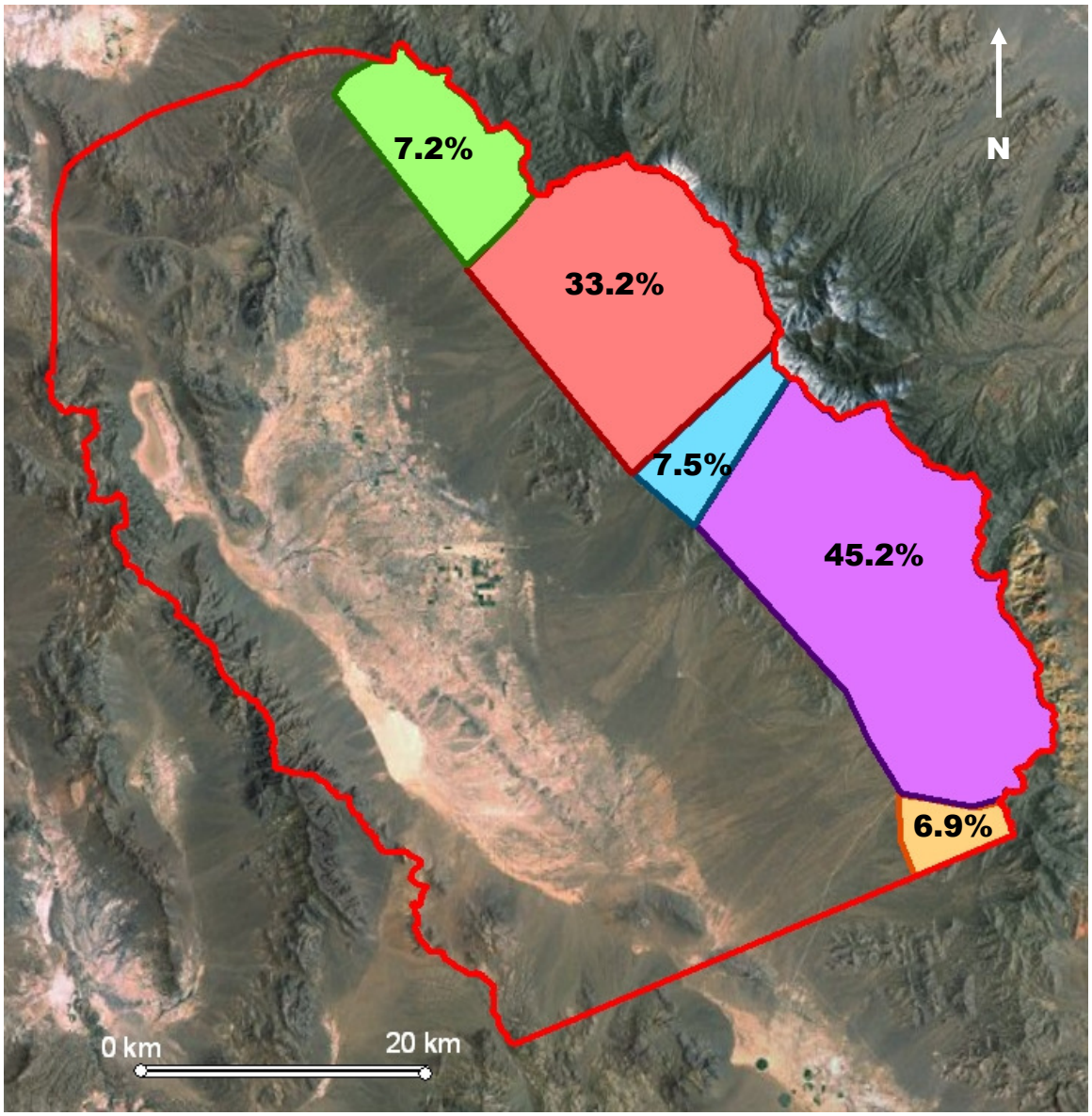

Figure 20. Simulated areas recharge (Spring Mountains). Percentages illustrate how much recharge was implemented in each zone based on the total amount of recharge attributed to each watershed by the Nichols method. Note the significant amount of recharge in Watershed 4 (purple).

2.2.5 Discharge

Total groundwater discharge for the model domain is calculated as the sum of evapotranspiration by phreatophytes, groundwater extraction rates from pumping and estimated outflows from the basin. Both ET and groundwater extraction rates are

estimated from independent methods, while outflow from the basin is computed by the model.

Pumpage:

The Nevada Division of Water Resources (NVDWR) and USGS DVRFS pumpage database supplies the spatial distribution and quantity for five major types of wells: household, industrial, irrigation, commercial and public. Data provided from the USGS-DVRFS pumpage database ranges from 1913- 2003, and data from the DWR ranges from 1913-2008. Pumping rates from both the NVDWR and USGS are not synonymous (Figure 21). The DWR database is missing a significant amount of data between 1913 and 1952, and assumes that the average annual pumpage per household was 1 ac-ft/yr. In contrast, the USGS database provides consistent annual pumping estimates while it incorporates a minimum, median and maximum for each category of pumping. Though the USGS database is based on records contained within the NVDWR database, it provides additional total pumpage estimates where the NVDWR had incomplete data and was used for this model.

A constant rate of 1.69 m^3/d (0.5 ac-ft/yr) is applied to all domestic wells in this study based on revised estimates of household use by the NVDWR (Felling, 2009 personnel communication). Water pumped for domestic uses eventually replenishes some of the extracted groundwater via septic systems, and is also accounted for in this pumping rate. Irrigation estimates for this study were calibrated to NWDWR total irrigation estimates to account for both incomplete data (1913-1950) and uncertainty in applied irrigation rates. A crop use of 1.5 m (5.0 ft) is typically applied to irrigated acreage.

Calibration of the USGS pumpage database to the NVDWR database values was achieved by changing crop use coefficients in the range of 1.37 m (4.5 ft) to 1.98 m (6.5 ft) until the NVDWR and USGS pumpage database annual totals were equal (Figure 21).

Long-term irrigation and industrial wells are spatially distributed via the USGS pumpage database to represent variability in pumping and the general shift from predominantly irrigation to domestic wells (Figure 22). Not all public and community well locations are known, and therefore, pumping is spatially distributed amongst wells of known positions with given pumping rates. Groundwater extractions from the basin fill aquifer are simulated using a negative specified flux applied to cells in Layer 1 using MODFLOW's well package. Annual pumping data are found in Appendix A.

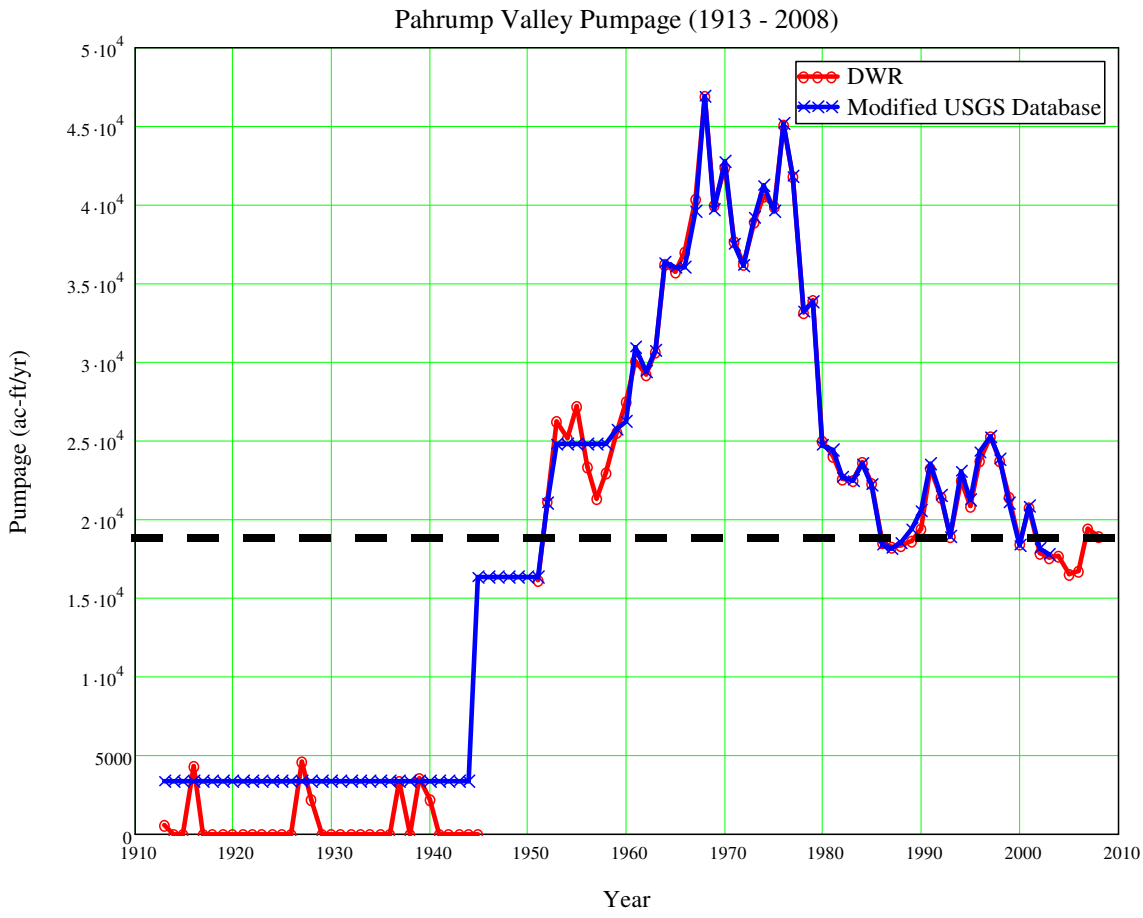

Figure 21. Annual groundwater pumpage inventories in Pahrump from 1913 to 2008; the black line is the sustainable basin yield estimated by Harrill (1986) of 19,000 ac-ft/yr (64,166 m^3/d). Note that pumping between 1960 and 1980 greatly exceeded the sustainable basin yield, and that current pumping rates are approaching the sustainable basin yield.

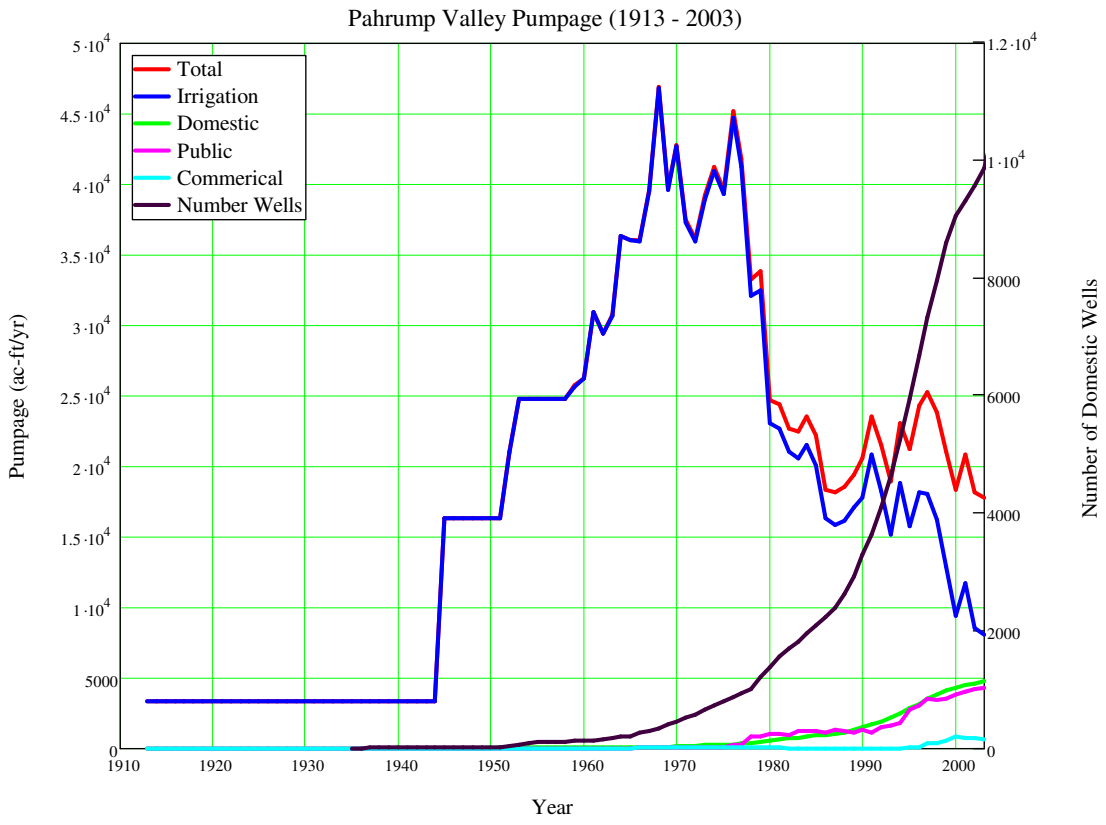

Figure 22. Graph distinguishing the different types of pumpage within Pahrump Valley. Up until the 1970s, irrigation accounted for almost all of the pumpage. Afterwards, the shift from agriculture to domestic uses is evident as public, domestic and commercial pumpage increased and irrigation decreased. As the population increases, the difference between irrigation and total pumpage also increases.

Evapotranspiration:

Delineation of phreatophytes is based on updating a digitized version of the 1962 map created by Malmberg using National Agriculture Imagery Program (NAIP) maps on Geographic Information Systems (GIS). These updated phreatophyte areas (Figure 23) are also mapped to distinguish changes between the 1962 map and present conditions. As the population growth increased in Pahrump Valley, areas of saltgrass, saltbush, saltcedar and cottonwood diminished. Mesquite, however, further expanded southwesterly within the basin, particularly in low-elevation areas with relatively shallow water table elevations. Currently, mesquite is the only significant source of evapotranspiration within

the valley, save a few isolated salt cedar strands. An evapotranspiration rate of 42,215 m^3/d (12,500 ac-ft/yr) is implemented as a negative recharge value using the recharge package in MODFLOW. This rate is determined by taking the current area of phreatophytes and multiplying it by a rate of use of 1.006 meter (3.3 ft), used by Malmberg in 1967 (Table 8). Current areas of mesquite are highlighted in green (Figure 23), simulated phreatophyte regions are outlined in black. The density of mesquite is over represented in the figure; areas of simulated ET were concentrated to the densest areas of phreatophytes.

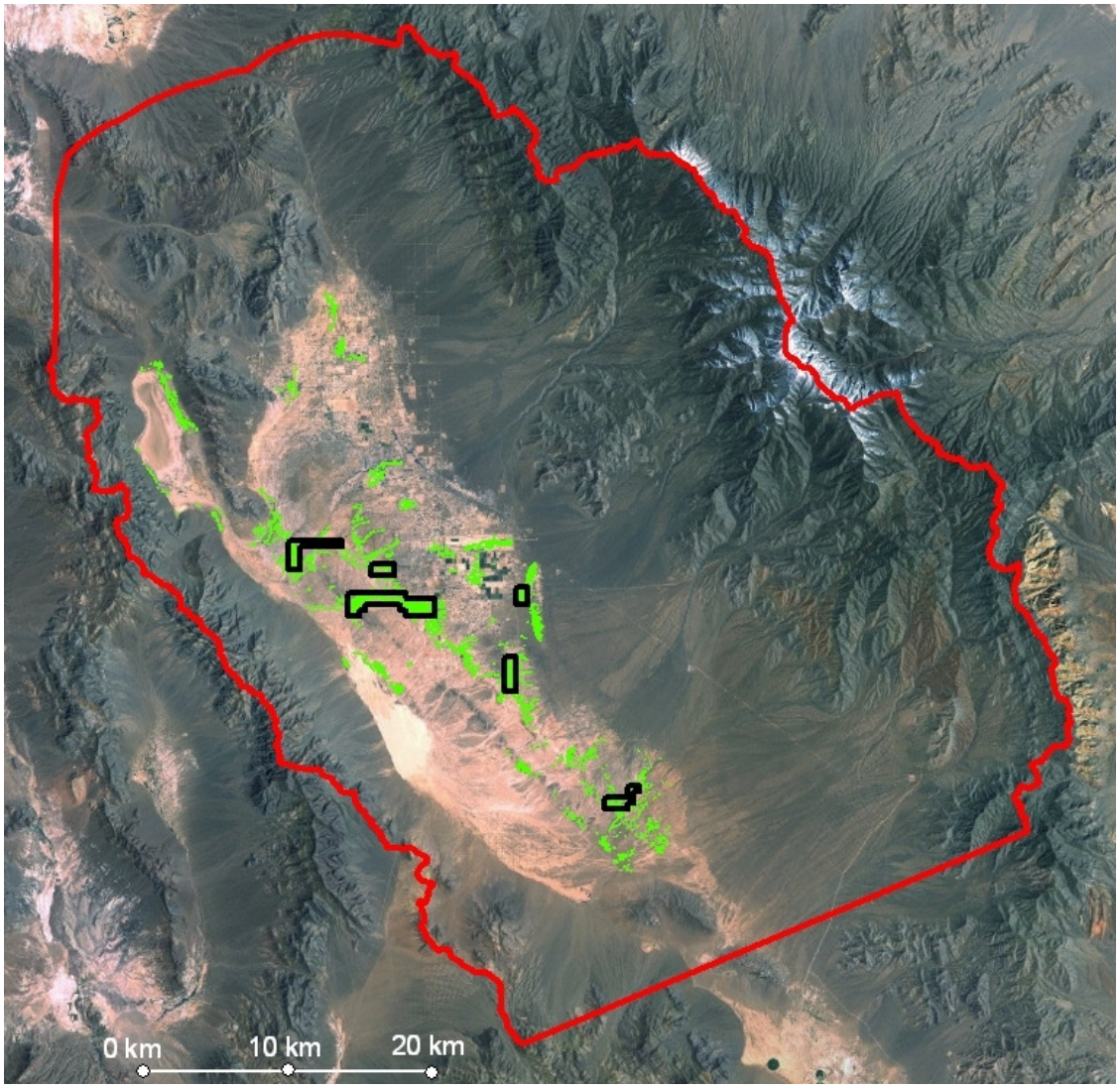

Figure 23. Delineated phreatophyte areas (mesquite) based on 2004 agriculture maps are highlighted in green. Regions outlined in black delineate where phreatophytes were simulated in the model. The density of phreatophytes is over represented by the green in the figure, areas of simulated ET were concentrated to dense areas of phreatophytes.

Table 8. Total ET calculations. First estimate is from Malmberg (1967); second estimate was derived from delineating phreatophyte zones from Malmberg (1967) into GIS. Last estimate is updated phreatophyte zones using 2004 agriculture map. Rates of use estimates obtained from Malmberg (1967) and DeMeo (2003).

Year	Phreatophyte Type	Area (km^2)	Rate of Use (m)	Source	ET (m^3)	Total ET (m^3/d)
Malmberg	*Saltgrass and saltbush*	1.821	0.914	Malmberg	4,559.17	
1959-1962	*Cottonwood*	0.040	1.68	Malmberg	185.74	
	Saltcedar	0.142	1.83	Malmberg	709.20	
	Mesquite	10.522	1.006	Malmberg	28,976.04	34,430
Malmberg	*Saltgrass*	1.772	0.914	Malmberg	4,435.17	
(Using GIS)	*Cottonwood*	0.056	1.68	Malmberg	258.98	
1959-1962	*Saltcedar*	0.153	1.83	Malmberg	764.36	
	Saltbrush	1.784	0.914	Malmberg	4,466.82	
	Mesquite	13.049	1.006	Malmberg	35,935.31	45,861
2004 NAIP Map	*Mesquite*	15.338	0.914	DeMeo	38,398.32	38,398
			1.006	Malmberg	42,238.16	**42,238**

Springs:

Spring discharge data is not simulated by the model. The small amount of spring discharge comprises only a small portion of the water budget. Both Manse and Bennetts springs also ceased flow in 1959 and 1979, respectively, although Manse Spring recently started to flow (or more correctly "seep") again in 2006 following a period of heavy winter precipitation. Bennetts Spring ceased flow before there was significant pumping in Pahrump Valley in the 1960s and 1970s. Manse Spring had small discharge rates of less than 5,065 m^3/d (1,500 ac-ft/yr), respectively, compared to the significant amount of pumping for agriculture at the time which averaged over 135,100 m^3/d (40,000 ac-ft/yr). Moreover, there is a high degree of uncertainty exhibited in the incomplete spring data (Figure 5 and Figure 24), and the springs are located in areas for which the model

simulates lower than observed head level elevations. Simulating the springs would only further decrease the simulated head elevations in these regions and cause additional inaccuracy to the model.

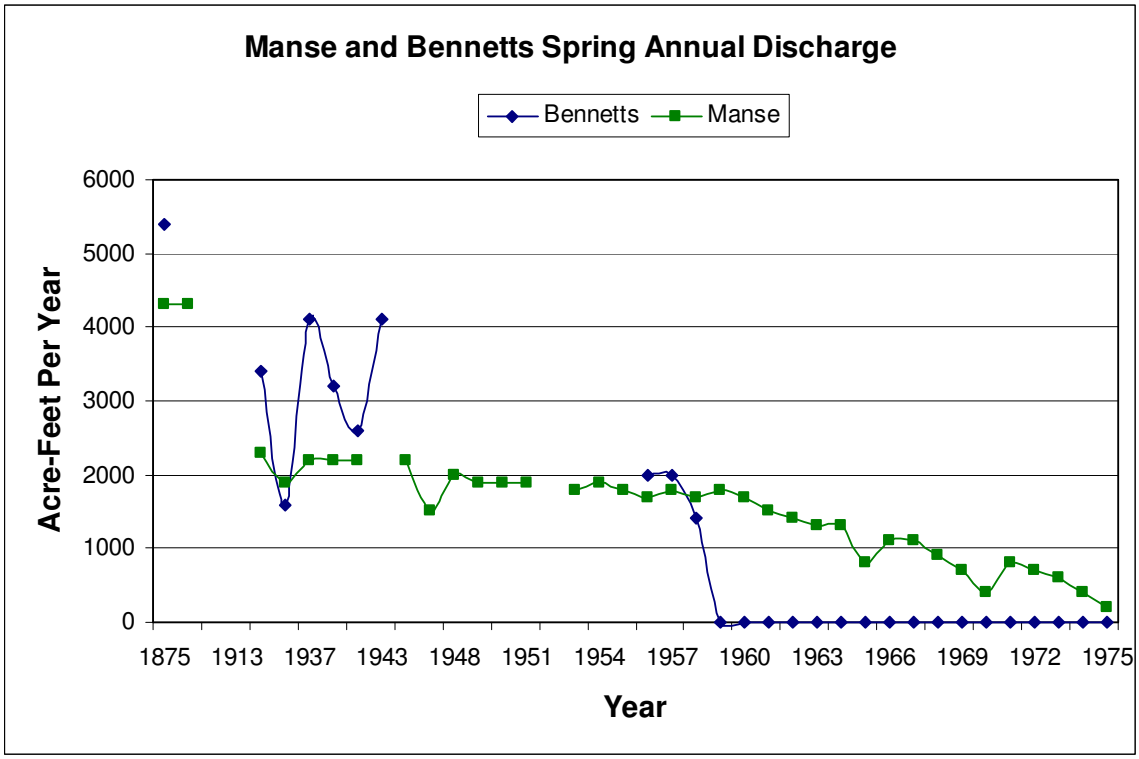

Figure 24. Annual discharge from Manse and Bennetts Springs. Bennetts Spring ceased flow in 1959 and Manse in 1979. Neither spring has a significant impact on the water budget and data is incomplete and inconsistent. Data modified from the NVDWR, Malmberg (1967) and Harrill (1986).

2.2.6 Hydraulic Parameters

Ranges of hydraulic parameters for the HGUs within the Pahrump Valley model were obtained from the DVRFS model (2004) and Harrill (1986) to help guide preliminary value selection prior for model calibration (Table 9). The complex geology of Pahrump Valley was represented by designating different *K* values based on the HGUs provided by the DVRFS hydrogeologic framework model. Inverse computation of hydraulic parameters during calibration is described in detail in Section 3.

Table 9. Previous estimates of hydraulic parameters from the DVRFS model from Belcher et al, (2004) and Harrill (1986).

		DVRFS		
Rock Type	**Typical Materials**	***K* at Average Depth (m/d)**	**Specific Storage m^{-1}**	**Specific Yield**
LCA	–	1.26E-03	1.5E-08 - 6.3E-02	2.0E-01
LCA_T1	–	2.57E-02	1.5E-08 - 6.3E-02	–
LCCU	–	6.0E-05	1.5E-08 - 6.3E-02	–
LCCU_T1	–	6.0E-05	1.5E-08 - 6.3E-02	–
XCU	–	–	–	–
VSU-Upper	–	4.17E+0	4.7E-07 - 4E-02	1.0E-03 - 4.7E-01
VSU-Lower	–	4.92E-01	9.7E-07 - 2.0E-02	–

		Harrill		
Rock Type	**Typical Materials**	**Range of *K* (m/d)**	**Specific Storage m^{-1}**	**Specific Yield**
playa deposit	clay and silt	1.0E-03 – 3.0E+00	1.00E-03	5.0E-02 - 1.3E-01
	very fine sand	1.0E-01 - 1.6E-01	1.00E-03	5.0E-02 - 1.3E-01
Lacustrine and associated fine-grained deposits	silt and clay	1.0E-01 - 5.0E-01	2.0E-03 - 2.0E-02	5.0E-02 - 1.3E-01
	fine sand	1.0E+00 - 4.0E+00	–	–
Fanglomerate and associated coarse gravel	mostly silt, sand and gravel	1.0E+00 - 4.0E+00	8.0E-04 - 2.0E-03	1.3E-01 - 2.5E-01
	sand	4.0E+00 - 30+	–	3.0E-01
	gravel	20E+00 - 150+	2.00E-03	3.0E-01

2.2.7 Depth Decay of Hydraulic Conductivity

Systematic decreases in hydraulic conductivity with depth are rarely accounted for in regional groundwater flow models outside of southern Nevada (Jiang et al., 2009). Ground water flow systems in southern Nevada consist of very thick sequences of permeable carbonates underlying thick packages of basin fill sediment. The presence of deep water tables, high overburden stresses at depth, and nonlinear decreases in borehole

flow with depth (IT Corporation, 1996) suggest that depth decay is a viable mechanism to scale the hydraulic conductivity of units at depth.

Previous numerical models that include depth decay of hydraulic conductivity for Nye County and surrounding areas include Beard et al. (2004) and Belcher et al. (2004). The study of Beard et al. (2004) noted that the lack of depth decay of hydraulic conductivity and flow anisotropy generated unrealistically deep flow paths and under simulation of observed discharge within Oasis Valley. The application of depth decay in hydraulic conductivity to the DVRFS model was found to alleviate these problems and enhance model calibration. Depth decay in hydraulic conductivity was also used in the DVRFS model based on previous estimates by IT Corporation (1996) to zones within the LCCU, SCU, XCU and ICU (Belcher et al., 2004), and was also found to enhance model calibration.

Depth decay of hydraulic conductivity is implemented in the model for two reasons: (1) the large vertical extent of the model (land surface down to -4000 m amsl), and (2) better calibration results, including more accurate simulation of the observed hydraulic gradient across the valley floor, once depth decay was implemented. Individual depth decay constants were applied to each hydrogeologic zone:

$$K(z) = K_{Land\ Surface} \cdot 10^{-\lambda z} \quad (5)$$

where $K(z)$ is the hydraulic conductivity at a specific depth, $K_{Land\ Surface}$ is the hydraulic conductivity at land surface, λ is the depth decay coefficient and z is depth below land surface. Belcher et al. (2004) noted that depth decay can produce unrealistically low K values at depth. This problem is addressed in the model by applying a lower K threshold value where appropriate. This is further explained in Section 3.

Table 10. Initial depth decay parameter values used in the DVRFS model; these values were used as a guide for preliminary depth decay values during model calibration. (IT Corporation, 1996).

Hydrogeologic Unit	Initial Depth Decay Parameter Values Used in DVRFS Model (λ)
LCA	1.02E-03
LCA_T1	1.02E-03
LCCU	1.02E-03
LCCU_T1	1.02E-03
VSU- Upper	4.00E-03
VSU-Lower	4.00E-03
XCU	1.50E-03

2.3 Model Calibration

The transient model has a total of 91 annual stress periods – encompassing 1913 to 2003 – and is configured so that steady-state is achieved for the first stress period, with the remaining 90 stress periods in transient mode. Recharge, pumping and evapotranspiration are held constant during each stress period. A single time step is implemented per annual stress period. The groundwater flow model was calibrated in confined mode, as the model did not consistently converge in unconfined mode. The lack of consistent convergence in unconfined mode is attributed to the high degree of head drop (400 m +) across the valley and mountain block.

Model calibration involves adjusting hydraulic parameters (hydraulic conductivity, specific storage, specific yield, depth decay and recharge) to minimize the difference between simulated and observed head levels from 1946-2003. Only water level data within a month of October 6th of any year were included in the calibration. The use of a specific date interval prevents calibration errors caused by seasonal variations

between head observations. In some circumstances, well observations were also eliminated if the well locations or head levels were unknown. These criteria restricted the total number of monitoring wells to 143 with a total of 899 water level measurements to serve as calibration targets. The spatial distribution and number of water level measurements of the monitoring wells is shown in Figure 26. The locations of the long-term monitoring wells (highlighted in red) are distributed throughout the populated areas within the valley. These wells provide a large amount of data to calibrate to in areas of significant pumping. It should also be noted that many of the newer wells drilled in 2000 are also well dispersed throughout the town of Pahrump (yellow dots).

The majority of the monitoring well data spans between the years 1966 to 1976 and from 2000 to 2003 (Figure 25). The period of 1966-1976 reflects the onset of high pumpage rates to a peak in 1967 and subsequent decline thereafter. The stressing of the aquifer during this time period provides a good opportunity for calibration of a groundwater flow model. However, the relative absence of data between 1968 and 2000 provides challenges in calibrating the model to current water levels. Of the 143 wells, only 6 monitoring wells have consistent, long-term data for calibration (Figure 26). Monitoring well data is provided in Appendix B.

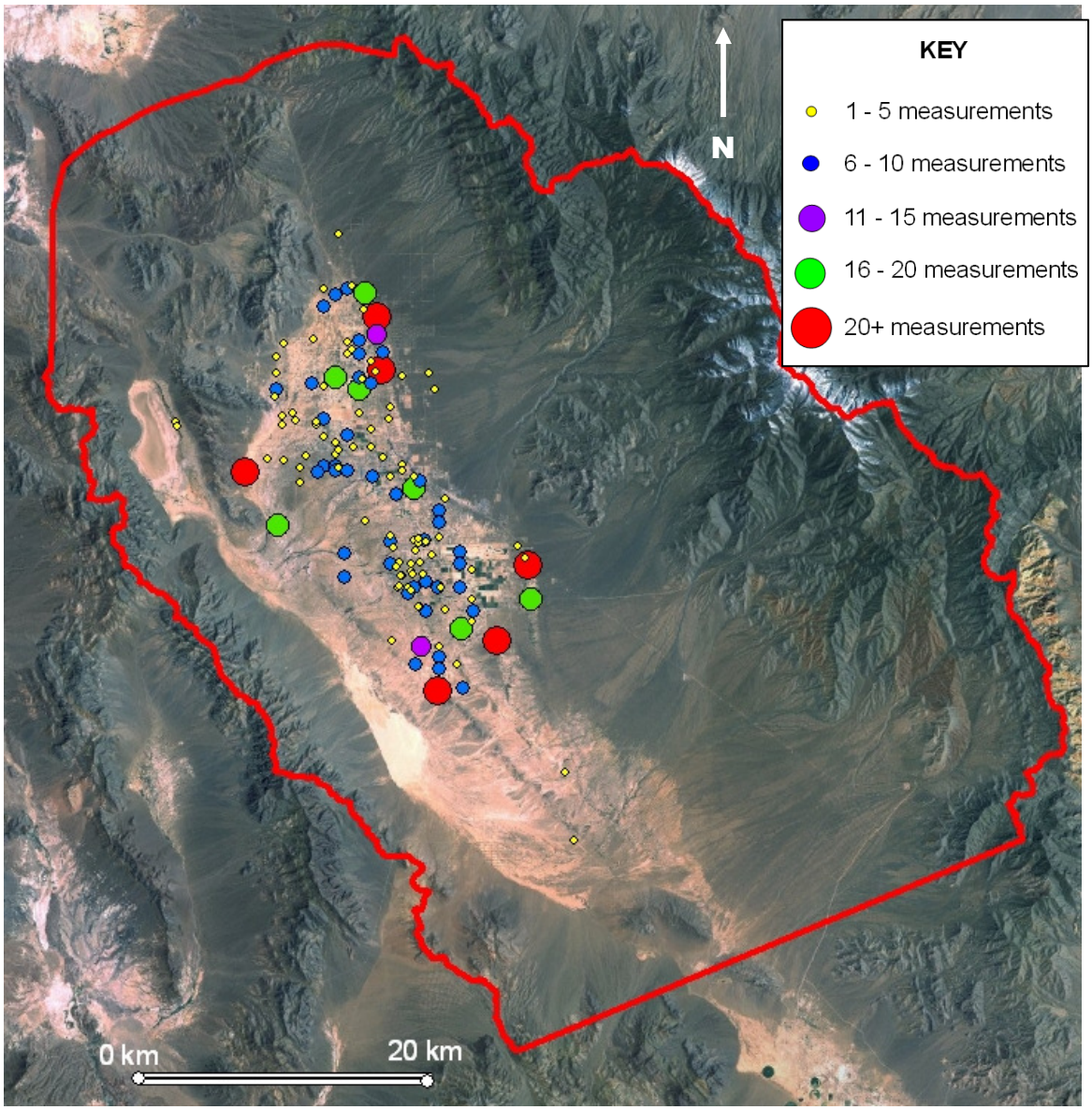

Figure 25. Locations of the 143 monitoring wells. Dot size is proportional to the number of well observations. The large red dots denote the six monitoring wells with long-term data. Also note the spatial distribution of monitoring wells with 16-20 water level measurements (green dots).

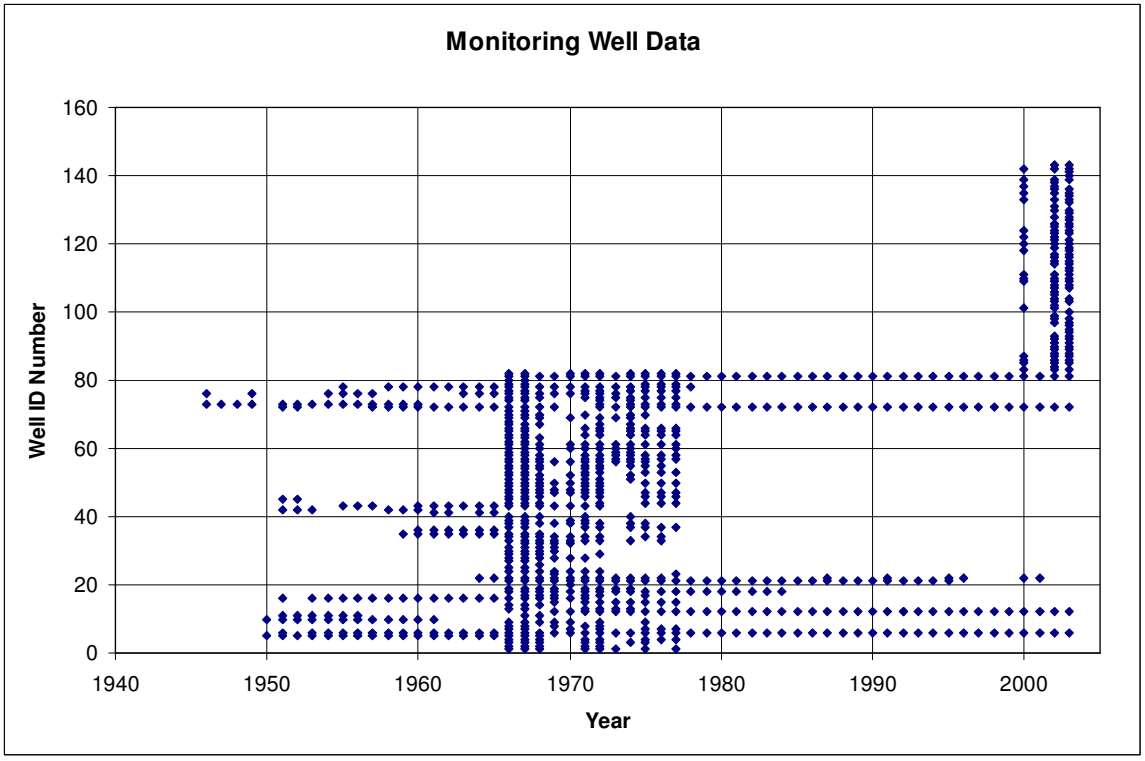

Figure 26. Graph of available monitoring well data based on the number of data points per well and the year. The majority of data falls from 1966-1976 and from 2000-2003. There are 143 monitoring wells with a total of 899 data points.

The model calibration process involves both manual calibration of individual hydraulic parameters and automatic calibration using PEST. Final values of hydraulic parameters (hydraulic conductivity, depth decay of hydraulic conductivity, specific yield and specific storage) are assigned to each hydrogeologic zone, based on a combination of PEST and manual calibration. Several different approaches were implemented during model calibration and are described in detail in Section 3.

3.0 RESULTS AND DISCUSSION

Study results include details on the various approaches used to calibrate the transient flow model, the final geologic configuration of the flow model, calibrated hydraulic parameters, and comparisons of simulated and observed water levels and

drawdown. Calibrating the model was an extremely intensive process due to the long time period used for calibration, a vast amount of monitoring well data, and the temporal and spatial distribution of pumpage and its uncertainty within the valley. Additionally, calibration of the model required the investigation of multiple conceptualizations of recharge and geology.

3.1 Model Calibration

The calibration process involves minimizing the difference between observed and simulated head values. The level of accuracy between observed and simulated head levels is calculated using root mean squared error (RMSE) which is an unbiased metric. The RMSE is defined as:

$$RMSE = \sqrt{\sum_{i=1}^{n} \frac{(O_i - E_i)^2}{n}} \tag{6}$$

where O is the observed value, E, is the simulated value and n is the number of observation data pairs (Anderson and Woessner, 2002). First, manual calibration is used to minimize the RMSE, followed by an automated calibration using PEST to finely tune values once manual calibration helps determine general range of parameter values. After each manual or automatic run, discrepancies between observed and simulated head elevations and drawdown values are analyzed. Parameters are then changed to lower the disparity between observed and simulated head levels and drawdown values.

The model calibration process additionally utilized a preferential weighting scheme for head observations: monitoring well data preceding 1980 were given a weight of 1.0; well data from 1980 to 2003 were given a weight of 3.0; and well data that

consistently produced erroneous head level matches are given a weight of 0.1. The year 1980 is chosen as the divide between more recent and less recent well data due to the abrupt change in pumpage and shift towards predominantly domestic pumping. The higher weighting of observations also places more confidence on more recent records, particularly pumping.

Initial model calibration involved holding the basin fill *K* at 1 m/d and LCCU at 1.0×10^{-5} m/d and calibrating *K* of the carbonate aquifer. Borehole specific data suggest that a *K* value of 1 m/d is best to simulate the basin fill (Figure 27). Calibration attempts that assigned separate hydraulic parameters (*K*, specific storage and specific yield) to LCA-t1 and LCCU-t1 yielded no advantage over simulations where these units are grouped with LCA and LCCU respectively. This calibration technique underestimated simulated head elevations closest to mountain block and overestimated in the western portion of the model.

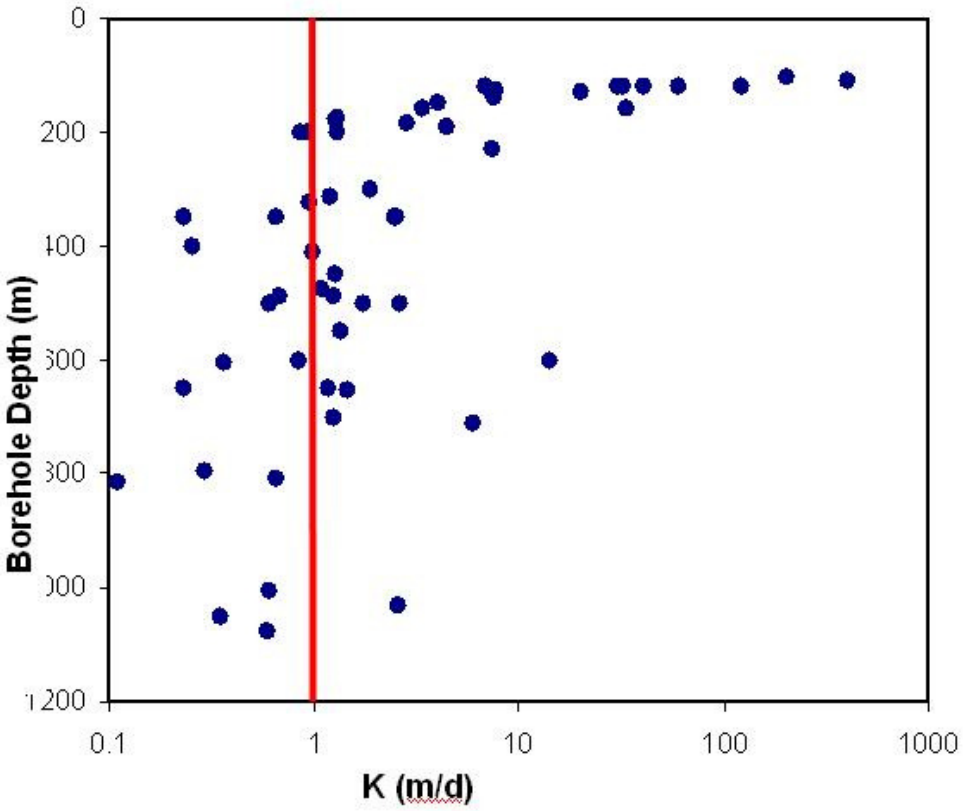

Figure 27. Graph of borehole depth versus *K* computed from single well specific capacity tests suggests an average basin fill *K* value of 1 m/d. The very high *K* values computed from 0 to 200 m amsl are most likely caused by specific capacity tests with high pumping rates and short screens. This combination tends to produce erroneously high *K* values.

3.1.1 Basin Fill Delineation

Initial model results using the hydrogeologic framework model depicted in Figure 15 resulted in problematic head values. Specifically, a very flat water table profile resulted in heads severely underestimated at the mountain block/valley fill interface, and heads that are overestimated in the eastern half of the basin fill. This prompted the division of the basin fill into designated basin fill *K* zones, each with distinct hydraulic parameters (Figure 28). This approach assumed that the basin fill *K* exerts the greatest impact on the simulated head measurements since all of the monitoring wells are located within the basin fill.

The basin fill *K* zones were differentiated from simulated head results that were systematically too high, too low or within five meters of the observed head values. The delineation of the basin fill involved mapping simulated groundwater level trends in GIS to determine areas where the model produces low, neutral or high groundwater levels. The basin fill zones were then outlined accordingly to target specific monitoring wells and produce neutral simulated head zones. Initially, only three zones were created, but after trying to focus closely on specific groundwater level trends, the number of zones was increased to five. Numerous adjustments were made to these zones during model calibration as an attempt to calibrate simulated heads in the basin fill (Figures 28 through 31).

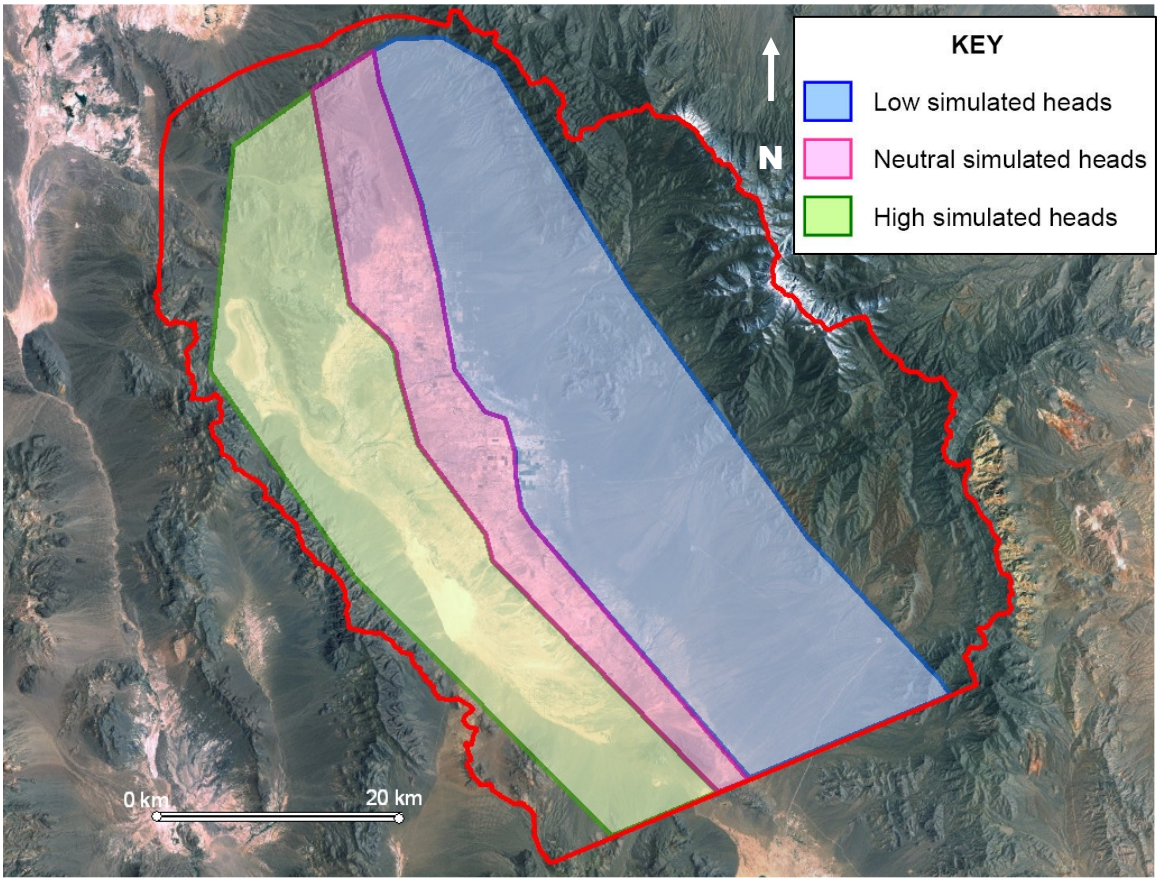

Figure 28. Original basin fill *K* zone delineation with three zones. The blue zone is given lower *K* values since the model produced lower than observed head measurements. The green zone is given higher *K* values to account for the higher than observed simulated head measurements. The pink zone produces the most accurate simulated heads and was considered the neutral zone.

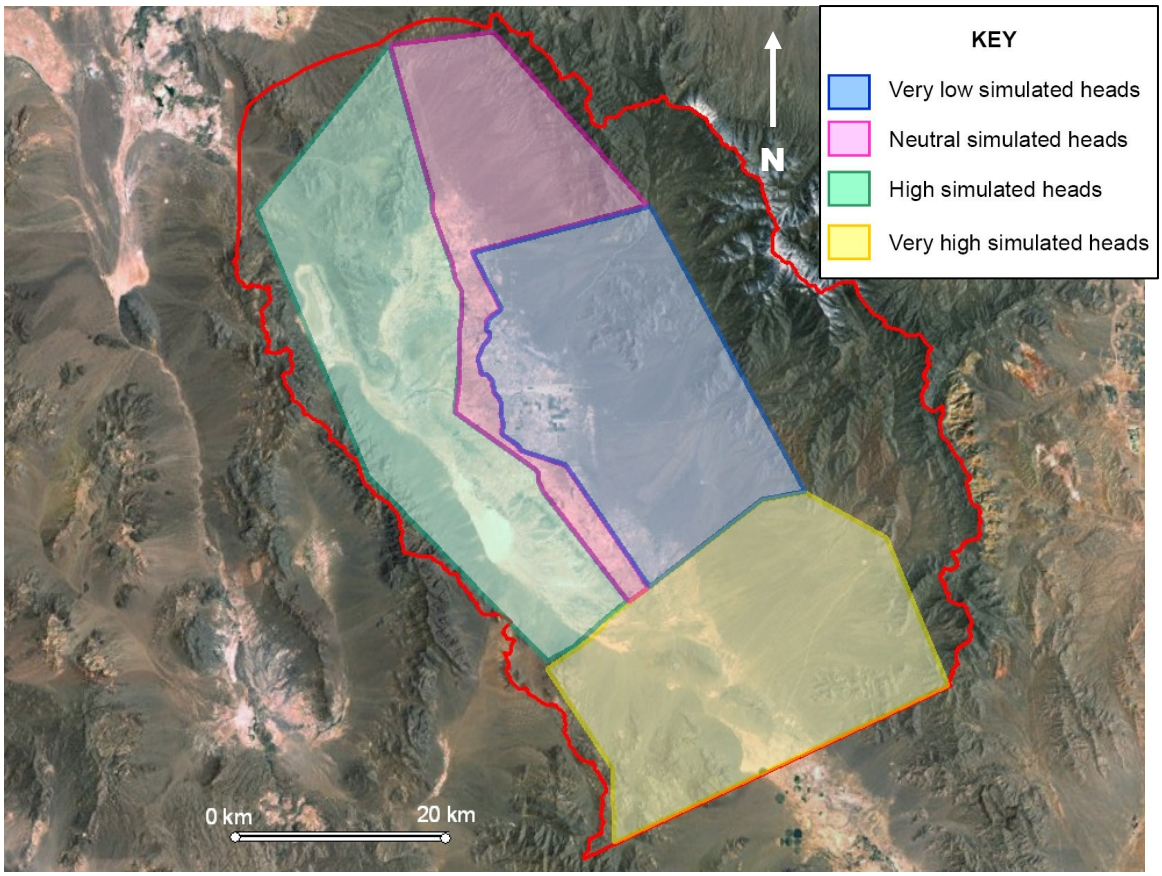

Figure 29. Example of one of the many delineated basin fill *K* zones created to simulate the curvature of groundwater flow off the Spring Mountains. The trial-and-error process involves varying the number of *K* zones since the three zones did not produce accurate simulated head measurements. Changing the shapes of the *K* zones is efficient in determining the direct effects of varying *K* for specific wells. The fourth zone is created for this trial because of the severely high simulated heads in the southern portion of the basin. The neutral zone (pink) is also expanded further northeast while restricting the very low simulated head zone (blue).

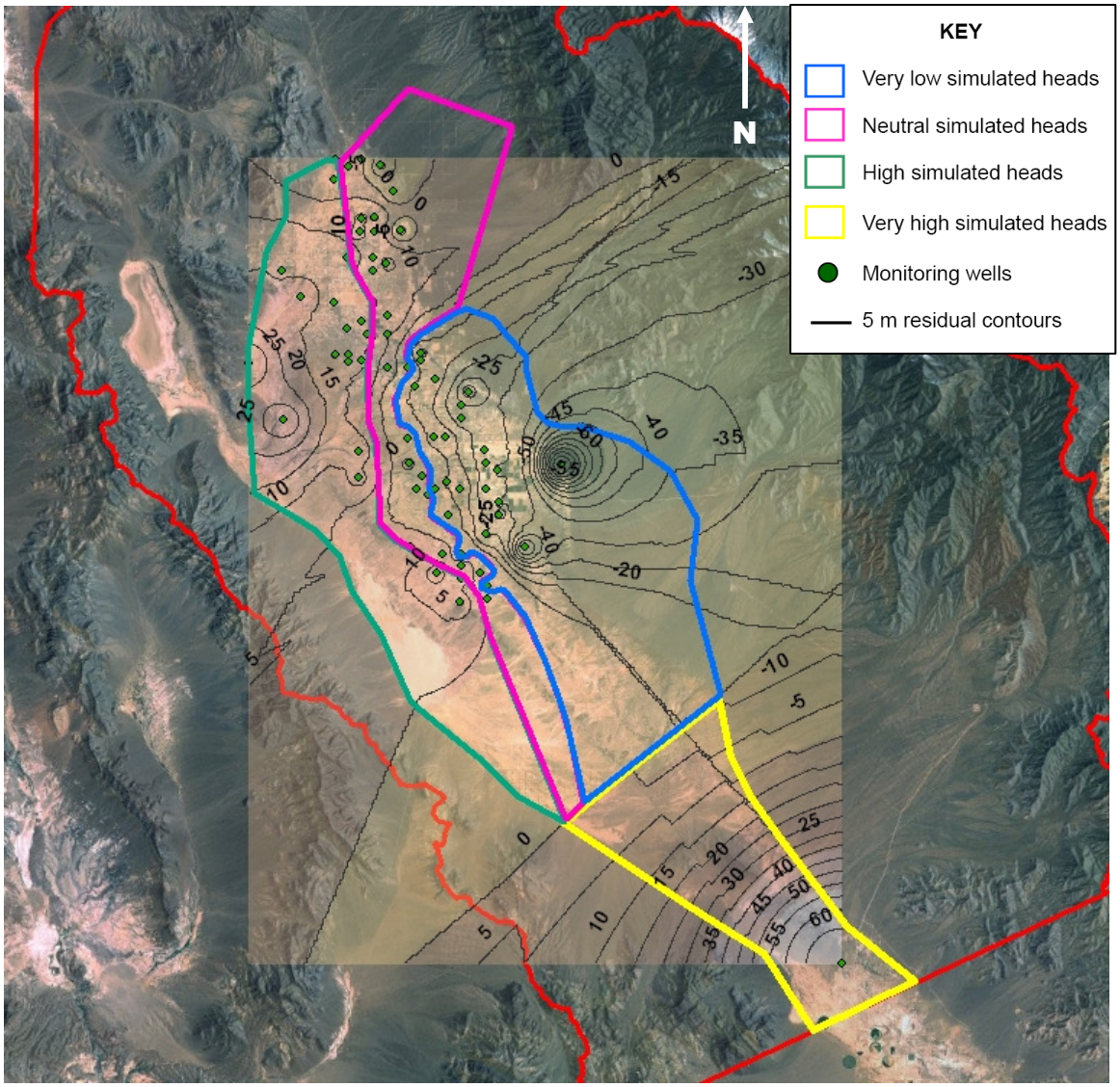

Figure 30. Figure of residual field snapshots of the year with the most groundwater pumping (1968) and delineated *K* zones. This residual map is developed during the trial-and-error process to create the best basin fill *K* zones. Note that all head measurements are located within the basin fill, and that any head contours extending into the mountain block are an artifact of the contouring program.

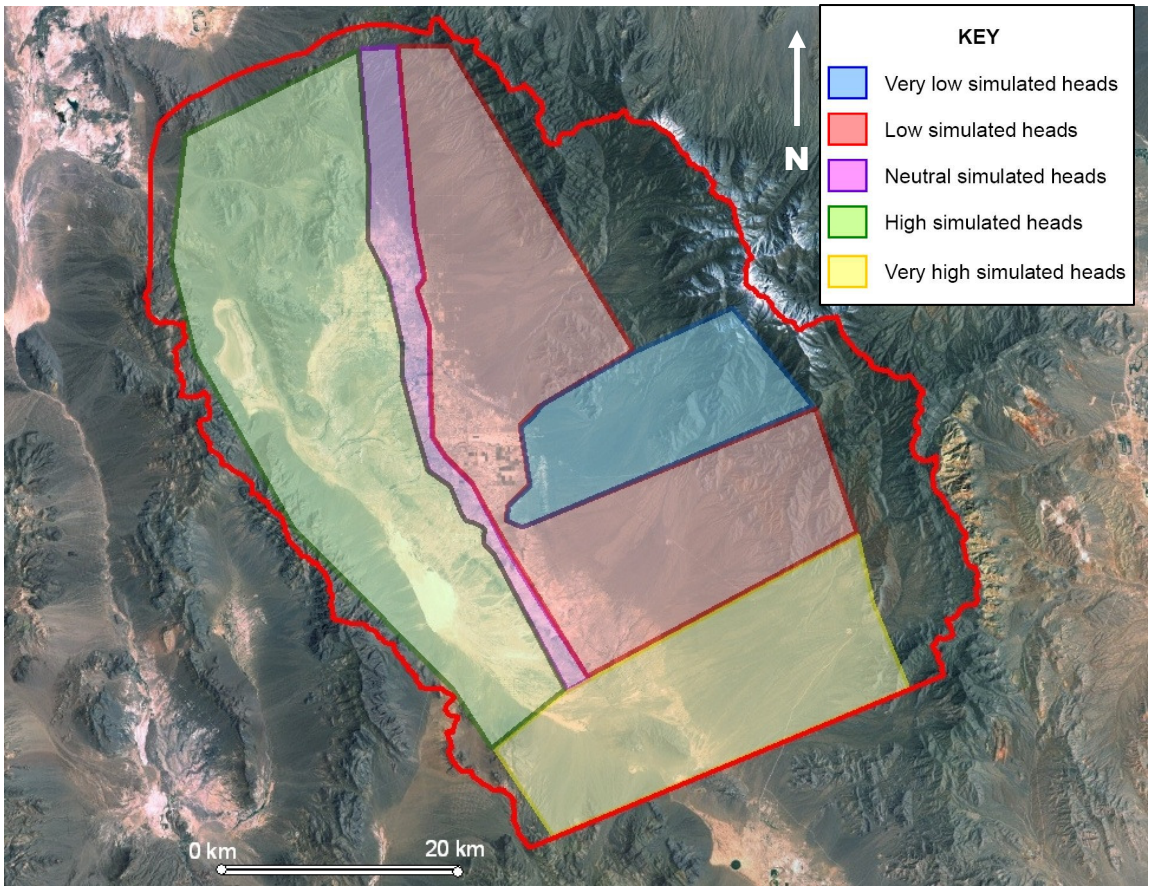

Figure 31. Example of one of the many basin fill *K* zone formations based on simulated head values. This configuration has five zones. Red and blue zones produce significantly lower simulated values than observed. Unfortunately, this basin fill delineation is also unable to suitably simulate the curvature of the mountain block.

After each basin fill delineation, calibration involved varying hydraulic conductivity, specific storage and specific yield both manually and using PEST. RMSE is then calculated for each zone to focus on the zonal match of simulated to observed head values. In several cases, specific wells repeatedly exhibit extremely inaccurate simulated head values, drastically affecting the overall RMSE. Monitoring wells: 67, 68, 72, 73 and 78 (located in the western part of the blue zone in Figure 31) consistently exhibit very low head measurements on the order of 50-70 meters below observed heads. These low simulated head measurements are attributed to the significant amount of groundwater

pumping for irrigation in the area which, coupled with low bedrock permeability values and thin amount of basin fill, lead to high simulated drawdown. The lowest RMSE using the delineated basin fill including all observation wells was ~34 m. Despite numerous approaches implementing various basin fill zone configurations, none of these configurations lead to significant improvement over a single basin fill unit with a *K* value of 1 m/d. This implies that hydraulic conductivity values in the basin fill are not the primary control on head values in the basin fill. This finding lead to the abandonment of the basin fill zone approach, and lead to delineation of the underlying carbonate aquifer as described below.

3.1.2 Carbonate Aquifer Delineation

The poor calibration resulting from the zonation of the basin fill indicates that the basin fill only exerts a secondary control on the water levels. The next calibration attempt involved determining the sensitivity of the LCA and LCCU on head levels. The LCCU is a low-permeability confining unit that transmits little flow. Consequently, calibration involved calibrating the LCA while holding the basin fill constant at a *K* of 1 m/d and the LCCU constant at 10^{-5} m/d. This approach did not dramatically improve the calibration (RMSE= ~ 33.8 m).

Two northwest-southwest trending transects of monitoring wells were constructed to better visualize the hydraulic gradient across the valley during calibration. Selection of the transects involved representing the northern and central portions of the valley and using monitoring wells with comparable sampling dates (Figure 32, Table 11). It was discovered during numerous manual calibration attempts, that the LCCU was responsible for the unrealistic flat gradient across the valley floor that produced the very high RMSE

values. The exclusion of this unit in subsequent model runs greatly improved the match between observed and simulated hydraulic gradients across the valley.

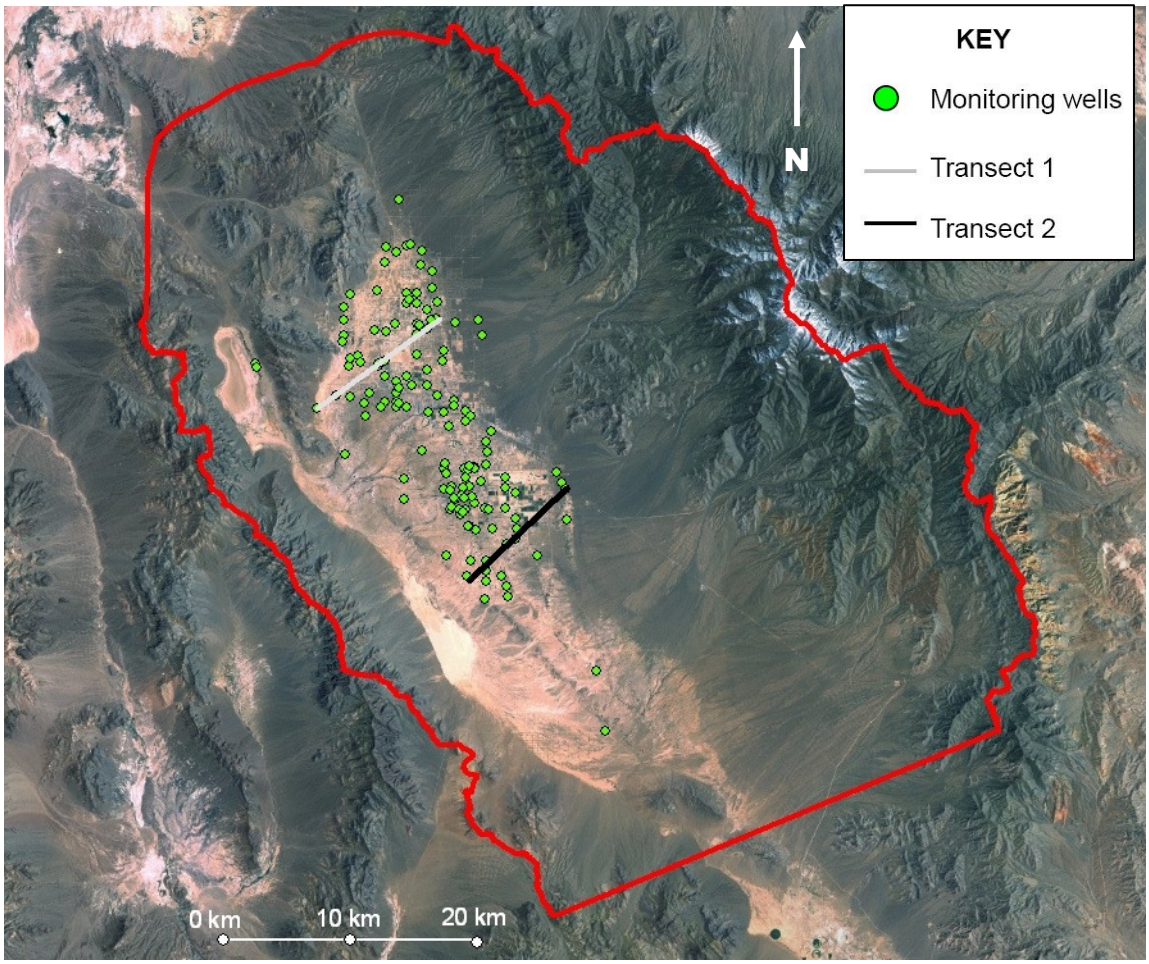

Figure 32. Locations of Transect 1 and 2; corresponding monitoring wells in Table 11.

Table 11. Monitoring wells in Transects 1 and 2. The order of wells transcends from the northeast point of the transect to the southwest point of the transect.

Transect 1 Well IDs	Transect 2 Well IDs
12	72
19	77
18	120
24	76
116	62
91	65
121	64
21	

The LCCU is a low-permeability confining unit that "cups" the carbonate aquifer at depth and precludes flow from exiting the southwestern portion of the model, save for a geologic window of LCA. The focused outflow through only a specific portion of the LCA is what is thought to have lead to the flat gradient. To remedy this, the LCCU was removed from the model by substituting all LCCU with LCA. Additionally, the XCU, located in the southwest corner of the model domain away from nearly all head observations, was found to exert little control over groundwater flow and was also removed from subsequent simulation.

Calibration to the transects also revealed that the model is unable to correctly simulate the hydraulic gradients across the valley with a single LCA unit. The LCA was further delineated into three zones: LCA1, LCA2, and LCA3. The zones represent portion of the carbonate aquifer in the surrounding mountain block, central portion of the valley, and west of the PVFZ, respectively (Figure 33). This delineation is necessary to simulate the mountain block fault and steep hydraulic gradient in the Spring Mountains. It also helps reproduce the flatter gradient in the basin fill and southwest portion of the valley that may result from PVFZ acting as a weak barrier to transverse flow.

Hydraulic parameters for each of the carbonate zones are varied to produce the most accurate simulated head measurements when utilizing both manual and automatic calibration methods. Calibration of the carbonate zones included focusing on *K* values assigned to LCA1, while holding *K* constant for LCA2 and LCA3. Once optimal *K* values for LCA1 are selected, LCA2 and LCA3 are calibrated together using PEST. RMSE is lowered and more accurate results are produced when LCA2 and LCA3 are calibrated by

PEST separately. This iterative process reduced error dramatically in the northern and central parts of the model. Errors are still present when trying to simulate head levels in at the mountain block/valley fill interface. The significant amount of pumping near the mountain block, combined with relatively thin basin fill and low hydraulic conductivity of the mountain block, causes a significant amount of drawdown in the region. The pumping, in conjunction with the natural curvature of hydraulic gradient in this region, causes the model to significantly underestimate head levels. These wells are highlighted in Figure 34.

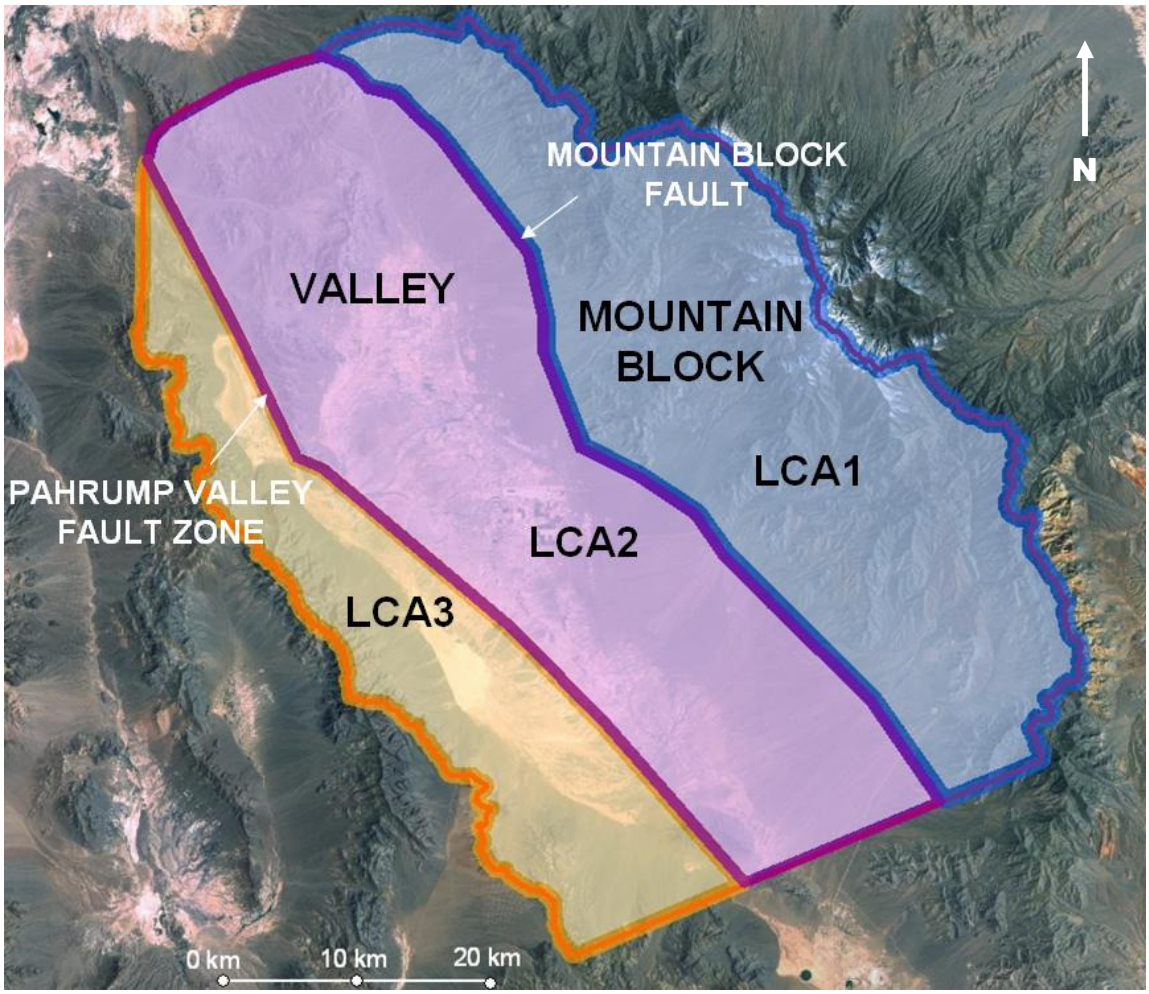

Figure 33. Carbonate zone delineation for calibration. The carbonate zones were divided to delineate the mountain block, basin fill and PVFZ. Note the locations of LCA1, LCA2 and LCA3.

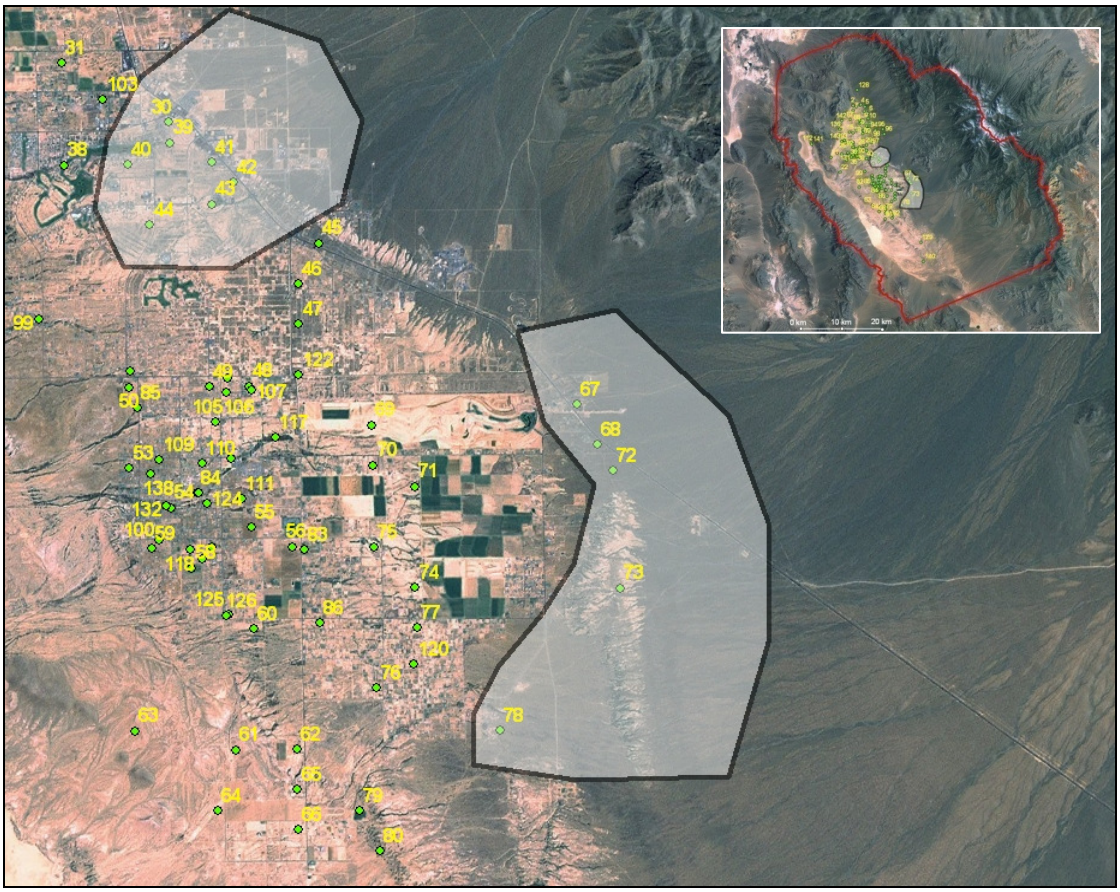

Figure 34. Regions at the mountain block and valley fill interface where the model significantly underestimates head levels. This is attributed to significant pumping in these areas and structural controls that the model cannot reproduce.

Profiles for Transects 1 and 2 were used to visualize changes to the hydraulic gradient during calibration. Final calibrated water levels along these transects are displayed in Figures 35 and 36. The first two wells in the Transect 1 profile have lower than observed head elevations (Figure 35). Transect 2 highlighted in Figure 36 shows a lower hydraulic gradient near the mountain block, but adequately represents wells within the valley.

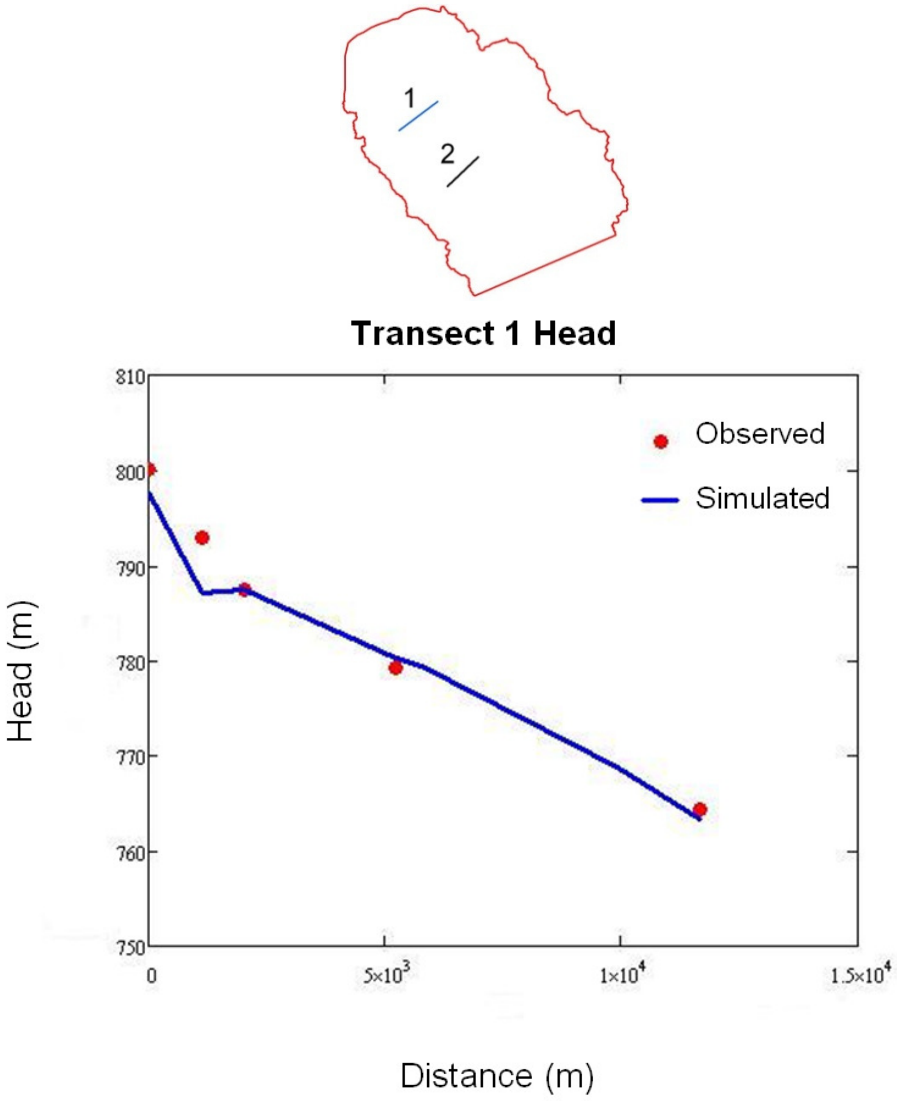

Figure 35. Transect 1 profile from the mountain block to west portion of the valley using the three LCA zones. Lower than observed values are found closest to the mountain block and more accurate groundwater elevations are found in the central part of the valley where most of the groundwater pumping occurs.

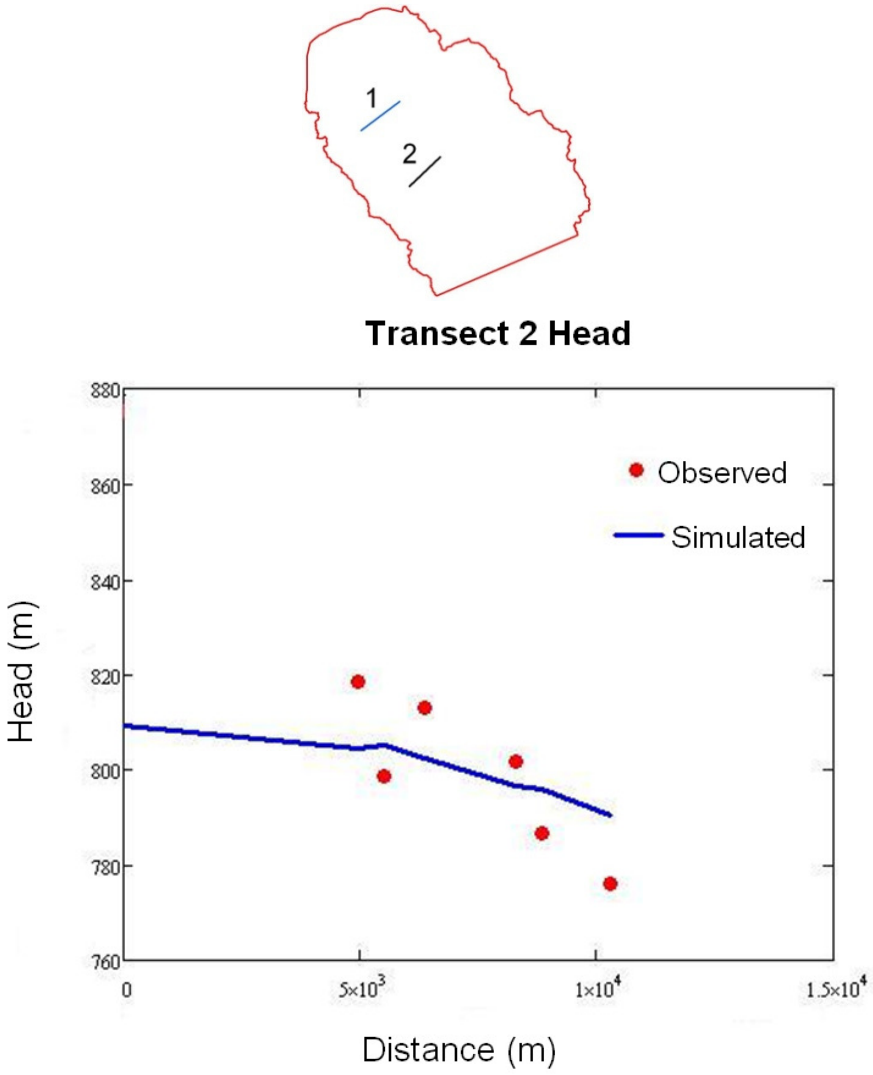

Figure 36. Transect 2 profile from the mountain block to west portion of the valley using the three LCA zones.

3.1.3 Incorporation of Depth Decay

Numerous properties of the Pahrump Valley model require the implementation of depth decay in hydraulic conductivity not only to simulate groundwater levels, but to also simulate realistic *K* values at the depth within the model domain. As shown in Figure 4 from Malmberg (1967), the naturally occurring recharge pathways from the Spring Mountains are curved. Consequently, the application of depth decay in *K* was required to adjust the hydraulic gradient to adequately form the curvature off of the mountain block.

Additionally, the large vertical extent of the domain along with the depth of the basin fill dictates lower basin *K* values at depth adjacent to the carbonates. The removal of the LCCU from the model domain requires depth decay in the deeper portions of the LCA to match the low permeability of the LCCU.

Initial depth decay parameter values are obtained from the IT Corporation (1996). Depth decay optimization was largely performed manually through the adjustment of the depth decay constants for each carbonate zone and the basin fill. The mountain block carbonate zones contain different depth decay constants to help simulate the curvature of groundwater flow off the mountain block. With the exception of the LCA3, the basin fill has the greatest depth decay constant causing a very steep decay in *K* with depth. This is attributed to the compaction and subsequent porosity loss of the unconsolidated basin fill with depth. The basin fill depth decay was simulated so that *K* could not drop below 10^{-3} m/d to represent accurate estimates of *K* in the basin fill. Contrastingly, the three carbonate zones were given smaller initial depth decay constants to simulate the missing LCCU that cups the LCA and basin fill. LCA1 is given a smaller depth decay constant to simulate the LCCU-t1 that was removed in the northern section of the valley and create the curved hydraulic gradient and raise water level elevations at the base of the mountain block. LCA2 is given the lowest constant to regulate the groundwater elevations at land surface while simulating the low permeability of the excluded LCCU at lower depths of the model. The LCA3 was given a higher depth decay constant to represent the large volume of LCCU in the region that is closer to land surface than other places in the basin. Depth decay proved to be highly effective as the RMSE of the model lowered considerably, and head profiles along the valley were more accurately simulated. Specific

examples of hydraulic conductivity versus depth from each carbonate zone are shown in Figure 37. Values found in Layer 10 show evidence that the carbonate *K* values are within range assigned to the LCCU, between 10^{-4} and 10^{-5} m/d.

Table 12. Calibrated depth decay constants for each carbonate zone and the basin fill.

Geologic Unit	Depth Decay Constant (λ)
LCA1	4.5E-04
LCA2	8.2E-04
LCA3	8.4E-03
Basin Fill	2.6E-03

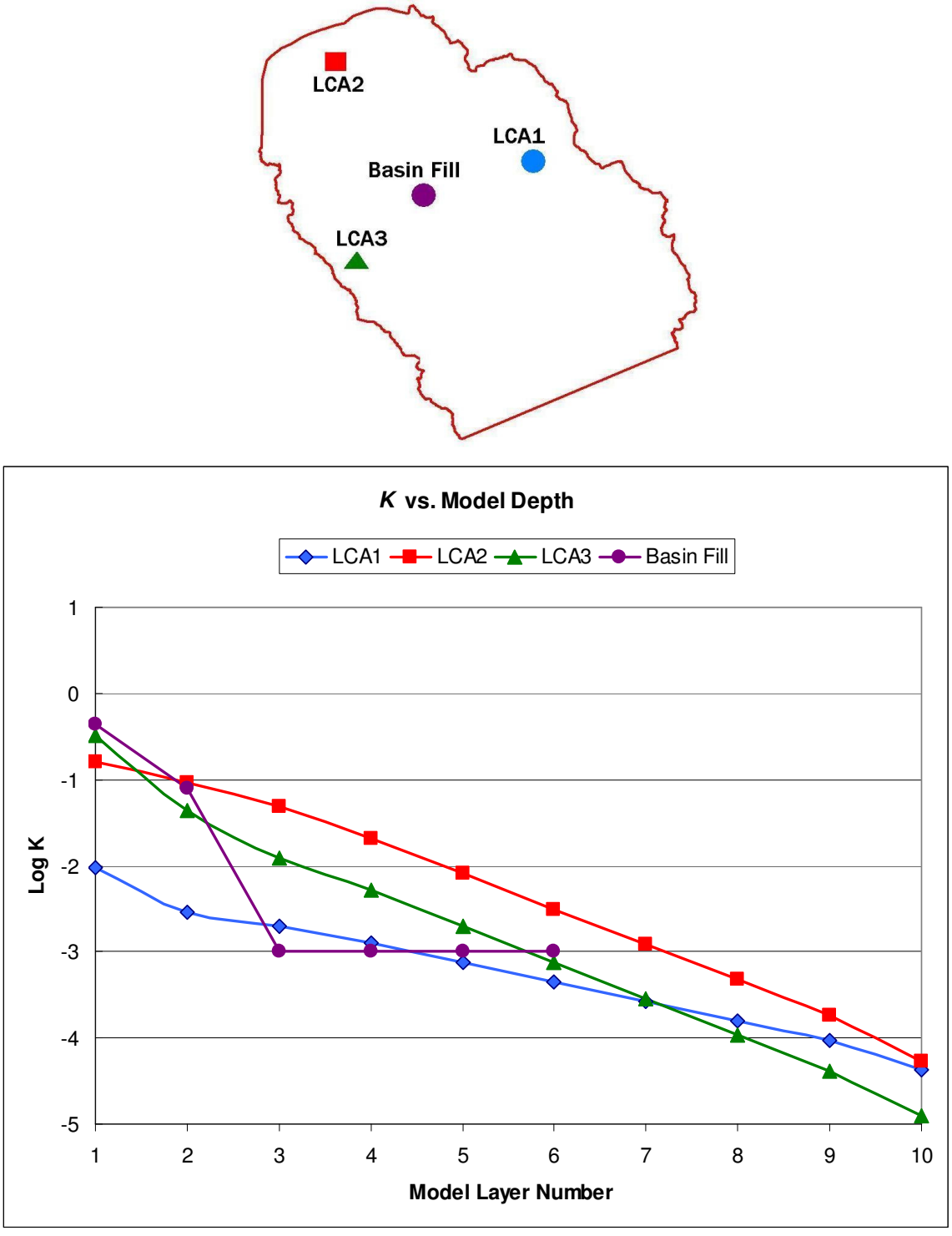

Figure 37. Example of hydraulic conductivity values versus depth for specific locations in the model. Note that the basin fill reaches the maximum threshold of 10^{-3} m/d to represent accurate estimates of *K*. The bottom of the model shows evidence that the carbonate *K* values are within range assigned to the LCCU between 10^{-4} and 10^{-5} m/d.

3.1.4 Recharge Optimization

Hydraulic conductivity and recharge are the most influential parameters in groundwater flow models of semi-arid basins. After calibration to hydraulic conductivity, the next step of the calibration process involves optimizing recharge contributions within each of the mountain block watersheds. PRISM, which estimates the amount of precipitation in a region based on precipitation-elevation regressions and uses a smoothing method to distribute isohyets to each grid cell (Epstein, 2004), was used to compute the amount of precipitation in each mountain block watershed. These volumes were then correlated to recharge using the empirically-derived Nichols recharge coefficients.

The contributions of recharge for each watershed, expressed as a percentage, were calibrated using both manual and automatic calibration methods. The initial percentages of these watershed contribution metrics were first given a range for Watersheds 1, 2 and 3 for automatic calibration in PEST. Watersheds 4 and 5 were then assigned the remaining recharge as the difference between the applied recharge of 87,806 m^3/yr (26,000 ac-ft/yr) and the sum of applied recharge for Watersheds 1, 2 and 3 (Figure 37). Recharge values were shifted significantly. Watershed 1 was optimized with a recharge of 0% while Watershed 2 was increased to 50% and Watershed 3 shifted to 12.5%. These calibration results may be attributed to the presence of the low permeability LCCU-t1 in the northern portion of the valley that may restrict recharge in Watershed 1.

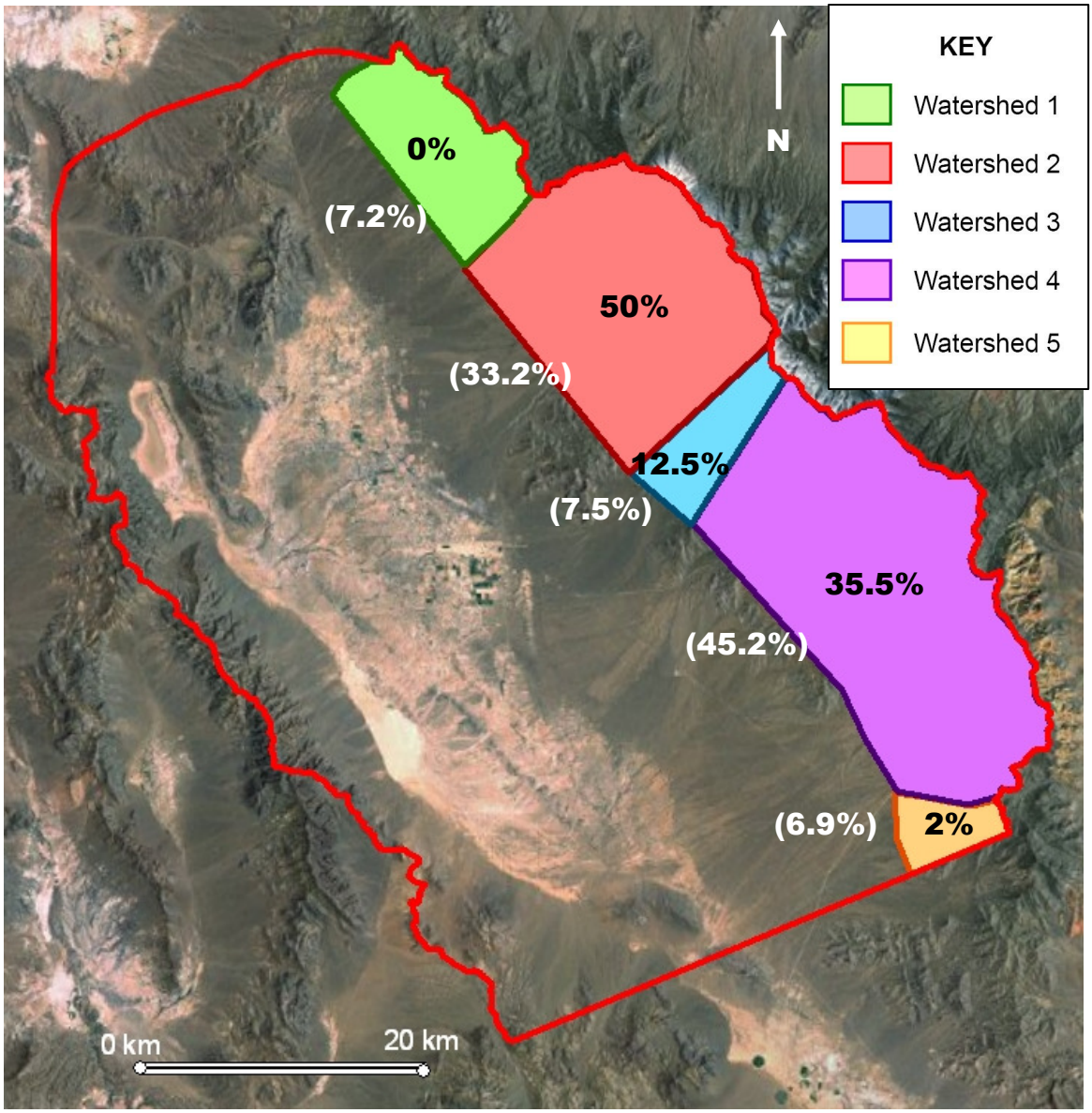

Figure 38. Delineated watersheds and the percentages of total recharge allocated to each watershed. Calibrated recharge percentages are shown in black, while original recharge percentages are shown in white. Note the dramatic increase in recharge percentages in Watersheds 1 and 2 to account for the consistently lower than observed groundwater elevations at the base of the mountain block. Recharge was eliminated from Watershed 1 because it is the location of LCCU-t1.

3.1.5 Pilot Point Calibration

To optimize *K* in the top layer of the model, 82 pilot points are created from cells with monitoring wells. This method involves using PEST to calibrate *K* for each of the 82 wells and interpret between areas of unknown data using a log-inverse distance weighting

algorithm. This complex process requires running parallel PEST with 20 processors to inversely provide a heterogeneity structure to the basin fill.

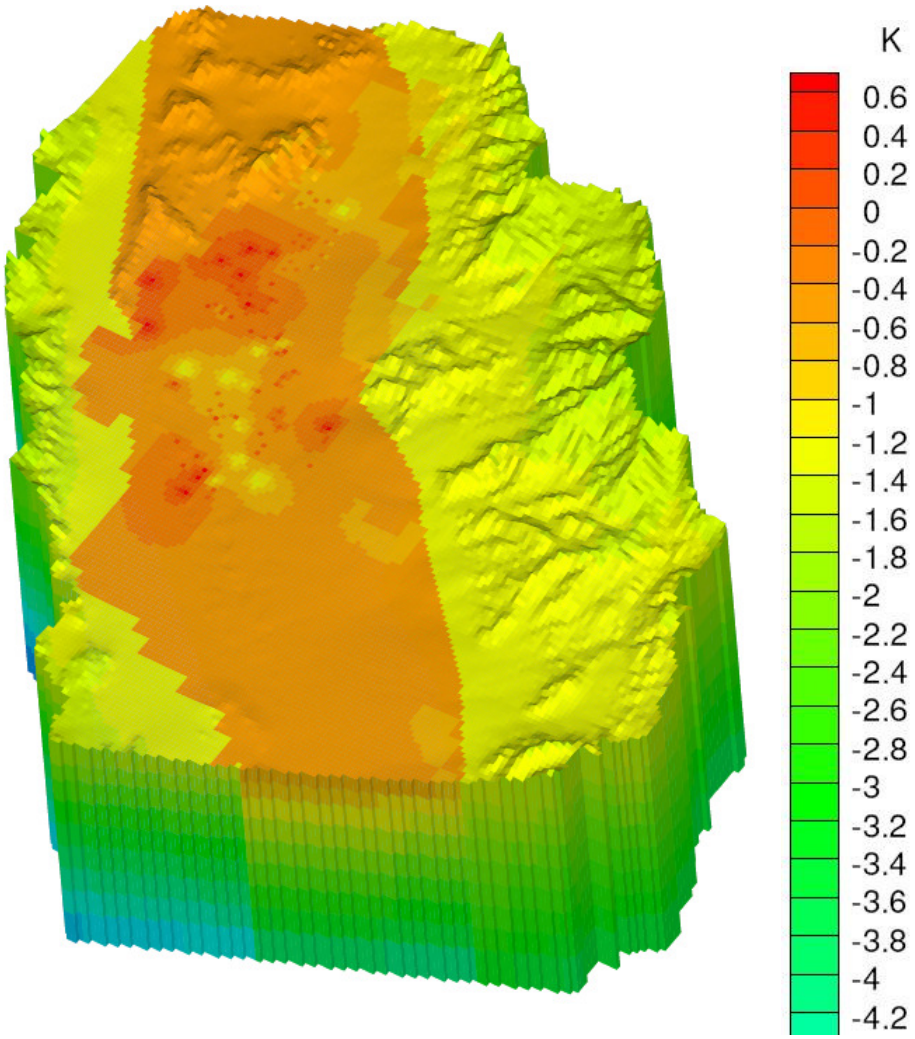

Figure 39. Simulation of heterogeneity of *K*(m/s) using the pilot point method. This figure also demonstrates depth decay as the *K* gradually lowers with depth to simulate the less permeable LCCU and XCU.

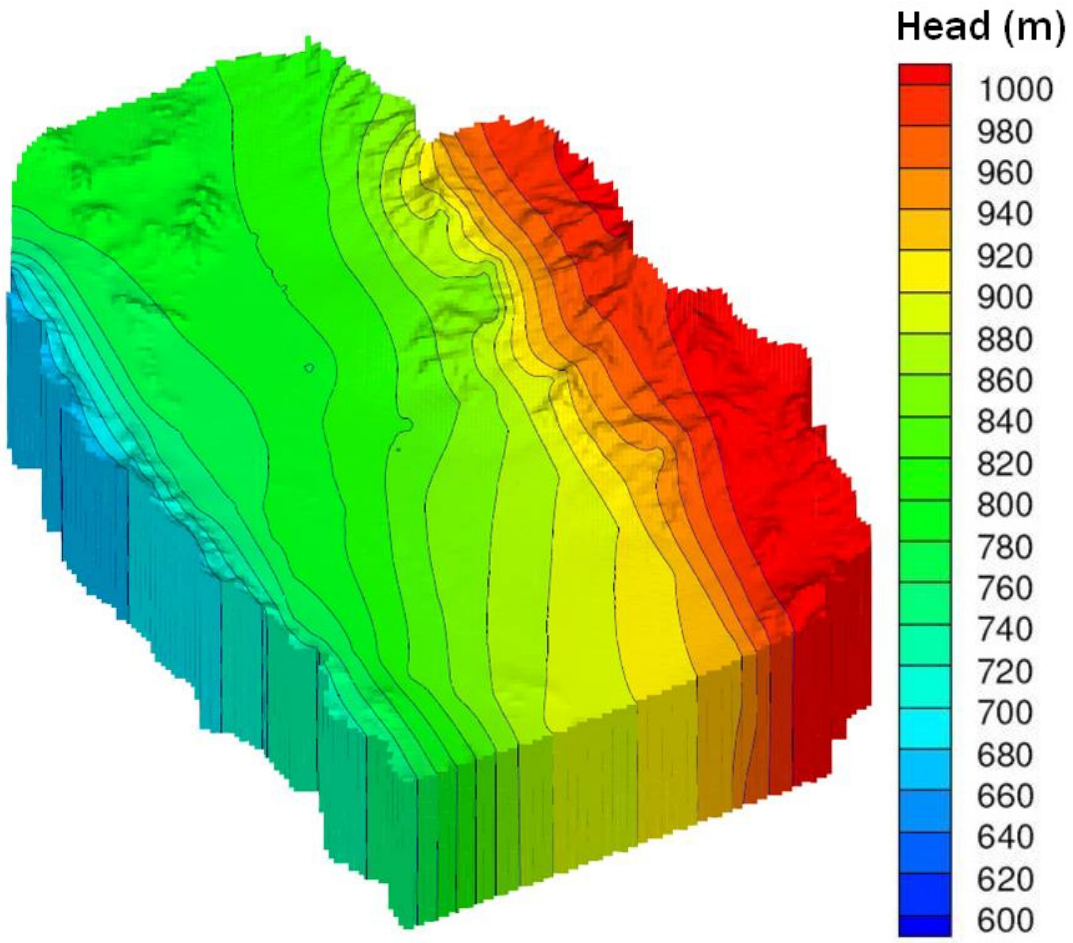

Figure 40. Head field in meters from 1968, the year with the most groundwater pumping. Note that the model simulates the southwesterly groundwater flow trend.

3.2 Calibrated Parameters and Volumetric Budget

Calibrating the hydraulic parameters to the carbonate zones, optimizing recharge, incorporating depth decay and using pilot point calibration, provides final optimized parameters (Table 13).

Table 13. Calibrated carbonate zone parameters with the homogeneous basin fill.

Geologic Unit	K_{ls} (m/d)	Depth Decay Constant (λ)	Specific Storage (1/m)	Specific Yield
LCA1	7.4E-02	4.5E-04	1.0E-04	0.05
LCA2	5.2E-01	8.2E-04	1.0E-04	0.05
LCA3	6.2E-02	8.4E-03	1.0E-04	0.05
Basin Fill	1.0	2.6E-03	1.0E-04	0.25

The transient model was run from 1913-2003. Table 14 displays the simulated annual water budget for 2003 (stress period 56). Recharge wells simulate the recharge from precipitation from the Spring Mountains. Discharge wells include domestic, irrigation, public, community and municipal wells. Annual recharge, pumpage, evapotranspiration and constant head output are found in Appendix C.

Table 14. Simulated water budget for 1968, the year with the most groundwater pumping.

VOLUMETRIC BUDGET FOR TRANSIENT MODEL, STRESS PERIOD 56 (m^3/d)			
IN:		**OUT:**	
STORAGE	152,250	STORAGE	5,237
CONSTANT HEAD	106	CONSTANT HEAD	34,458
WELLS	87,864	WELLS	158,453
EVAPOTRANSPIRATION	0	EVAPOTRANSPIRATION	42,243
TOTAL IN	240,221	**TOTAL OUT**	240,389
IN-OUT	-168		
PERCENT DISCREPANCY	-0.07		

3.3 Accuracy and Precision of Pahrump Valley Model

The final RMSE when all wells are incorporated is16.5 meters. However, when problem wells are excluded (large red dots in Figure 41), the RMSE drops to 9.7 meters. Uncertainty in pumpage within the model is not completely understood. Some cells

containing monitoring wells assign effective pumping rates to the center of the cell (node) for three or more pumping wells. As a result, some cells may have much greater drawdown than observed and overestimate pumping in the center of the cell. Contrastingly, some areas of the model may not incorporate pumping where it actually occurs (missed pumping). However, the lack of systematic drawdown bias over time indicates that storage parameters in the model are appropriate. Final monitoring well calibration shows that the most inaccurate wells are located closest to the mountain block as the model has trouble accurately simulating the curvature of groundwater flow off the mountain block. However, the model is able to adequately simulate head elevations in areas with significant pumping within the valley floor where most of the population resides.

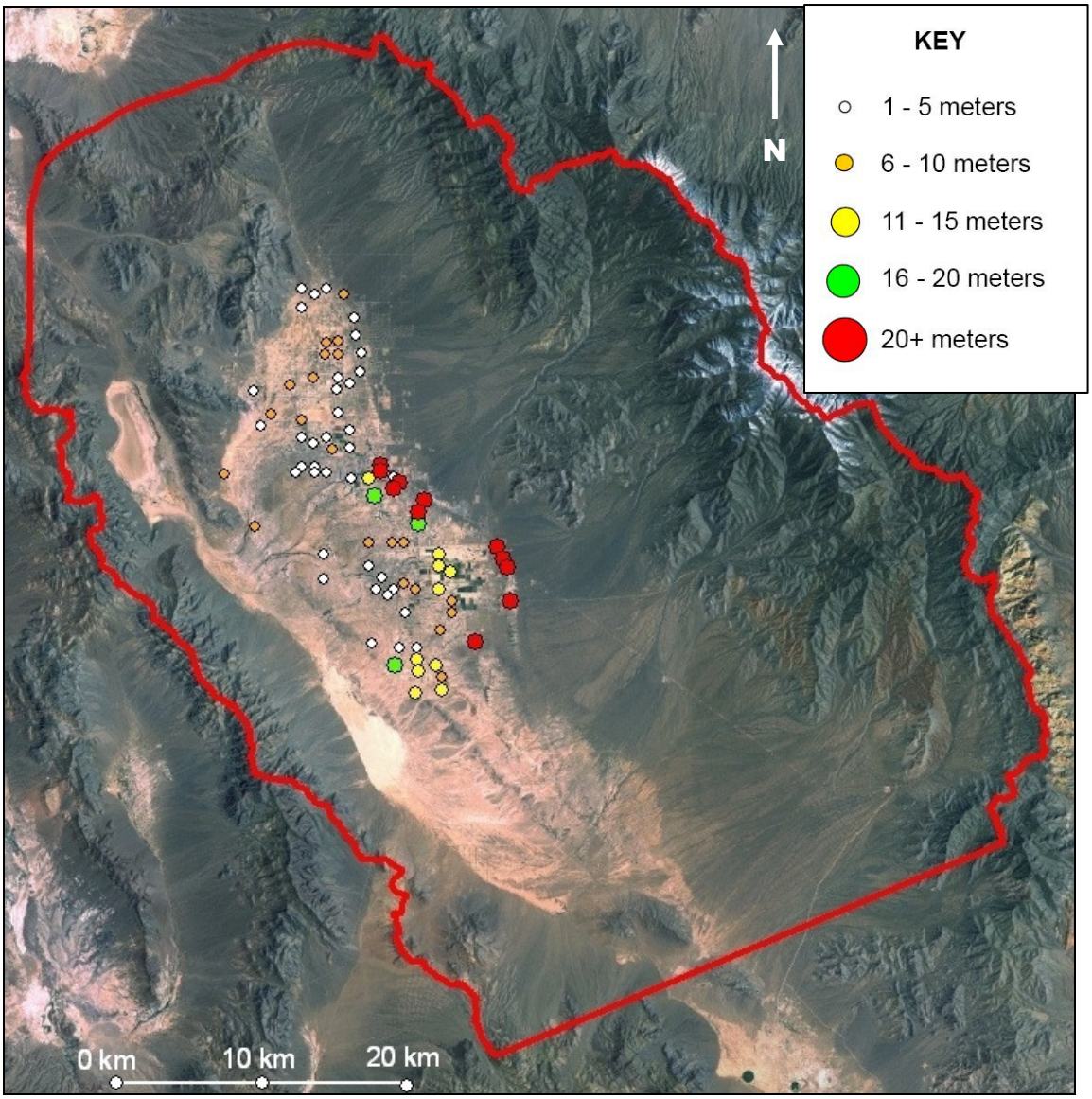

Figure 41. Monitoring well calibration using a graduated legend. The dot size is proportional to the accuracy of simulated head elevations versus observed head elevations. Note that the most inaccurate wells are closest to the mountain block.

Below, specific monitoring well data showing simulated versus observed heads are displayed to demonstrate the lack of systematic drawdown bias throughout the valley. The first set of graphs in Figure 42 demonstrate some accurate water level elevations simulated by the model. Figure 43 displays examples where inaccurate head elevations are produced by the model, but drawdown is adequately modeled. Lastly, Figure 44

shows wells where neither head levels nor drawdown measurements are simulated adequately. These cases may be regions of missed pumping or overestimated pumping and had significant effects on the overall RMSE of the model. Graph s of drawdown for two long-term monitoring wells (Well 6 and 12) are found in Figure 45. Both of these wells are located next to the alluvial fan show signs of recovery subsequent to 1980.

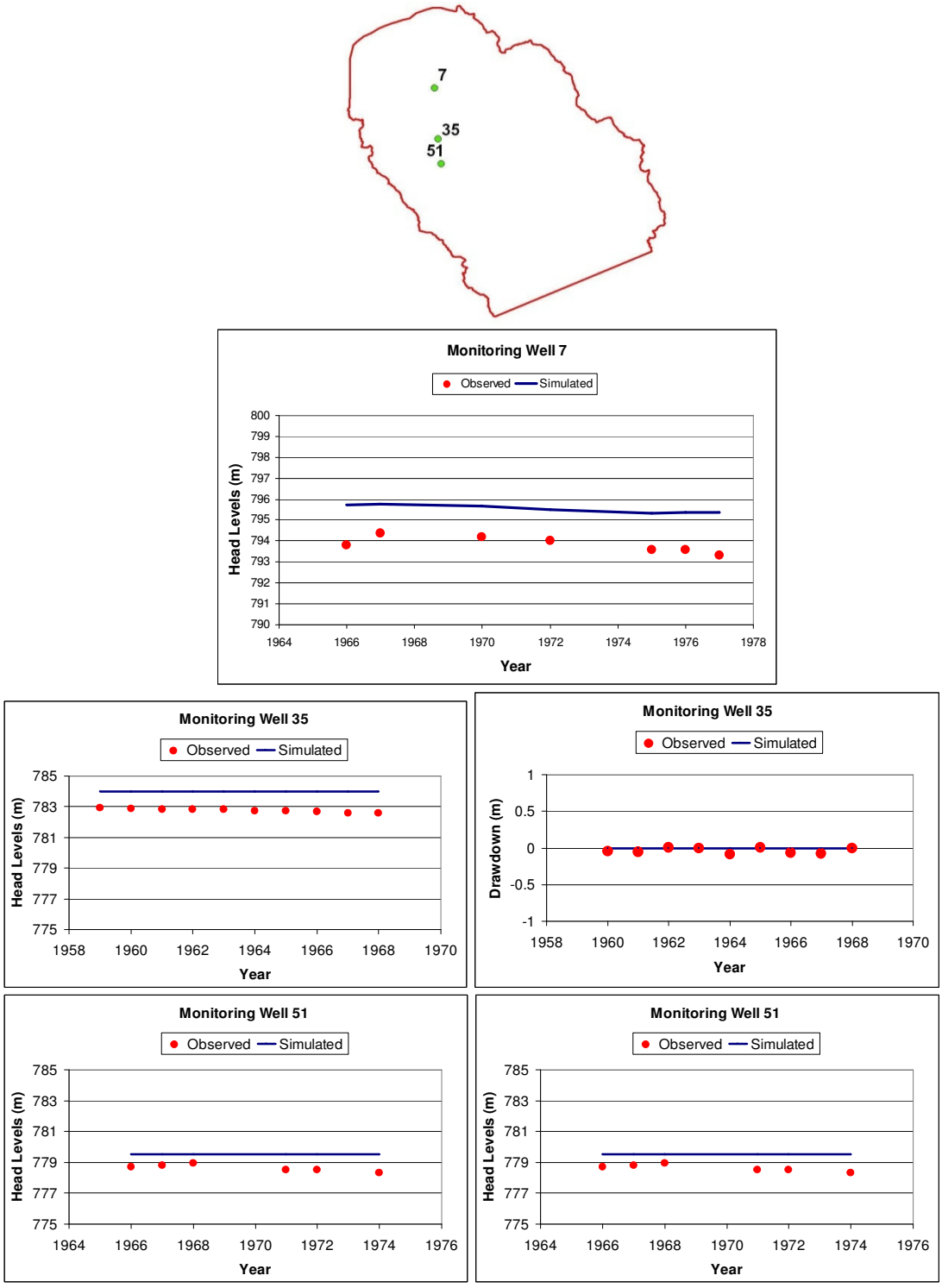

Figure 42. Graphs of simulated versus observed head elevations and drawdown measurements for monitoring wells 7, 35 and 51. In these cases, accurate simulated head values are produced along with adequately modeled drawdown values.

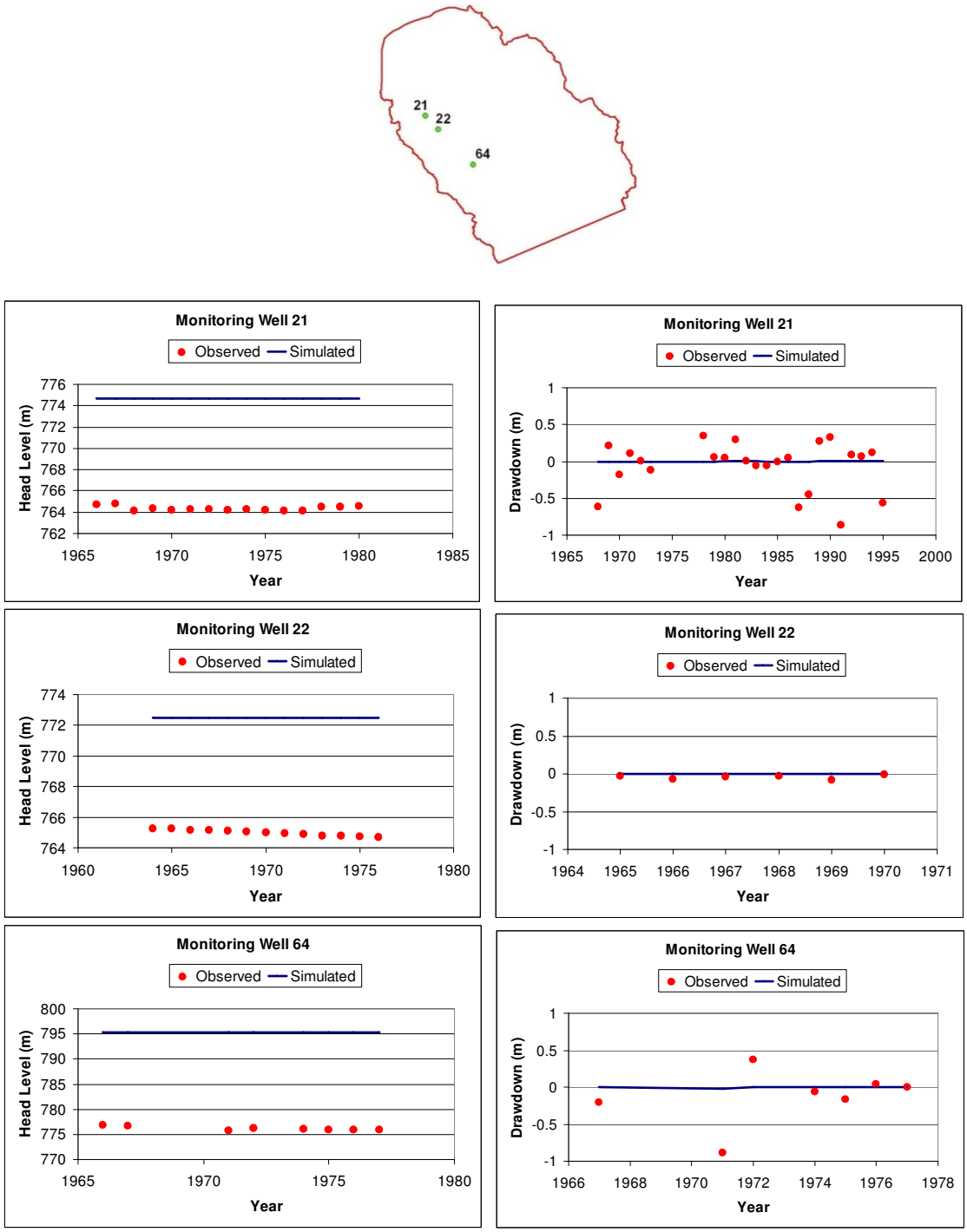

Figure 43. Graphs display monitoring wells where inaccurate head levels are produced (left side) but the model adequately simulates drawdown (right side). Wells 21 and 64 depict errors in the pumpage schedule with periods of both under-and over-simulation of pumpage.

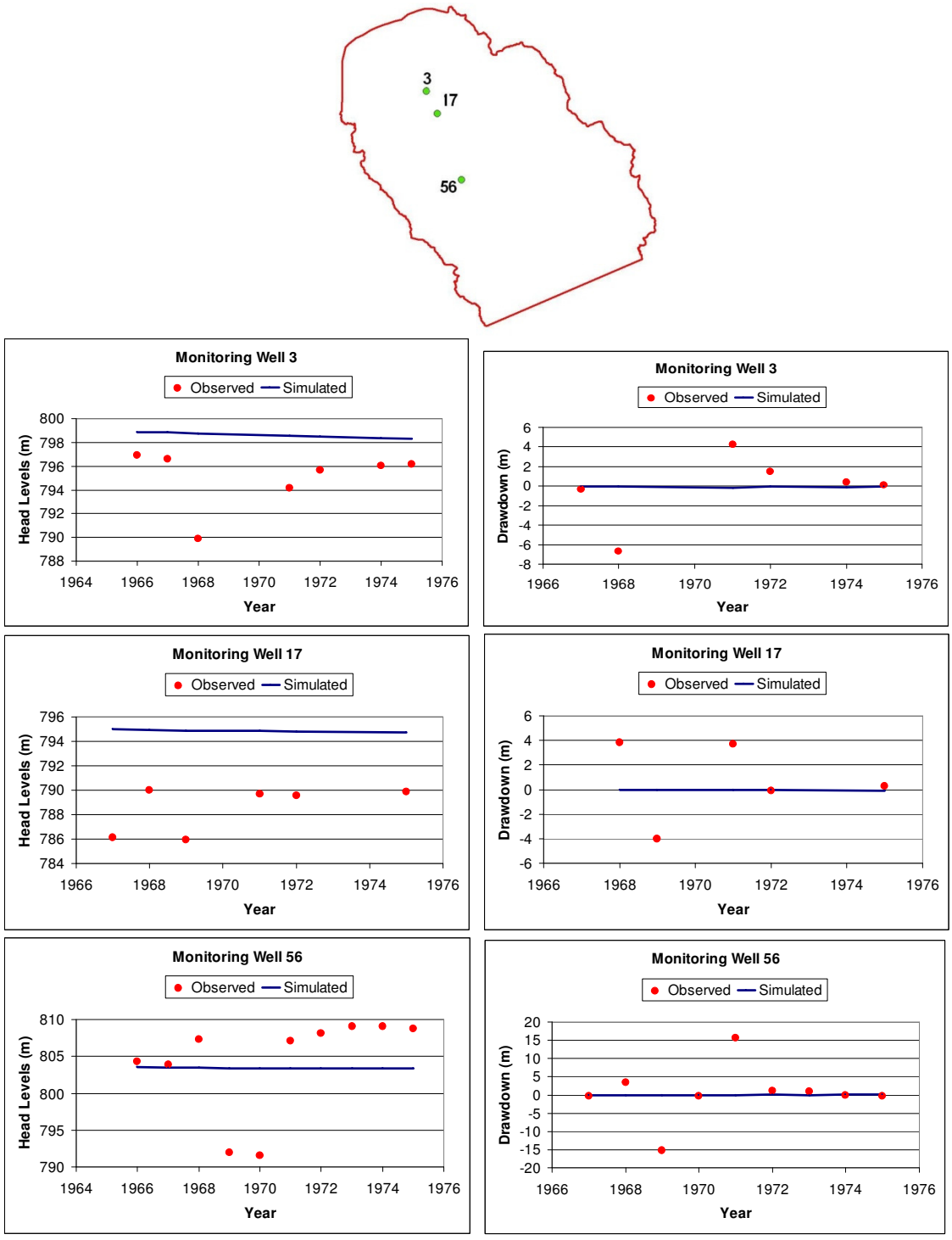

Figure 44. Graphs of specific wells where there are potential applied pumpage errors. In these cases, too much or too little pumpage may be applied to cells because some locations of wells are unknown, causing the pumping to be spatially distributed incorrectly. In these cases, the model does not produce suitable simulated head or drawdown values.

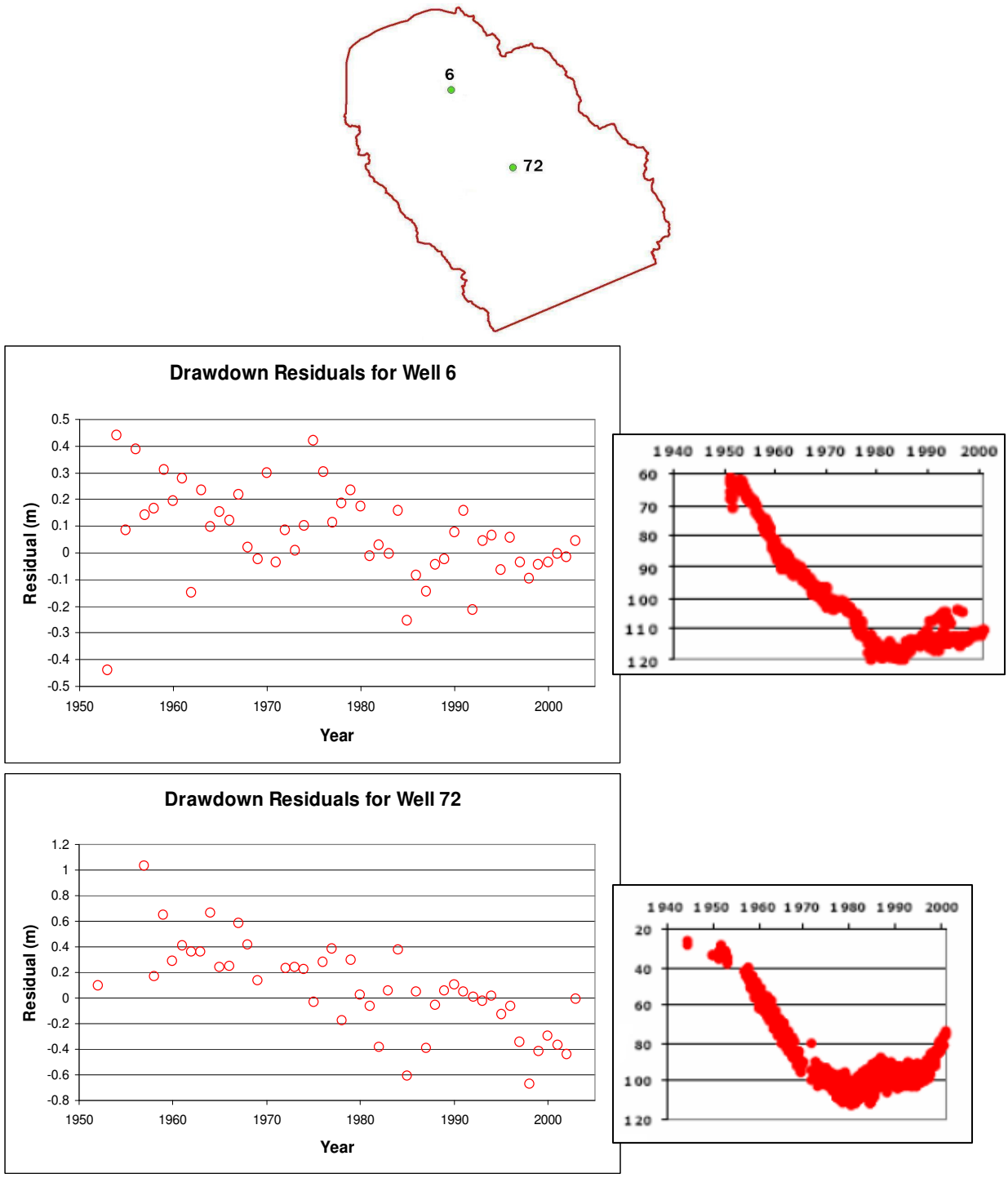

Figure 45. Graphs of two long-term monitoring wells that were highlighted in Figure 2 (Buqo, 2006). Simulated drawdown residuals for the two wells are shown in the graphs on the left. Hydrographs from Buqo, 2006 for the wells are shown on the right. Graphs on the right show depth to groundwater in feet. Note that both wells are located close to the alluvial fan and show signs of recovery after 1980.

Final head and drawdown residuals show the model adequately simulates head and is precise at simulating drawdown (Figures 46 and 47). General head trends reveal that the model generally underestimates head elevations located at the valley fill/mountain block interface (Figures 34, 41 and 46(a)) as previously discussed; the model produces unbiased head measurements for the rest of the valley (Figures 39 and 43b). A relative error of error of 5% is calculated based on the RMSE of 9.7 meters over the 182 meter head drop across the valley.

(a)

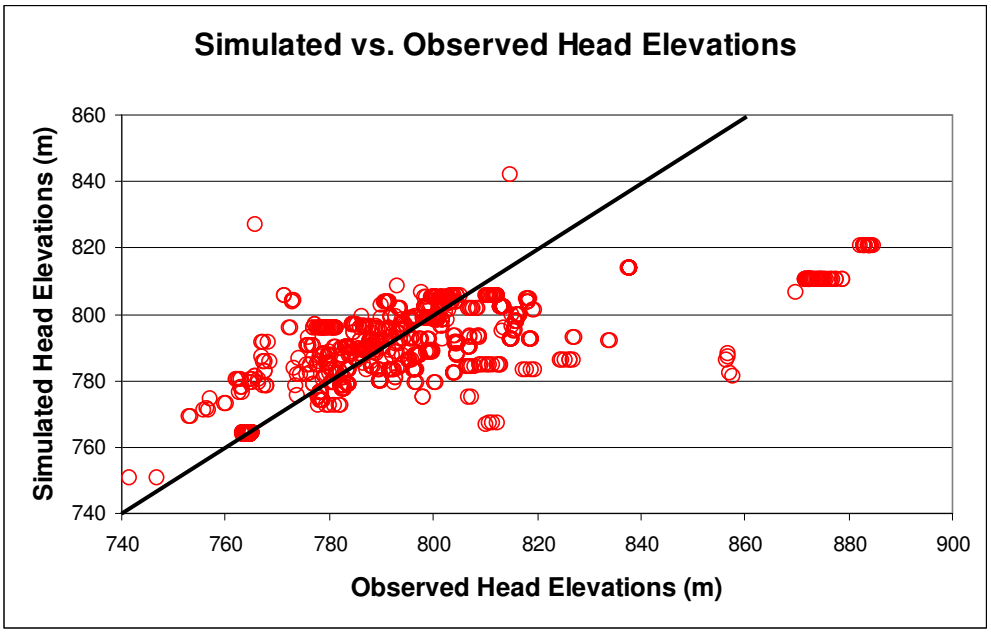

(b)

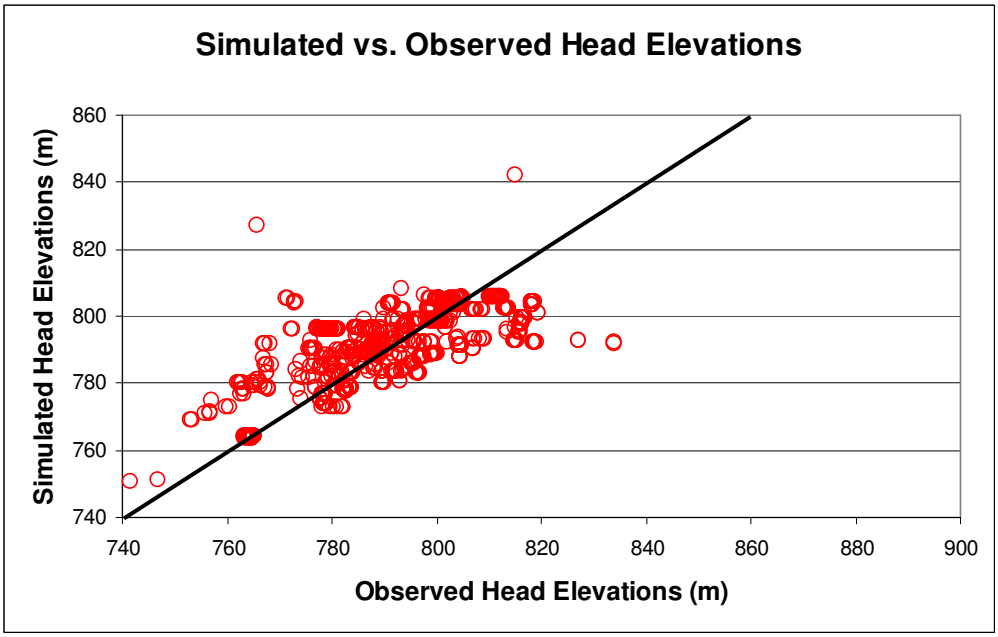

Figure 46. (a) Head residuals incorporating all monitoring well data. (b) Head residuals with the exclusion of the problematic observations near the mountain block (highlighted in red in Figure 41). The model bias is symmetric around 0 meters.

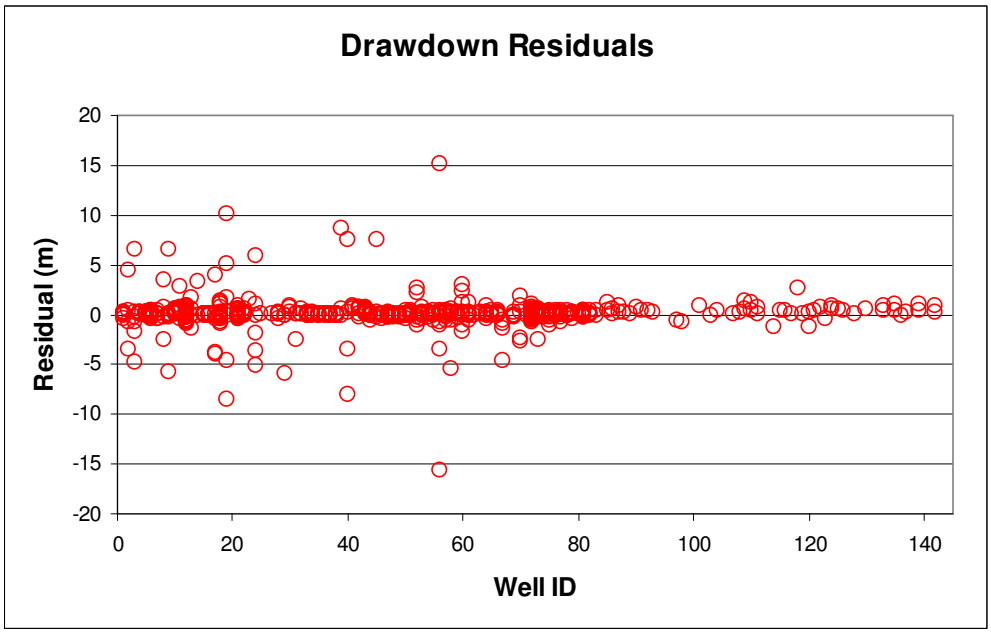

Figure 47. The model is more precise in terms of drawdown than it is accurate in terms of water level elevations. Very large drawdown residuals are attributed to errors associated with the pumpage database.

4.0 CONCLUSIONS

The objective of this thesis was to develop a numerical groundwater flow model of Pahrump Valley, Nevada in MODFLOW, and calibrate the model to observed head measurements. The complexity of groundwater pumping in Pahrump Valley was temporally and spatially represented through pumpage from over 11,000 wells. The final product will be used as a tool by Nye County to examine future water management scenarios.

The complex geology and groundwater pumping history of Pahrump Valley caused model calibration to be an extremely strenuous process. Influences of the hydrogeologic units within the model domain were assessed and it was demonstrated that a hydrogeologic framework consisting of fewer HGUs produced more accurate simulated head elevations. The incorporation of depth decay was successful in producing more

accurate simulated heads, while also lowering hydraulic conductivity at depth representative of the excluded LCCU hydrogeologic unit.

The model reproduces the dominant southwest groundwater flow direction towards Tecopa and Shoshone. The final overall RMSE is equal to 9.7 meters, excluding problem wells at the mountain block and valley fill interface. This is an acceptable value considering the 182 meter head drop across the valley and the significant errors associated with pumpage complexity and calculations produced by a linear solver. The relative error of error of 5% is calculated based on the RMSE of 9.7 meters over the 182 meter head drop across the valley. Though the model does not consistently produce accurate head levels over the entire domain, it adequately simulates drawdown.

5.0 MODEL LIMITATIONS

This groundwater flow model is unique because it incorporates a vast amount of monitoring well data spanning several decades, uncommon in many groundwater flow models. However, modeling, of any kind, integrates an undeniable amount of uncertainty. One particular model limitation is that the model is confined. Observation points 81, 112, 140 and 141 (Figure 48) indicate that the simulated head is above land surface in a few locations where the land surface elevation is the lowest in the valley. This is the result of a confined solution where a linear head gradient is propagated across the valley regardless of the configuration of the land surface. An unconfined solution would better represent the natural curvature of the land surface and subsequent water table configuration. The unconfined version of this model did not consistently converge during calibration attempts due to the large topography contrast and associated water

table curvature across the valley and mountain block. Despite the lack of convergence, an unconfined model is desired for Pahrump Valley due to the large amount of pumpage in this hydrologic basin, and the better ability of unconfined models in simulating drawdown.

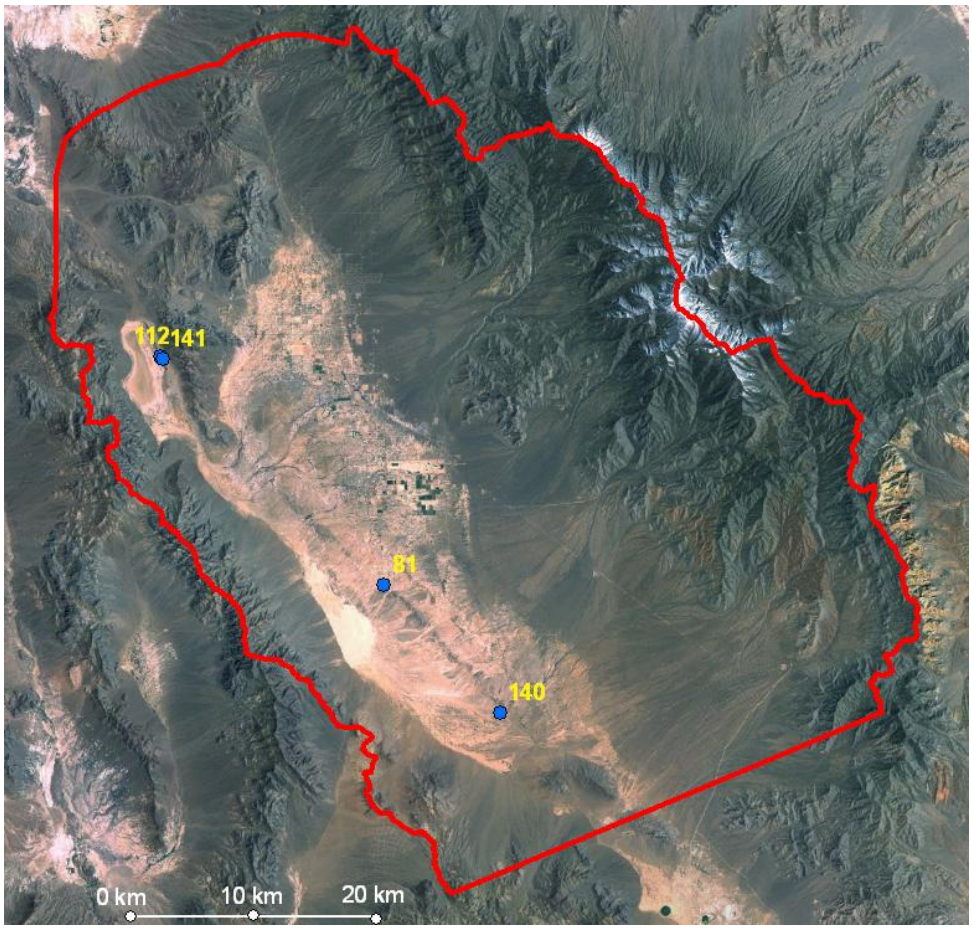

Figure 48. Locations of wells with simulated heads above land surface. This is the consequence of a confined solution where the linear head is propagated across the valley, regardless of the elevation of land surface. The four wells are located in areas with the lowest land surface elevations within the valley and are in areas with minimal pumping.

Although the model includes data from 143 monitoring wells, there are still large gaps in the records that affected model construction and calibration. Most of the monitoring well data is from 1966-1976 and 2000-2003. Only six wells provide data

spanning several decades and the majority of all wells include less than five observations. Unknown locations and perforation measurements from monitoring wells limited the accuracy of the data and required a thicker vertical cell size of 300 meters in the top layer. The lack of more recent water levels hinders the ability of the model to accurately reproduce water levels in more recent time periods.

Additionally, many monitoring wells are near areas with significant pumping; this caused some inaccurate simulated head measurements. Nodes in the center of the cell in MODFLOW are the location of all pumping. When a cell contains multiple wells, all pumping is extracted from the node and not spatially distributed within the cell. Furthermore, locations for some of the irrigation, public and community wells were unavailable, and pumping is spatially distributed to wells with known locations. As a result, some cells most likely over simulate groundwater pumping.

Observed precipitation varies from year to year, providing regions with varying recharges rates annually. However, even the most updated PRISM data averages precipitation of a region spanning several decades. To simulate recharge from the Spring Mountains, flux zones were implemented on the northeastern portion of the basin by injection wells. There is natural recharge variability around the constant applied recharge value for each stress period. Seasonal changes in precipitation were not accounted for as injection wells input water into the model at a constant rate. Upon investigation of annual precipitation measurements, it was revealed that 2002 was a particularly dry year in Pahrump Valley (Figure 49). This dry trend may also influence the simulated heads in 2003, if most of the precipitation occurred during November and December of that year after the monitoring well data measurements. This trend plays a major influence on

calibrating the model because 12% of the monitoring well data is from 2002 and 2003 and is given a weight three times higher than data prior to 1980.

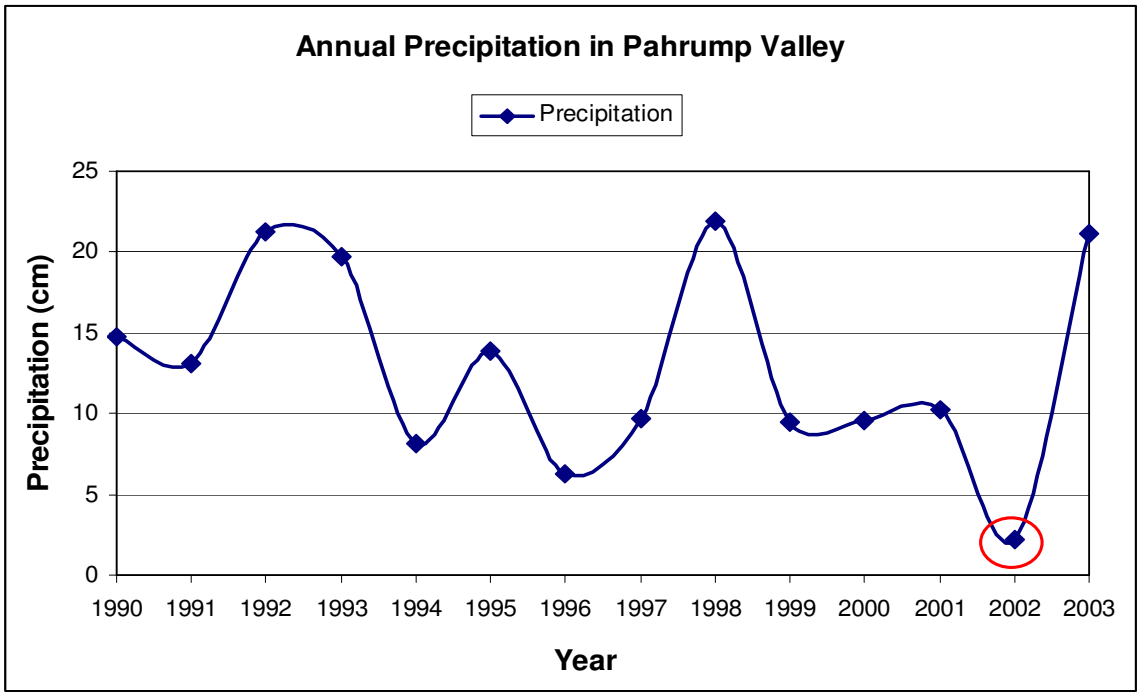

Figure 49. Annual precipitation in Pahrump Valley (cm) from 1990 to 2003. The year 2002 was a particularly dry year with only 2.25 cm of precipitation.

6.0 RECOMMENDATIONS FOR FUTURE WORK

To improve the accuracy of the model, particularly by simulating the curvature of groundwater flow off the mountain block, would require the use of a non-linear solver and converting the model to unconfined mode. The use of either MODFLOW-SURFACT or the new USGS Newton-Raphson solver may potentially increases model convergence and provide more accurate simulated head elevations.

Modeling the intricacy of the groundwater system in Pahrump Valley requires significant long-term monitoring well data throughout the basin for calibration. Most of the monitoring well data occurs from 1966-1976 and from 2000-2003. Since there are only six long-term monitoring wells, it is essential that the new wells drilled in 2000

continue to be well-maintained and monitored to accrue more long-term data. Additionally, the numerical framework provided by this study could be used in studies involving the land subsidence and optimization of well placement and extraction rates within Pahrump Valley.

Currently, perforation measurements for many of the older monitoring wells are not available or are inconsistent and could be updated. Monitoring wells could also be drilled throughout the California side of the basin to help further investigate the impacts of the PVFZ on groundwater flow, particularly in the southern regions. This additional data could improve the uncertainty in the hydraulic function of the PVFZ and increase predictive capabilities of the model. Lastly, little information is known about the extinction depth of mesquite, and this issue will become more important if the water levels continue to drop in Pahrump due to pumpage overdrafts.

7.0 REFERENCES

Allen, R.G., Pereira, L.S., Raes, D. and Smith, M., 1998. Crop evapotranspiration – Guidelines for computing crop water requirements. Chapter 6. *FAO Irrigation and Drainage Paper 56.*

Anderman E. R. and LeFrancois, M., 2003. MODFLOW-2000, the U.S. Geological Survey Modular Ground-Water Model – Documentation of Hufprint, and Evaluation Program for the Hydrogeologic-Unit Flow (HUF) Package.

Anderson, M.P. and Woessner, W.W., 2002. Applied Groundwater Modeling: Simulation of Flow and Advective Transport. Academic Press. 220p.

Beard T., Brooks, K., DeNovia, N., Ewing, J., Farnham, I., Fryer, W., Jones, T., McCord, J., Pickens, J. and Rose, J., 2004. Phase II Hydrologic Data for the Groundwater Flow and Contaminant Transport Model of Correction Action Unit 98: Frenchman Flat, Nye County, Nevada. *U.S Department of Energy – Contract No. DE- AC52-03NA99205.*

Belcher, W.R., Bedinger, M.S., Blainely, J.B., D'Agnese, F.A., Faunt, C.C., Harrill, J.R., Laczniak, R.J., O'Brien, G.M., Potter, C.J., Putnam, H.M., San Juan, C.A., and Sweetkind, D.J., 2004. Death Valley Regional Ground-Water Flow System, Nevada and California- Hydrogeologic Framework and Transient Ground-Water Flow Model. *U.S. Geological Survey Open-File-Report 2004-5205.*

Blakely, R.J., Morin, R.L., McKee, E.H., Schmidt, K.M., Langenheim, V.E., and Dixon, G.L., 1998. Three-dimensional model of pre-Cenozoic basement beneath Amargosa Desert and Pahrump Valley, California and Nevada — Implications for tectonic evolution and water resources: *U.S. Geological Survey Open-File-Report 98-496, 29.*

Buqo, T., 2006. Long-Term Water Level Trends in Pahrump Valley. Nye County Nuclear Waste Repository Office. Devil's Hole Workshop, May 2007.

Buqo, T., 2004. Nye County Water Resources Plan. Department of Natural Resources and Federal Facilities.

Daly, C., Taylor, G. and Gibson, W., 1997. The PRISM approach to mapping precipitation and temperature. In 10th Conference on Applied Climatology, Reno, Nevada. p.10-12.

D'Agnese, G. A., O'Brien, G.M., Faunt, C.C., Belcher, W.R., and San Huan, C., 2002. A three-dimensional numerical model of prepumping conditions in Death Valley regional ground-water flow system, Nevada and California: *U.S. Geological Survey Open-File-Report 02-4102.* 114 p.

DeMeo,G.A., Laczniak, R.J., Boyd, R.A., Smith, J.L., and Nylund, W.E., 2003. Estimated Ground-Water Discharge by Evapotranspiration from Death Valley, California, 1997-2001. *U.S. Geological Survey Open-File-Report 03-4254.*

Doherty, R.E., 2004. Model-Independent Parameter Estimation, PEST. Watermark Numerical Computing.

Felling, R., 2009. Personnel communication.

Harbaugh, A.W., Banta, E.R., Hill, M.C. and McDonald, M.G., 2000. MODFLOW-2000: The U.S. Geological Survey Modular Groundwater Model - User Guide to Modularization Concepts and Ground-Water Flow Processes. *U.S. Geological Survey Open File Report 00-92,* 221 p.

Harrill, J.R.,1986. Ground-Water Storage Depletion in Pahrump Valley, Nevada-California, 1962-1975. *US. Geologic Survey Water-Supply Paper 2279.*

Hoffard, J.L., 1991. Quaternary tectonics and basin history of Pahrump and Stewart Valleys, Nevada and California, M.S. Thesis, University of Nevada, Reno.

IT Corporation, 1996. Underground Test Area subproject, Phase 1 data analysis task, volume IV, Hydrologic parameter data documentation package. Report ITLV/10972-181 prepared for the U.S Department of Energy, 8 volumes.

Jiang, X-W. L. Wan, X-S. Wang, S. Ge, J. Liu. 2009. Effect of Exponential Decay in Hydraulic Conductivity with Depth on Regional Groundwater Flow. *Geophy. Res. Lett., 36,* L24402.

Malmberg, G.T. 1967. Hydrology of the Valley-fill and carbonate-rock reservoirs, Pahrump Valley, Nevada-California. *US. Geologic Survey Water-Supply Paper 1832.*

Maxey, G.B., and T. E. Eakin, 1949. Ground water in White River Valley, White Pine, Nye and Lincoln Counties, Nevada. No. 8, State of Nevada Office of the State Engineer in cooperation with the United States Department of the Interior Geological Survey, Carson City, Nevada.

Maxey, G.B., and Jameson, C.H., 1948. Geology and Water Resources of Las Vegas, Pahrump, and Indian Spring Valleys, Clark and Nye Counties, Nevada. *Nevada Water Resources Bulletin, 5.*

Moreo, M.T, Halford, K.J., La Camera, R.J. and Laczniak R.J. 2003. Estimated Ground-Water Withdrawals from the Death Valley Regional Flow System, Nevada and California, 1913-98. *U.S. Geological Survey Open-File-Report 03-4245.*

Nichols, W.D., 2000. Regional ground-water evapotranspiration and ground-water budget, Great Basin, Nevada: *United States Geological Survey Professional Paper 1628.*

Shields, G., Allander, K., Brigham, R., Crosbie, R., Trimble, L., Sleeman, M., Tucker, R., Hongbin, Z., and Louie J.N. 1997. Shallow Geophysical Survey Across the Pahrump Valley Fault Zone, California-Nevada Border. *Bulletin of Seismological Society of America v.88.* p. 270-275.

Strober, I. and Bucher, K., 2006. Hydraulic Properties of the crystalline basement. *Hydrogeology Journal.* p.213-224

Sweetkind, D. S. 2003. Stratigraphic inferences derived from borehole data of Tertiary basin-filling rocks of the Pahrump Valley basin, Nevada and California. *U.S. Geological Survey Open-File-Report 2003-51.*

U.S Geological Survey. 1995. Ground Water Atlas of the United States - Segment 1 California Nevada.

Waring, G.A. Ground water in Pahrump, Mesquite and Iavanpah Valley, Nevada and California Edition. *U.S Geological Survery Paper 450.*

Winograd, I. J., and W. Thordarson. 1975. Hydrogeologic and hydrochemical framework, south-central Great Basin, Nevada-California, with special reference to Nevada Test Site. U.S. Geological Survey Professional Paper 712-C.

APPENDIX A: Annual Pumpage Estimates using updated USGS and DWR data.

Time Step	Year	m^3/day	ac-ft/yr
1	1913	11270.30	3335.00
2	1914	11270.30	3335.00
3	1915	11270.30	3335.00
4	1916	11270.30	3335.00
5	1917	11270.30	3335.00
6	1918	11270.30	3335.00
7	1919	11270.30	3335.00
8	1920	11270.30	3335.00
9	1921	11270.30	3335.00
10	1922	11270.30	3335.00
11	1923	11270.30	3335.00
12	1924	11270.30	3335.00
13	1925	11270.30	3335.00
14	1926	11270.30	3335.00
15	1927	11270.30	3335.00
16	1928	11270.30	3335.00
17	1929	11270.30	3335.00
18	1930	11270.30	3335.00
19	1931	11270.30	3335.00
20	1932	11270.30	3335.00
21	1933	11270.30	3335.00
22	1934	11270.30	3335.00
23	1935	11270.30	3335.00
24	1936	11270.30	3335.00
25	1937	11270.30	3335.00
26	1938	11270.30	3335.00
27	1939	11270.30	3335.00
28	1940	11270.30	3335.00
29	1941	11270.30	3335.00
30	1942	11270.30	3335.00
31	1943	11270.30	3335.00
32	1944	11270.30	3335.00
33	1945	54923.70	16252.50
34	1946	54923.70	16252.50
35	1947	54923.70	16252.50
36	1948	54923.70	16252.50
37	1949	54923.70	16252.50
38	1950	54923.70	16252.50
39	1951	54925.39	16253.00
40	1952	70838.98	20962.00
41	1953	83719.56	24773.50
42	1954	83721.26	24774.00
43	1955	83724.63	24775.00

Time Step	Year	m^3/day	ac-ft/yr
44	1956	83724.63	24775.00
45	1957	83724.63	24775.00
46	1958	83726.33	24775.50
47	1959	86766.09	25675.00
48	1960	88596.04	26216.50
49	1961	104531.60	30932.00
50	1962	99314.66	29388.25
51	1963	103713.80	30690.00
52	1964	122785.40	36333.50
53	1965	121779.40	36035.80
54	1966	121653.30	35998.50
55	1967	133776.90	39586.00
56	1968	158452.50	46887.75
57	1969	134107.40	39683.80
58	1970	144470.00	42750.20
59	1971	126453.80	37419.00
60	1972	122054.10	36117.10
61	1973	132322.10	39155.50
62	1974	136807.30	40482.71
63	1975	133847.90	39607.00
64	1976	152670.50	45176.81
65	1977	141339.30	41823.80
66	1978	112381.30	33254.80
67	1979	114111.20	33766.70
68	1980	83201.18	24620.10
69	1981	81621.80	24152.75
70	1982	76364.30	22597.00
71	1983	76002.70	22490.00
72	1984	79582.34	23549.25
73	1985	74775.98	22127.00
74	1986	61916.52	18321.75
75	1987	61208.54	18112.25
76	1988	62420.90	18471.00
77	1989	65558.67	19399.50
78	1990	69358.80	20524.00
79	1991	79579.80	23548.50
80	1992	72707.79	21515.00
81	1993	63745.62	18863.00
82	1994	77778.24	23015.40
83	1995	71674.02	21209.10
84	1996	82085.95	24290.10
85	1997	85417.03	25275.80
86	1998	80425.34	23798.70
87	1999	70902.17	20980.70
88	2000	61777.97	18280.75
89	2001	70343.05	20815.25

Time Step	Year	m^3/day	ac-ft/yr
90	2002	61100.40	18080.25
91	2003	59896.48	17724.00

APPENDIX B: Monitoring well data.

Well Name	Well ID	UTM_E (NAD 83 Zone 11)	UTM_N (NAD 83 Zone 11)	Measure Date	Water Level Elevation (m)	Well Elevation (m)
162 S19 E52 36CA 1	1	582500	4012465	1966	780.98	783.00
162 S19 E52 36CA 1	1	582500	4012465	1967	780.84	783.00
162 S19 E52 36CA 1	1	582500	4012465	1968	780.64	783.00
162 S19 E52 36CA 1	1	582500	4012465	1971	780.42	783.00
162 S19 E52 36CA 1	1	582500	4012465	1972	780.41	783.00
162 S19 E52 36CA 1	1	582500	4012465	1973	780.75	783.00
162 S19 E52 36CA 1	1	582500	4012465	1975	780.69	783.00
162 S19 E52 36CA 1	1	582500	4012465	1977	780.74	783.00
162 S19 E53 08BD 1	2	585800	4019430	1966	769.74	783.00
162 S19 E53 08BD 1	2	585800	4019430	1967	765.24	783.00
162 S19 E53 08BD 1	2	585800	4019430	1968	765.98	783.00
162 S19 E53 08BD 1	2	585800	4019430	1971	765.51	783.00
162 S19 E53 08BD 1	2	585800	4019430	1972	768.97	783.00
162 S19 E53 08DA 1	3	586627	4019038	1966	796.94	806.00
162 S19 E53 08DA 1	3	586627	4019038	1967	796.60	806.00
162 S19 E53 08DA 1	3	586627	4019038	1968	789.89	806.00
162 S19 E53 08DA 1	3	586627	4019038	1971	794.17	806.00
162 S19 E53 08DA 1	3	586627	4019038	1972	795.67	806.00
162 S19 E53 08DA 1	3	586627	4019038	1974	796.06	806.00
162 S19 E53 08DA 1	3	586627	4019038	1975	796.15	806.00
162 S19 E53 09BD 1	4	587446	4019446	1966	799.62	809.00
162 S19 E53 09BD 1	4	587446	4019446	1967	799.35	809.00
162 S19 E53 09BD 1	4	587446	4019446	1968	799.01	809.00
162 S19 E53 09BD 1	4	587446	4019446	1971	798.71	809.00
162 S19 E53 09BD 1	4	587446	4019446	1972	798.59	809.00
162 S19 E53 09BD 1	4	587446	4019446	1975	798.46	809.00
162 S19 E53 09BD 1	4	587446	4019446	1976	798.38	809.00
162 S19 E53 09BD 1	4	587446	4019446	1977	798.34	809.00
162 S19 E53 10CB 1	5	588672	4019089	1950	812.42	821.00
162 S19 E53 10CB 1	5	588672	4019089	1951	812.38	821.00
162 S19 E53 10CB 1	5	588672	4019089	1952	812.30	821.00
162 S19 E53 10CB 1	5	588672	4019089	1953	812.12	821.00
162 S19 E53 10CB 1	5	588672	4019089	1954	812.09	821.00
162 S19 E53 10CB 1	5	588672	4019089	1955	811.93	821.00
162 S19 E53 10CB 1	5	588672	4019089	1956	811.90	821.00
162 S19 E53 10CB 1	5	588672	4019089	1957	811.76	821.00
162 S19 E53 10CB 1	5	588672	4019089	1958	811.62	821.00
162 S19 E53 10CB 1	5	588672	4019089	1959	811.43	821.00
162 S19 E53 10CB 1	5	588672	4019089	1960	811.24	821.00
162 S19 E53 10CB 1	5	588672	4019089	1961	810.97	821.00
162 S19 E53 10CB 1	5	588672	4019089	1962	810.97	821.00
162 S19 E53 10CB 1	5	588672	4019089	1963	810.82	821.00

Well Name	Well ID	UTM_E (NAD 83 Zone 11)	UTM_N (NAD 83 Zone 11)	Measure Date	Water Level Elevation (m)	Well Elevation (m)
162 S19 E53 10CB 1	5	588672	4019089	1964	810.67	821.00
162 S19 E53 10CB 1	5	588672	4019089	1965	810.54	821.00
162 S19 E53 10CB 1	5	588672	4019089	1966	810.40	821.00
162 S19 E53 10CB 1	5	588672	4019089	1967	810.27	821.00
162 S19 E53 10CB 1	5	588672	4019089	1968	810.19	821.00
162 S19 E53 15DB 1	6	589410	4017459	1951	804.70	811.00
162 S19 E53 15DB 1	6	589410	4017459	1953	805.13	811.00
162 S19 E53 15DB 1	6	589410	4017459	1954	804.67	811.00
162 S19 E53 15DB 1	6	589410	4017459	1955	804.56	811.00
162 S19 E53 15DB 1	6	589410	4017459	1956	804.14	811.00
162 S19 E53 15DB 1	6	589410	4017459	1957	803.96	811.00
162 S19 E53 15DB 1	6	589410	4017459	1958	803.75	811.00
162 S19 E53 15DB 1	6	589410	4017459	1959	803.39	811.00
162 S19 E53 15DB 1	6	589410	4017459	1960	803.15	811.00
162 S19 E53 15DB 1	6	589410	4017459	1961	802.82	811.00
162 S19 E53 15DB 1	6	589410	4017459	1962	802.92	811.00
162 S19 E53 15DB 1	6	589410	4017459	1963	802.64	811.00
162 S19 E53 15DB 1	6	589410	4017459	1964	802.50	811.00
162 S19 E53 15DB 1	6	589410	4017459	1965	802.31	811.00
162 S19 E53 15DB 1	6	589410	4017459	1966	802.16	811.00
162 S19 E53 15DB 1	6	589410	4017459	1967	801.92	811.00
162 S19 E53 15DB 1	6	589410	4017459	1968	801.88	811.00
162 S19 E53 15DB 1	6	589410	4017459	1969	801.89	811.00
162 S19 E53 15DB 1	6	589410	4017459	1970	801.58	811.00
162 S19 E53 15DB 1	6	589410	4017459	1971	801.61	811.00
162 S19 E53 15DB 1	6	589410	4017459	1972	801.52	811.00
162 S19 E53 15DB 1	6	589410	4017459	1973	801.51	811.00
162 S19 E53 15DB 1	6	589410	4017459	1974	801.41	811.00
162 S19 E53 15DB 1	6	589410	4017459	1975	800.99	811.00
162 S19 E53 15DB 1	6	589410	4017459	1976	800.69	811.00
162 S19 E53 15DB 1	6	589410	4017459	1977	800.58	811.00
162 S19 E53 15DB 1	6	589410	4017459	1978	800.40	811.00
162 S19 E53 15DB 1	6	589410	4017459	1979	800.17	811.00
162 S19 E53 15DB 1	6	589410	4017459	1980	800.00	811.00
162 S19 E53 15DB 1	6	589410	4017459	1981	800.02	811.00
162 S19 E53 15DB 1	6	589410	4017459	1982	800.00	811.00
162 S19 E53 15DB 1	6	589410	4017459	1983	800.01	811.00
162 S19 E53 15DB 1	6	589410	4017459	1984	799.86	811.00
162 S19 E53 15DB 1	6	589410	4017459	1985	800.12	811.00
162 S19 E53 15DB 1	6	589410	4017459	1986	800.21	811.00
162 S19 E53 15DB 1	6	589410	4017459	1987	800.36	811.00
162 S19 E53 15DB 1	6	589410	4017459	1988	800.41	811.00
162 S19 E53 15DB 1	6	589410	4017459	1989	800.44	811.00
162 S19 E53 15DB 1	6	589410	4017459	1990	800.37	811.00
162 S19 E53 15DB 1	6	589410	4017459	1991	800.22	811.00

Well Name	Well ID	UTM_E (NAD 83 Zone 11)	UTM_N (NAD 83 Zone 11)	Measure Date	Water Level Elevation (m)	Well Elevation (m)
162 S19 E53 15DB 1	6	589410	4017459	1992	800.44	811.00
162 S19 E53 15DB 1	6	589410	4017459	1993	800.40	811.00
162 S19 E53 15DB 1	6	589410	4017459	1994	800.34	811.00
162 S19 E53 15DB 1	6	589410	4017459	1995	800.41	811.00
162 S19 E53 15DB 1	6	589410	4017459	1996	800.36	811.00
162 S19 E53 15DB 1	6	589410	4017459	1997	800.40	811.00
162 S19 E53 15DB 1	6	589410	4017459	1998	800.50	811.00
162 S19 E53 15DB 1	6	589410	4017459	1999	800.55	811.00
162 S19 E53 15DB 1	6	589410	4017459	2000	800.59	811.00
162 S19 E53 15DB 1	6	589410	4017459	2001	800.60	811.00
162 S19 E53 15DB 1	6	589410	4017459	2002	800.62	811.00
162 S19 E53 15DB 1	6	589410	4017459	2003	800.58	811.00
162 S19 E53 17BA 1	7	585788	4018197	1966	793.80	802.00
162 S19 E53 17BA 1	7	585788	4018197	1967	794.37	802.00
162 S19 E53 17BA 1	7	585788	4018197	1970	794.21	802.00
162 S19 E53 17BA 1	7	585788	4018197	1972	794.03	802.00
162 S19 E53 17BA 1	7	585788	4018197	1975	793.56	802.00
162 S19 E53 17BA 1	7	585788	4018197	1976	793.58	802.00
162 S19 E53 17BA 1	7	585788	4018197	1977	793.34	802.00
162 S19 E53 21CA 1	8	587433	4015779	1966	789.43	795.00
162 S19 E53 21CA 1	8	587433	4015779	1967	786.02	795.00
162 S19 E53 21CA 1	8	587433	4015779	1969	785.99	795.00
162 S19 E53 21CA 1	8	587433	4015779	1971	788.62	795.00
162 S19 E53 21CA 1	8	587433	4015779	1972	787.93	795.00
162 S19 E53 21DA 1	9	588256	4015818	1966	792.72	799.00
162 S19 E53 21DA 1	9	588256	4015818	1967	786.21	799.00
162 S19 E53 21DA 1	9	588256	4015818	1968	791.87	799.00
162 S19 E53 21DA 1	9	588256	4015818	1969	791.83	799.00
162 S19 E53 21DA 1	9	588256	4015818	1970	791.74	799.00
162 S19 E53 21DA 1	9	588256	4015818	1972	791.73	799.00
162 S19 E53 21DA 1	9	588256	4015818	1975	791.84	799.00
162 S19 E53 22AC 1	10	589475	4016231	1950	804.54	809.00
162 S19 E53 22AC 1	10	589475	4016231	1951	804.41	809.00
162 S19 E53 22AC 1	10	589475	4016231	1952	804.19	809.00
162 S19 E53 22AC 1	10	589475	4016231	1953	803.83	809.00
162 S19 E53 22AC 1	10	589475	4016231	1954	803.63	809.00
162 S19 E53 22AC 1	10	589475	4016231	1955	803.26	809.00
162 S19 E53 22AC 1	10	589475	4016231	1956	803.01	809.00
162 S19 E53 22AC 1	10	589475	4016231	1957	802.94	809.00
162 S19 E53 22AC 1	10	589475	4016231	1958	802.32	809.00
162 S19 E53 22AC 1	10	589475	4016231	1959	802.01	809.00
162 S19 E53 22AC 1	10	589475	4016231	1960	801.86	809.00
162 S19 E53 22AC 1	10	589475	4016231	1961	801.34	809.00
162 S19 E53 27AA 1	11	589886	4015034	1951	808.72	813.00
162 S19 E53 27AA 1	11	589886	4015034	1952	808.38	813.00

Well Name	Well ID	UTM_E (NAD 83 Zone 11)	UTM_N (NAD 83 Zone 11)	Measure Date	Water Level Elevation (m)	Well Elevation (m)
162 S19 E53 27AA 1	11	589886	4015034	1953	807.70	813.00
162 S19 E53 27AA 1	11	589886	4015034	1954	806.99	813.00
162 S19 E53 27AA 1	11	589886	4015034	1955	807.31	813.00
162 S19 E53 27AA 1	11	589886	4015034	1956	806.79	813.00
162 S19 E53 27AA 1	11	589886	4015034	1967	803.19	813.00
162 S19 E53 27AA 1	11	589886	4015034	1968	802.59	813.00
162 S19 E53 27DD 1	12	589797	4013796	1969	800.76	811.00
162 S19 E53 27DD 1	12	589797	4013796	1970	800.75	811.00
162 S19 E53 27DD 1	12	589797	4013796	1971	800.91	811.00
162 S19 E53 27DD 1	12	589797	4013796	1972	800.10	811.00
162 S19 E53 27DD 1	12	589797	4013796	1973	799.98	811.00
162 S19 E53 27DD 1	12	589797	4013796	1974	799.46	811.00
162 S19 E53 27DD 1	12	589797	4013796	1975	799.55	811.00
162 S19 E53 27DD 1	12	589797	4013796	1976	798.87	811.00
162 S19 E53 27DD 1	12	589797	4013796	1977	799.01	811.00
162 S19 E53 27DD 1	12	589797	4013796	1978	798.05	811.00
162 S19 E53 27DD 1	12	589797	4013796	1979	798.91	811.00
162 S19 E53 27DD 1	12	589797	4013796	1980	798.74	811.00
162 S19 E53 27DD 1	12	589797	4013796	1981	798.66	811.00
162 S19 E53 27DD 1	12	589797	4013796	1982	799.15	811.00
162 S19 E53 27DD 1	12	589797	4013796	1983	798.85	811.00
162 S19 E53 27DD 1	12	589797	4013796	1984	799.37	811.00
162 S19 E53 27DD 1	12	589797	4013796	1985	799.49	811.00
162 S19 E53 27DD 1	12	589797	4013796	1986	800.26	811.00
162 S19 E53 27DD 1	12	589797	4013796	1987	800.83	811.00
162 S19 E53 27DD 1	12	589797	4013796	1988	801.12	811.00
162 S19 E53 27DD 1	12	589797	4013796	1989	800.66	811.00
162 S19 E53 27DD 1	12	589797	4013796	1990	800.19	811.00
162 S19 E53 27DD 1	12	589797	4013796	1991	800.25	811.00
162 S19 E53 27DD 1	12	589797	4013796	1992	800.40	811.00
162 S19 E53 27DD 1	12	589797	4013796	1992	800.91	811.00
162 S19 E53 27DD 1	12	589797	4013796	1993	800.69	811.00
162 S19 E53 27DD 1	12	589797	4013796	1994	800.72	811.00
162 S19 E53 27DD 1	12	589797	4013796	1995	800.87	811.00
162 S19 E53 27DD 1	12	589797	4013796	1996	800.90	811.00
162 S19 E53 27DD 1	12	589797	4013796	1997	801.00	811.00
162 S19 E53 27DD 1	12	589797	4013796	1998	801.67	811.00
162 S19 E53 27DD 1	12	589797	4013796	1999	801.93	811.00
162 S19 E53 27DD 1	12	589797	4013796	2000	801.94	811.00
162 S19 E53 27DD 1	12	589797	4013796	2001	802.72	811.00
162 S19 E53 27DD 1	12	589797	4013796	2002	801.85	811.00
162 S19 E53 27DD 1	12	589797	4013796	2003	801.89	811.00
162 S19 E53 28AA 1	13	588240	4014986	1966	791.71	811.00
162 S19 E53 28AA 1	13	588240	4014986	1967	791.66	811.00
162 S19 E53 28AA 1	13	588240	4014986	1971	789.64	811.00

Well Name	Well ID	UTM_E (NAD 83 Zone 11)	UTM_N (NAD 83 Zone 11)	Measure Date	Water Level Elevation (m)	Well Elevation (m)
162 S19 E53 28AA 1	13	588240	4014986	1972	790.91	811.00
162 S19 E53 28AA 1	13	588240	4014986	1973	790.90	811.00
162 S19 E53 28AA 1	13	588240	4014986	1974	790.29	811.00
162 S19 E53 28BA 1	14	587416	4014978	1966	788.24	794.00
162 S19 E53 28BA 1	14	587416	4014978	1967	784.82	794.00
162 S19 E53 28BA 1	14	587416	4014978	1968	784.74	794.00
162 S19 E53 31AD 1	15	584942	4012889	1969	779.96	782.00
162 S19 E53 31AD 1	15	584942	4012889	1971	780.01	782.00
162 S19 E53 31AD 1	15	584942	4012889	1972	779.97	782.00
162 S19 E53 31AD 1	15	584942	4012889	1973	779.88	782.00
162 S19 E53 31AD 1	15	584942	4012889	1974	779.79	782.00
162 S19 E53 31AD 1	15	584942	4012889	1975	779.75	782.00
162 S19 E53 31AD 1	15	584942	4012889	1976	779.63	782.00
162 S19 E53 31AD 1	15	584942	4012889	1977	779.55	782.00
162 S19 E53 32AA 1	16	586585	4013336	1951	783.45	786.00
162 S19 E53 32AA 1	16	586585	4013336	1953	783.49	786.00
162 S19 E53 32AA 1	16	586585	4013336	1954	783.60	786.00
162 S19 E53 32AA 1	16	586585	4013336	1955	783.68	786.00
162 S19 E53 32AA 1	16	586585	4013336	1956	783.69	786.00
162 S19 E53 32AA 1	16	586585	4013336	1957	783.66	786.00
162 S19 E53 32AA 1	16	586585	4013336	1958	783.64	786.00
162 S19 E53 32AA 1	16	586585	4013336	1959	783.64	786.00
162 S19 E53 32AA 1	16	586585	4013336	1960	783.58	786.00
162 S19 E53 32AA 1	16	586585	4013336	1961	783.56	786.00
162 S19 E53 32AA 1	16	586585	4013336	1962	783.56	786.00
162 S19 E53 32AA 1	16	586585	4013336	1963	783.55	786.00
162 S19 E53 32AA 1	16	586585	4013336	1964	783.45	786.00
162 S19 E53 32AA 1	16	586585	4013336	1965	783.45	786.00
162 S19 E53 32AA 1	16	586585	4013336	1966	783.34	786.00
162 S19 E53 32AA 1	16	586585	4013336	1967	783.28	786.00
162 S19 E53 32AA 1	16	586585	4013336	1968	783.20	786.00
162 S19 E53 32AA 1	16	586585	4013336	1969	783.15	786.00
162 S19 E53 32AA 1	16	586585	4013336	1970	783.11	786.00
162 S19 E53 32AA 1	16	586585	4013336	1971	783.06	786.00
162 S19 E53 33AA 1	17	588232	4013353	1967	786.13	795.00
162 S19 E53 33AA 1	17	588232	4013353	1968	789.97	795.00
162 S19 E53 33AA 1	17	588232	4013353	1969	785.96	795.00
162 S19 E53 33AA 1	17	588232	4013353	1971	789.69	795.00
162 S19 E53 33AA 1	17	588232	4013353	1972	789.57	795.00
162 S19 E53 33AA 1	17	588232	4013353	1975	789.85	795.00
162 S19 E53 33DA 1	18	588215	4012552	1966	789.23	792.00
162 S19 E53 33DA 1	18	588215	4012552	1967	789.10	792.00
162 S19 E53 33DA 1	18	588215	4012552	1968	787.80	792.00
162 S19 E53 33DA 1	18	588215	4012552	1969	788.62	792.00
162 S19 E53 33DA 1	18	588215	4012552	1970	788.83	792.00

Well Name	Well ID	UTM_E (NAD 83 Zone 11)	UTM_N (NAD 83 Zone 11)	Measure Date	Water Level Elevation (m)	Well Elevation (m)
162 S19 E53 33DA 1	18	588215	4012552	1971	789.08	792.00
162 S19 E53 33DA 1	18	588215	4012552	1972	787.48	792.00
162 S19 E53 33DA 1	18	588215	4012552	1973	788.09	792.00
162 S19 E53 33DA 1	18	588215	4012552	1974	786.97	792.00
162 S19 E53 33DA 1	18	588215	4012552	1975	786.79	792.00
162 S19 E53 33DA 1	18	588215	4012552	1976	787.07	792.00
162 S19 E53 33DA 1	18	588215	4012552	1977	787.43	792.00
162 S19 E53 33DA 1	18	588215	4012552	1978	786.67	792.00
162 S19 E53 33DA 1	18	588215	4012552	1979	786.57	792.00
162 S19 E53 33DA 1	18	588215	4012552	1980	786.51	792.00
162 S19 E53 33DA 1	18	588215	4012552	1981	786.65	792.00
162 S19 E53 33DA 1	18	588215	4012552	1982	786.93	792.00
162 S19 E53 33DA 1	18	588215	4012552	1983	786.93	792.00
162 S19 E53 33DA 1	18	588215	4012552	1984	786.89	792.00
162 S19 E53 34BD 1	19	589034	4012961	1966	794.07	797.00
162 S19 E53 34BD 1	19	589034	4012961	1967	784.20	797.00
162 S19 E53 34BD 1	19	589034	4012961	1968	788.99	797.00
162 S19 E53 34BD 1	19	589034	4012961	1969	784.18	797.00
162 S19 E53 34BD 1	19	589034	4012961	1971	784.22	797.00
162 S19 E53 34BD 1	19	589034	4012961	1972	792.89	797.00
162 S19 E53 34BD 1	19	589034	4012961	1973	793.04	797.00
162 S19 E53 34BD 1	19	589034	4012961	1974	791.53	797.00
162 S20 E52 12AB 1	20	582947	4010035	1970	773.97	776.00
162 S20 E52 22AA 1	21	580456	4006776	1966	764.72	769.00
162 S20 E52 22AA 1	21	580456	4006776	1967	764.77	769.00
162 S20 E52 22AA 1	21	580456	4006776	1968	764.15	769.00
162 S20 E52 22AA 1	21	580456	4006776	1969	764.36	769.00
162 S20 E52 22AA 1	21	580456	4006776	1970	764.18	769.00
162 S20 E52 22AA 1	21	580456	4006776	1971	764.29	769.00
162 S20 E52 22AA 1	21	580456	4006776	1972	764.30	769.00
162 S20 E52 22AA 1	21	580456	4006776	1973	764.18	769.00
162 S20 E52 22AA 1	21	580456	4006776	1974	764.24	769.00
162 S20 E52 22AA 1	21	580456	4006776	1975	764.17	769.00
162 S20 E52 22AA 1	21	580456	4006776	1976	764.13	769.00
162 S20 E52 22AA 1	21	580456	4006776	1977	764.11	769.00
162 S20 E52 22AA 1	21	580456	4006776	1978	764.46	769.00
162 S20 E52 22AA 1	21	580456	4006776	1979	764.52	769.00
162 S20 E52 22AA 1	21	580456	4006776	1980	764.57	769.00
162 S20 E52 22AA 1	21	580456	4006776	1981	764.87	769.00
162 S20 E52 22AA 1	21	580456	4006776	1982	764.88	769.00
162 S20 E52 22AA 1	21	580456	4006776	1983	764.82	769.00
162 S20 E52 22AA 1	21	580456	4006776	1984	764.76	769.00
162 S20 E52 22AA 1	21	580456	4006776	1985	764.76	769.00
162 S20 E52 22AA 1	21	580456	4006776	1986	764.81	769.00
162 S20 E52 22AA 1	21	580456	4006776	1987	764.18	769.00

Well Name	Well ID	UTM_E (NAD 83 Zone 11)	UTM_N (NAD 83 Zone 11)	Measure Date	Water Level Elevation (m)	Well Elevation (m)
162 S20 E52 22AA 1	21	580456	4006776	1988	763.73	769.00
162 S20 E52 22AA 1	21	580456	4006776	1989	764.00	769.00
162 S20 E52 22AA 1	21	580456	4006776	1990	764.33	769.00
162 S20 E52 22AA 1	21	580456	4006776	1991	763.46	769.00
162 S20 E52 22AA 1	21	580456	4006776	1992	763.55	769.00
162 S20 E52 22AA 1	21	580456	4006776	1993	763.62	769.00
162 S20 E52 22AA 1	21	580456	4006776	1994	763.74	769.00
162 S20 E52 22AA 1	21	580456	4006776	1995	763.18	768.00
162 S20 E52 36BD 1	22	582610	4003186	1964	765.27	768.00
162 S20 E52 36BD 1	22	582610	4003186	1965	765.24	768.00
162 S20 E52 36BD 1	22	582610	4003186	1966	765.17	768.00
162 S20 E52 36BD 1	22	582610	4003186	1967	765.13	768.00
162 S20 E52 36BD 1	22	582610	4003186	1968	765.10	768.00
162 S20 E52 36BD 1	22	582610	4003186	1969	765.02	768.00
162 S20 E52 36BD 1	22	582610	4003186	1970	765.01	768.00
162 S20 E52 36BD 1	22	582610	4003186	1971	764.94	768.00
162 S20 E52 36BD 1	22	582610	4003186	1972	764.91	768.00
162 S20 E52 36BD 1	22	582610	4003186	1973	764.78	768.00
162 S20 E52 36BD 1	22	582610	4003186	1974	764.78	768.00
162 S20 E52 36BD 1	22	582610	4003186	1975	764.71	768.00
162 S20 E52 36BD 1	22	582610	4003186	1976	764.66	768.00
162 S20 E52 36BD 1	22	582610	4003186	1987	764.05	768.00
162 S20 E52 36BD 1	22	582610	4003186	1991	763.80	768.00
162 S20 E52 36BD 1	22	582610	4003186	1995	763.57	768.00
162 S20 E52 36BD 1	22	582610	4003186	1996	763.51	768.00
162 S20 E52 36BD 1	22	582610	4003186	2000	763.31	768.00
162 S20 E52 36BD 1	22	582610	4003186	2001	763.23	768.00
162 S20 E53 04DA 1	23	588231	4010919	1969	788.29	768.00
162 S20 E53 04DA 1	23	588231	4010919	1977	786.48	768.00
162 S20 E53 05CD 1	24	585764	4010493	1966	776.45	782.00
162 S20 E53 05CD 1	24	585764	4010493	1967	780.02	782.00
162 S20 E53 05CD 1	24	585764	4010493	1968	773.90	782.00
162 S20 E53 05CD 1	24	585764	4010493	1969	775.62	782.00
162 S20 E53 05CD 1	24	585764	4010493	1970	774.44	782.00
162 S20 E53 05CD 1	24	585764	4010493	1971	779.33	782.00
162 S20 E53 05CD 1	24	585764	4010493	1972	779.26	782.00
162 S20 E53 06CB 1	25	583689	4010843	1966	776.97	779.00
162 S20 E53 06CB 1	25	583689	4010843	1967	776.92	779.00
162 S20 E53 08CA 1	26	585776	4009261	1968	778.78	781.00
162 S20 E53 08DD 1	27	586604	4008868	1966	782.87	785.00
162 S20 E53 08DD 1	27	586604	4008868	1967	782.71	785.00
162 S20 E53 09CA 1	28	587424	4009308	1966	783.59	786.00
162 S20 E53 09CA 1	28	587424	4009308	1967	783.94	786.00
162 S20 E53 09CA 1	28	587424	4009308	1968	783.85	786.00
162 S20 E53 09CA 1	28	587424	4009308	1969	783.71	786.00

Well Name	Well ID	UTM_E (NAD 83 Zone 11)	UTM_N (NAD 83 Zone 11)	Measure Date	Water Level Elevation (m)	Well Elevation (m)
162 S20 E53 09CA 1	28	587424	4009308	1970	783.69	786.00
162 S20 E53 09CA 1	28	587424	4009308	1971	783.48	786.00
162 S20 E53 10BD 1	29	589067	4009725	1966	785.34	795.00
162 S20 E53 10BD 1	29	589067	4009725	1967	785.30	795.00
162 S20 E53 10BD 1	29	589067	4009725	1968	785.30	795.00
162 S20 E53 10BD 1	29	589067	4009725	1972	790.99	795.00
162 S20 E53 14DC 1	30	591190	4007344	1966	812.33	818.00
162 S20 E53 14DC 1	30	591190	4007344	1967	811.42	818.00
162 S20 E53 14DC 1	30	591190	4007344	1968	810.74	818.00
162 S20 E53 14DC 1	30	591190	4007344	1969	810.06	818.00
162 S20 E53 15BA 1	31	589080	4008524	1966	787.16	793.00
162 S20 E53 15BA 1	31	589080	4008524	1967	789.68	793.00
162 S20 E53 15BA 1	31	589080	4008524	1968	789.64	793.00
162 S20 E53 15BA 1	31	589080	4008524	1969	789.51	793.00
162 S20 E53 16AB 1	32	587856	4008511	1967	782.31	788.00
162 S20 E53 16AB 1	32	587856	4008511	1968	781.66	788.00
162 S20 E53 16AB 1	32	587856	4008511	1969	781.52	788.00
162 S20 E53 16AB 1	32	587856	4008511	1970	781.45	788.00
162 S20 E53 17CD 1	33	585796	4007258	1966	778.59	781.00
162 S20 E53 17CD 1	33	585796	4007258	1967	778.66	781.00
162 S20 E53 17CD 1	33	585796	4007258	1968	778.65	781.00
162 S20 E53 17CD 1	33	585796	4007258	1969	778.52	781.00
162 S20 E53 17CD 1	33	585796	4007258	1970	778.52	781.00
162 S20 E53 17CD 1	33	585796	4007258	1971	778.40	781.00
162 S20 E53 17CD 1	33	585796	4007258	1972	778.31	781.00
162 S20 E53 17CD 1	33	585796	4007258	1974	778.33	781.00
162 S20 E53 17CD 1	33	585796	4007258	1976	778.11	781.00
162 S20 E53 17DD 1	34	586620	4007266	1966	782.78	785.00
162 S20 E53 17DD 1	34	586620	4007266	1967	782.77	785.00
162 S20 E53 17DD 1	34	586620	4007266	1968	782.64	785.00
162 S20 E53 17DD 1	34	586620	4007266	1969	782.59	785.00
162 S20 E53 17DD 1	34	586620	4007266	1970	782.46	785.00
162 S20 E53 17DD 1	34	586620	4007266	1971	782.39	785.00
162 S20 E53 17DD 1	34	586620	4007266	1972	782.40	785.00
162 S20 E53 17DD 1	34	586620	4007266	1975	782.20	785.00
162 S20 E53 17DD 1	34	586620	4007266	1976	782.12	785.00
162 S20 E53 20AA 1	35	586624	4006866	1959	782.93	785.00
162 S20 E53 20AA 1	35	586624	4006866	1960	782.88	785.00
162 S20 E53 20AA 1	35	586624	4006866	1961	782.82	785.00
162 S20 E53 20AA 1	35	586624	4006866	1962	782.83	785.00
162 S20 E53 20AA 1	35	586624	4006866	1963	782.83	785.00
162 S20 E53 20AA 1	35	586624	4006866	1964	782.74	785.00
162 S20 E53 20AA 1	35	586624	4006866	1965	782.75	785.00
162 S20 E53 20AA 1	35	586624	4006866	1966	782.68	785.00
162 S20 E53 20AA 1	35	586624	4006866	1967	782.60	785.00

Well Name	Well ID	UTM_E (NAD 83 Zone 11)	UTM_N (NAD 83 Zone 11)	Measure Date	Water Level Elevation (m)	Well Elevation (m)
162 S20 E53 20AA 1	35	586624	4006866	1968	782.59	785.00
162 S20 E53 20BB 1	36	585400	4006854	1960	777.97	780.00
162 S20 E53 20BB 1	36	585400	4006854	1961	777.91	780.00
162 S20 E53 20BB 1	36	585400	4006854	1962	777.93	780.00
162 S20 E53 20BB 1	36	585400	4006854	1963	777.91	780.00
162 S20 E53 20BB 1	36	585400	4006854	1964	777.84	780.00
162 S20 E53 20BB 1	36	585400	4006854	1965	777.81	780.00
162 S20 E53 21BA 1	37	587448	4006874	1966	783.76	786.00
162 S20 E53 21BA 1	37	587448	4006874	1967	783.67	786.00
162 S20 E53 21BA 1	37	587448	4006874	1971	783.55	786.00
162 S20 E53 21BA 1	37	587448	4006874	1972	783.55	786.00
162 S20 E53 21BA 1	37	587448	4006874	1974	783.57	786.00
162 S20 E53 21BA 1	37	587448	4006874	1975	783.70	786.00
162 S20 E53 21BA 1	37	587448	4006874	1976	783.57	786.00
162 S20 E53 21BA 1	37	587448	4006874	1977	783.51	786.00
162 S20 E53 22BD 1	38	589125	4006490	1966	790.00	792.00
162 S20 E53 22BD 1	38	589125	4006490	1967	789.87	792.00
162 S20 E53 22BD 1	38	589125	4006490	1968	789.72	792.00
162 S20 E53 22BD 1	38	589125	4006490	1969	789.65	792.00
162 S20 E53 22BD 1	38	589125	4006490	1970	789.80	792.00
162 S20 E53 22BD 1	38	589125	4006490	1971	789.71	792.00
162 S20 E53 22BD 1	38	589125	4006490	1972	789.79	792.00
162 S20 E53 22BD 1	38	589125	4006490	1974	789.86	792.00
162 S20 E53 22BD 1	38	589125	4006490	1975	789.88	792.00
162 S20 E53 23AB 1	39	591194	4006943	1966	807.27	813.00
162 S20 E53 23AB 1	39	591194	4006943	1967	806.69	813.00
162 S20 E53 23AB 1	39	591194	4006943	1970	798.13	813.00
162 S20 E53 23AB 1	39	591194	4006943	1971	798.19	813.00
162 S20 E53 23BC 1	40	590374	4006503	1966	796.85	803.00
162 S20 E53 23BC 1	40	590374	4006503	1967	796.65	803.00
162 S20 E53 23BC 1	40	590374	4006503	1968	800.15	803.00
162 S20 E53 23BC 1	40	590374	4006503	1971	792.62	803.00
162 S20 E53 23BC 1	40	590374	4006503	1974	800.64	803.00
162 S20 E53 24BC 1	41	592022	4006551	1961	819.56	825.00
162 S20 E53 24BC 1	41	592022	4006551	1962	818.85	825.00
162 S20 E53 24BC 1	41	592022	4006551	1964	817.93	825.00
162 S20 E53 24BC 1	41	592022	4006551	1965	817.40	825.00
162 S20 E53 24CA 1	42	592451	4006155	1951	827.02	830.00
162 S20 E53 24CA 1	42	592451	4006155	1952	826.27	830.00
162 S20 E53 24CA 1	42	592451	4006155	1953	826.41	830.00
162 S20 E53 24CA 1	42	592451	4006155	1958	825.47	830.00
162 S20 E53 24CA 1	42	592451	4006155	1959	824.84	830.00
162 S20 E53 24CA 1	42	592451	4006155	1960	824.63	830.00
162 S20 E53 24CC 1	43	592031	4005719	1955	813.06	817.00
162 S20 E53 24CC 1	43	592031	4005719	1956	813.02	817.00

Well Name	Well ID	UTM_E (NAD 83 Zone 11)	UTM_N (NAD 83 Zone 11)	Measure Date	Water Level Elevation (m)	Well Elevation (m)
162 S20 E53 24CC 1	43	592031	4005719	1957	812.79	817.00
162 S20 E53 24CC 1	43	592031	4005719	1960	812.24	817.00
162 S20 E53 24CC 1	43	592031	4005719	1961	811.56	817.00
162 S20 E53 24CC 1	43	592031	4005719	1962	810.86	817.00
162 S20 E53 24CC 1	43	592031	4005719	1963	810.61	817.00
162 S20 E53 24CC 1	43	592031	4005719	1964	809.93	817.00
162 S20 E53 24CC 1	43	592031	4005719	1965	809.40	817.00
162 S20 E53 24CC 1	43	592031	4005719	1966	808.84	817.00
162 S20 E53 24CC 1	43	592031	4005719	1967	808.15	817.00
162 S20 E53 24CC 1	43	592031	4005719	1968	807.46	817.00
162 S20 E53 24CC 1	43	592031	4005719	1969	807.05	817.00
162 S20 E53 24CC 1	43	592031	4005719	1970	806.84	817.00
162 S20 E53 24CC 1	43	592031	4005719	1971	806.51	817.00
162 S20 E53 24CC 1	43	592031	4005719	1972	806.35	817.00
162 S20 E53 26BA 1	44	590811	4005306	1966	803.99	807.00
162 S20 E53 26BA 1	44	590811	4005306	1967	803.99	807.00
162 S20 E53 26BA 1	44	590811	4005306	1968	804.07	807.00
162 S20 E53 26BA 1	44	590811	4005306	1972	803.90	807.00
162 S20 E53 26BA 1	44	590811	4005306	1975	804.41	807.00
162 S20 E53 26BA 1	44	590811	4005306	1976	804.13	807.00
162 S20 E53 26BA 1	44	590811	4005306	1977	804.02	807.00
162 S20 E54 30BD 1	45	594113	4004940	1951	833.93	837.00
162 S20 E54 30BD 1	45	594113	4004940	1952	833.99	837.00
162 S20 E54 30BD 1	45	594113	4004940	1966	827.28	837.00
162 S20 E54 30BD 1	45	594113	4004940	1967	827.04	837.00
162 S20 E54 30CC 1	46	593722	4004135	1966	818.94	826.00
162 S20 E54 30CC 1	46	593722	4004135	1967	818.84	826.00
162 S20 E54 30CC 1	46	593722	4004135	1968	818.72	826.00
162 S20 E54 30CC 1	46	593722	4004135	1971	818.57	826.00
162 S20 E54 30CC 1	46	593722	4004135	1972	818.56	826.00
162 S20 E54 30CC 1	46	593722	4004135	1975	818.86	826.00
162 S20 E54 30CC 1	46	593722	4004135	1976	818.86	826.00
162 S20 E54 30CC 1	46	593722	4004135	1977	818.78	826.00
162 S20 E54 31BC 1	47	593730	4003334	1966	814.83	821.00
162 S20 E54 31BC 1	47	593730	4003334	1967	815.07	821.00
162 S20 E54 31BC 1	47	593730	4003334	1968	815.10	821.00
162 S20 E54 31BC 1	47	593730	4003334	1969	815.00	821.00
162 S20 E54 31BC 1	47	593730	4003334	1970	815.22	821.00
162 S20 E54 31BC 1	47	593730	4003334	1971	814.97	821.00
162 S20 E54 31BC 1	47	593730	4003334	1972	814.93	821.00
162 S20 E54 31BC 1	47	593730	4003334	1975	815.12	821.00
162 S20 E54 31BC 1	47	593730	4003334	1976	815.04	821.00
162 S20 E54 31BC 1	47	593730	4003334	1977	814.97	821.00
162 S21 E53 01BA 1	48	592744	4002091	1966	807.02	810.00
162 S21 E53 01BA 1	48	592744	4002091	1967	806.98	810.00

Well Name	Well ID	UTM_E (NAD 83 Zone 11)	UTM_N (NAD 83 Zone 11)	Measure Date	Water Level Elevation (m)	Well Elevation (m)
162 S21 E53 01BA 1	48	592744	4002091	1968	806.90	810.00
162 S21 E53 01BA 1	48	592744	4002091	1969	807.10	810.00
162 S21 E53 01BA 1	48	592744	4002091	1970	806.99	810.00
162 S21 E53 01BA 1	48	592744	4002091	1971	806.89	810.00
162 S21 E53 01BA 1	48	592744	4002091	1972	806.94	810.00
162 S21 E53 02AA 1	49	591969	4002083	1966	804.63	807.00
162 S21 E53 02AA 1	49	591969	4002083	1967	804.53	807.00
162 S21 E53 02AA 1	49	591969	4002083	1968	804.47	807.00
162 S21 E53 02AA 1	49	591969	4002083	1971	804.52	807.00
162 S21 E53 02AA 1	49	591969	4002083	1972	804.54	807.00
162 S21 E53 03AA 1	50	590395	4002066	1966	796.84	799.00
162 S21 E53 03AA 1	50	590395	4002066	1967	796.50	799.00
162 S21 E53 03AA 1	50	590395	4002066	1968	796.36	799.00
162 S21 E53 03AA 1	50	590395	4002066	1969	796.31	799.00
162 S21 E53 03AA 1	50	590395	4002066	1970	796.27	799.00
162 S21 E53 03AA 1	50	590395	4002066	1971	796.66	799.00
162 S21 E53 03AA 1	50	590395	4002066	1972	796.67	799.00
162 S21 E53 03AA 1	50	590395	4002066	1975	796.56	799.00
162 S21 E53 03AA 1	50	590395	4002066	1976	796.51	799.00
162 S21 E53 03AA 1	50	590395	4002066	1977	796.45	799.00
162 S21 E53 05DA 1	51	587255	4001233	1966	778.68	781.00
162 S21 E53 05DA 1	51	587255	4001233	1967	778.81	781.00
162 S21 E53 05DA 1	51	587255	4001233	1968	778.94	781.00
162 S21 E53 05DA 1	51	587255	4001233	1971	778.52	781.00
162 S21 E53 05DA 1	51	587255	4001233	1972	778.50	781.00
162 S21 E53 05DA 1	51	587255	4001233	1974	778.33	781.00
162 S21 E53 08DA 1	52	587271	3999600	1966	780.97	786.00
162 S21 E53 08DA 1	52	587271	3999600	1967	782.01	786.00
162 S21 E53 08DA 1	52	587271	3999600	1968	782.26	786.00
162 S21 E53 08DA 1	52	587271	3999600	1970	779.59	786.00
162 S21 E53 08DA 1	52	587271	3999600	1971	780.18	786.00
162 S21 E53 08DA 1	52	587271	3999600	1974	777.99	786.00
162 S21 E53 08DA 1	53	590412	4000464	1966	792.44	795.00
162 S21 E53 10AA 1	53	590412	4000464	1967	792.23	795.00
162 S21 E53 10AA 1	53	590412	4000464	1971	792.00	795.00
162 S21 E53 10AA 1	53	590412	4000464	1972	792.36	795.00
162 S21 E53 10AA 1	53	590412	4000464	1975	791.66	795.00
162 S21 E53 10AA 1	53	590412	4000464	1976	791.54	795.00
162 S21 E53 10AA 1	53	590412	4000464	1977	791.63	795.00
162 S21 E53 11CA 1	54	591220	3999671	1966	795.80	799.00
162 S21 E53 11CA 1	54	591220	3999671	1967	795.49	799.00
162 S21 E53 11CA 1	54	591220	3999671	1968	795.36	799.00
162 S21 E53 11CA 1	54	591220	3999671	1971	795.17	799.00
162 S21 E53 11CA 1	54	591220	3999671	1972	795.37	799.00
162 S21 E53 12CD 1	55	592799	3999287	1966	804.78	807.00

Well Name	Well ID	UTM_E (NAD 83 Zone 11)	UTM_N (NAD 83 Zone 11)	Measure Date	Water Level Elevation (m)	Well Elevation (m)
162 S21 E53 12CD 1	55	592799	3999287	1967	804.39	807.00
162 S21 E53 12CD 1	55	592799	3999287	1968	804.27	807.00
162 S21 E53 12CD 1	55	592799	3999287	1971	804.29	807.00
162 S21 E53 12CD 1	55	592799	3999287	1972	804.75	807.00
162 S21 E53 12CD 1	55	592799	3999287	1974	804.61	807.00
162 S21 E53 12CD 1	55	592799	3999287	1975	804.51	807.00
162 S21 E53 12CD 1	55	592799	3999287	1976	804.36	807.00
162 S21 E53 13AA 1	56	593603	3998895	1966	804.30	812.00
162 S21 E53 13AA 1	56	593603	3998895	1967	803.89	812.00
162 S21 E53 13AA 1	56	593603	3998895	1968	807.26	812.00
162 S21 E53 13AA 1	56	593603	3998895	1969	791.93	812.00
162 S21 E53 13AA 1	56	593603	3998895	1970	791.53	812.00
162 S21 E53 13AA 1	56	593603	3998895	1971	807.10	812.00
162 S21 E53 13AA 1	56	593603	3998895	1972	808.18	812.00
162 S21 E53 13AA 1	56	593603	3998895	1973	809.03	812.00
162 S21 E53 13AA 1	56	593603	3998895	1974	809.02	812.00
162 S21 E53 13AA 1	56	593603	3998895	1975	808.74	812.00
162 S21 E53 14AA 1	57	592028	3998878	1966	800.04	804.00
162 S21 E53 14AA 1	57	592028	3998878	1967	799.54	804.00
162 S21 E53 14AA 1	57	592028	3998878	1968	799.30	804.00
162 S21 E53 14AA 1	57	592028	3998878	1971	799.23	804.00
162 S21 E53 14AA 1	57	592028	3998878	1972	799.81	804.00
162 S21 E53 14AA 1	57	592028	3998878	1973	799.57	804.00
162 S21 E53 14AA 1	57	592028	3998878	1974	799.73	804.00
162 S21 E53 14AA 1	57	592028	3998878	1975	799.32	804.00
162 S21 E53 14AA 1	57	592028	3998878	1976	799.05	804.00
162 S21 E53 14AA 1	57	592028	3998878	1977	798.78	804.00
162 S21 E53 14AC 1	58	591632	3998474	1966	792.06	802.00
162 S21 E53 14AC 1	58	591632	3998474	1967	797.42	802.00
162 S21 E53 14AC 1	58	591632	3998474	1968	797.20	802.00
162 S21 E53 14AC 1	58	591632	3998474	1971	797.05	802.00
162 S21 E53 14AC 1	58	591632	3998474	1972	797.62	802.00
162 S21 E53 14AC 1	58	591632	3998474	1973	797.50	802.00
162 S21 E53 14AC 1	58	591632	3998474	1974	797.26	802.00
162 S21 E53 14AC 1	58	591632	3998474	1975	796.71	802.00
162 S21 E53 14AC 1	58	591632	3998474	1976	796.69	802.00
162 S21 E53 14AC 1	58	591632	3998474	1977	796.63	802.00
162 S21 E53 14BB 1	59	590853	3998866	1966	794.47	798.00
162 S21 E53 14BB 1	59	590853	3998866	1967	794.07	798.00
162 S21 E53 14BB 1	59	590853	3998866	1973	793.51	798.00
162 S21 E53 14BB 1	59	590853	3998866	1974	793.26	798.00
162 S21 E53 24BA 1	60	592845	3997254	1966	801.93	806.00
162 S21 E53 24BA 1	60	592845	3997254	1967	799.00	806.00
162 S21 E53 24BA 1	60	592845	3997254	1968	796.59	806.00
162 S21 E53 24BA 1	60	592845	3997254	1970	797.67	806.00

Well Name	Well ID	UTM_E (NAD 83 Zone 11)	UTM_N (NAD 83 Zone 11)	Measure Date	Water Level Elevation (m)	Well Elevation (m)
162 S21 E53 24BA 1	60	592845	3997254	1971	797.53	806.00
162 S21 E53 24BA 1	60	592845	3997254	1972	797.56	806.00
162 S21 E53 24BA 1	60	592845	3997254	1973	799.19	806.00
162 S21 E53 24BA 1	60	592845	3997254	1974	798.91	806.00
162 S21 E53 24BA 1	60	592845	3997254	1977	797.62	806.00
162 S21 E53 25CB 1	61	592496	3994847	1966	789.28	795.00
162 S21 E53 25CB 1	61	592496	3994847	1967	789.10	795.00
162 S21 E53 25CB 1	61	592496	3994847	1968	789.04	795.00
162 S21 E53 25CB 1	61	592496	3994847	1970	788.94	795.00
162 S21 E53 25CB 1	61	592496	3994847	1971	787.69	795.00
162 S21 E53 25CB 1	61	592496	3994847	1972	788.23	795.00
162 S21 E53 25CB 1	61	592496	3994847	1973	788.38	795.00
162 S21 E53 25CB 1	61	592496	3994847	1974	788.37	795.00
162 S21 E53 25CB 1	61	592496	3994847	1975	788.41	795.00
162 S21 E53 25CB 1	61	592496	3994847	1976	788.37	795.00
162 S21 E53 25CB 1	61	592496	3994847	1977	788.31	795.00
162 S21 E53 25DA 1	62	593696	3994859	1966	801.59	805.00
162 S21 E53 25DA 1	62	593696	3994859	1967	801.75	805.00
162 S21 E53 27AD 1	63	590516	3995227	1966	788.32	794.00
162 S21 E53 27AD 1	63	590516	3995227	1967	788.15	794.00
162 S21 E53 27AD 1	63	590516	3995227	1968	788.11	794.00
162 S21 E53 35AD 1	64	592133	3993641	1966	776.89	781.00
162 S21 E53 35AD 1	64	592133	3993641	1967	776.68	781.00
162 S21 E53 35AD 1	64	592133	3993641	1971	775.79	781.00
162 S21 E53 35AD 1	64	592133	3993641	1972	776.16	781.00
162 S21 E53 35AD 1	64	592133	3993641	1974	776.10	781.00
162 S21 E53 35AD 1	64	592133	3993641	1975	775.93	781.00
162 S21 E53 35AD 1	64	592133	3993641	1976	775.97	781.00
162 S21 E53 35AD 1	64	592133	3993641	1977	775.97	781.00
162 S21 E53 36AA 1	65	593705	3994058	1966	787.32	796.00
162 S21 E53 36AA 1	65	593705	3994058	1967	787.01	796.00
162 S21 E53 36AA 1	65	593705	3994058	1972	786.51	796.00
162 S21 E53 36AA 1	65	593705	3994058	1974	786.52	796.00
162 S21 E53 36AA 1	65	593705	3994058	1975	786.51	796.00
162 S21 E53 36AA 1	65	593705	3994058	1976	786.49	796.00
162 S21 E53 36AA 1	65	593705	3994058	1977	786.51	796.00
162 S21 E53 36DA 1	66	593713	3993257	1966	785.26	791.00
162 S21 E53 36DA 1	66	593713	3993257	1967	785.02	791.00
162 S21 E53 36DA 1	66	593713	3993257	1971	784.54	791.00
162 S21 E53 36DA 1	66	593713	3993257	1972	784.69	791.00
162 S21 E53 36DA 1	66	593713	3993257	1974	784.61	791.00
162 S21 E53 36DA 1	66	593713	3993257	1975	784.53	791.00
162 S21 E53 36DA 1	66	593713	3993257	1976	784.47	791.00
162 S21 E53 36DA 1	66	593713	3993257	1977	784.38	791.00
162 S21 E54 03BD 1	67	599170	4001730	1966	856.95	862.00

Well Name	Well ID	UTM_E (NAD 83 Zone 11)	UTM_N (NAD 83 Zone 11)	Measure Date	Water Level Elevation (m)	Well Elevation (m)
162 S21 E54 03BD 1	67	599170	4001730	1967	856.97	862.00
162 S21 E54 03BD 1	67	599170	4001730	1968	856.61	862.00
162 S21 E54 03BD 1	67	599170	4001730	1972	857.16	862.00
162 S21 E54 03BD 1	67	599170	4001730	1974	857.61	862.00
162 S21 E54 03DC 1	68	599579	4000933	1966	870.01	872.00
162 S21 E54 06DA 1	69	595151	4001316	1966	815.82	819.00
162 S21 E54 06DA 1	69	595151	4001316	1967	815.86	819.00
162 S21 E54 06DA 1	69	595151	4001316	1968	816.13	819.00
162 S21 E54 06DA 1	69	595151	4001316	1970	816.21	819.00
162 S21 E54 06DA 1	69	595151	4001316	1972	816.03	819.00
162 S21 E54 06DA 1	69	595151	4001316	1973	816.07	819.00
162 S21 E54 06DA 1	69	595151	4001316	1974	816.10	819.00
162 S21 E54 07AA 1	70	595185	4000515	1966	815.11	819.00
162 S21 E54 07AA 1	70	595185	4000515	1967	813.55	819.00
162 S21 E54 07AA 1	70	595185	4000515	1968	815.82	819.00
162 S21 E54 07AA 1	70	595185	4000515	1971	813.41	819.00
162 S21 E54 07AA 1	70	595185	4000515	1974	815.83	819.00
162 S21 E54 07AA 1	70	595185	4000515	1975	815.63	819.00
162 S21 E54 08BD 1	71	595990	4000092	1966	819.32	823.00
162 S21 E54 08BD 1	71	595990	4000092	1967	819.47	823.00
162 S21 E54 10AAC 1	72	599883	4000409	1951	878.91	882.00
162 S21 E54 10AAC 1	72	599883	4000409	1952	878.81	882.00
162 S21 E54 10AAC 1	72	599883	4000409	1957	877.77	882.00
162 S21 E54 10AAC 1	72	599883	4000409	1958	877.60	882.00
162 S21 E54 10AAC 1	72	599883	4000409	1959	876.95	882.00
162 S21 E54 10AAC 1	72	599883	4000409	1960	876.66	882.00
162 S21 E54 10AAC 1	72	599883	4000409	1961	876.25	882.00
162 S21 E54 10AAC 1	72	599883	4000409	1962	875.89	882.00
162 S21 E54 10AAC 1	72	599883	4000409	1963	875.53	882.00
162 S21 E54 10AAC 1	72	599883	4000409	1964	874.86	882.00
162 S21 E54 10AAC 1	72	599883	4000409	1965	874.62	882.00
162 S21 E54 10AAC 1	72	599883	4000409	1966	874.37	882.00
162 S21 E54 10AAC 1	72	599883	4000409	1967	873.78	882.00
162 S21 E54 10AAC 1	72	599883	4000409	1968	873.36	882.00
162 S21 E54 10AAC 1	72	599883	4000409	1969	873.22	882.00
162 S21 E54 10AAC 1	72	599883	4000409	1972	872.98	882.00
162 S21 E54 10AAC 1	72	599883	4000409	1973	872.74	882.00
162 S21 E54 10AAC 1	72	599883	4000409	1974	872.51	882.00
162 S21 E54 10AAC 1	72	599883	4000409	1975	872.54	882.00
162 S21 E54 10AAC 1	72	599883	4000409	1976	872.26	882.00
162 S21 E54 10AAC 1	72	599883	4000409	1977	871.87	882.00
162 S21 E54 10AAC 1	72	599883	4000409	1978	872.04	882.00
162 S21 E54 10AAC 1	72	599883	4000409	1979	871.74	882.00
162 S21 E54 10AAC 1	72	599883	4000409	1980	871.71	882.00
162 S21 E54 10AAC 1	72	599883	4000409	1981	871.77	882.00

Well Name	Well ID	UTM_E (NAD 83 Zone 11)	UTM_N (NAD 83 Zone 11)	Measure Date	Water Level Elevation (m)	Well Elevation (m)
162 S21 E54 10AAC 1	72	599883	4000409	1982	872.15	882.00
162 S21 E54 10AAC 1	72	599883	4000409	1983	872.09	882.00
162 S21 E54 10AAC 1	72	599883	4000409	1984	871.71	882.00
162 S21 E54 10AAC 1	72	599883	4000409	1985	872.31	882.00
162 S21 E54 10AAC 1	72	599883	4000409	1986	872.26	882.00
162 S21 E54 10AAC 1	72	599883	4000409	1987	872.65	882.00
162 S21 E54 10AAC 1	72	599883	4000409	1988	872.70	882.00
162 S21 E54 10AAC 1	72	599883	4000409	1989	872.64	882.00
162 S21 E54 10AAC 1	72	599883	4000409	1990	872.53	882.00
162 S21 E54 10AAC 1	72	599883	4000409	1991	872.48	882.00
162 S21 E54 10AAC 1	72	599883	4000409	1992	872.47	882.00
162 S21 E54 10AAC 1	72	599883	4000409	1993	872.49	882.00
162 S21 E54 10AAC 1	72	599883	4000409	1994	872.47	882.00
162 S21 E54 10AAC 1	72	599883	4000409	1995	872.59	882.00
162 S21 E54 10AAC 1	72	599883	4000409	1996	872.65	882.00
162 S21 E54 10AAC 1	72	599883	4000409	1997	872.99	882.00
162 S21 E54 10AAC 1	72	599883	4000409	1998	873.66	882.00
162 S21 E54 10AAC 1	72	599883	4000409	1999	874.07	882.00
162 S21 E54 10AAC 1	72	599883	4000409	2000	874.36	882.00
162 S21 E54 10AAC 1	72	599883	4000409	2001	874.72	882.00
162 S21 E54 10AAC 1	72	599883	4000409	2002	875.15	882.00
162 S21 E54 10AAC 1	72	599883	4000409	2003	875.15	882.00
162 S21 E54 15DA 1	73	600012	3998073	1946	884.12	887.00
162 S21 E54 15DA 1	73	600012	3998073	1947	884.29	887.00
162 S21 E54 15DA 1	73	600012	3998073	1948	884.11	887.00
162 S21 E54 15DA 1	73	600012	3998073	1949	884.15	887.00
162 S21 E54 15DA 1	73	600012	3998073	1951	883.94	887.00
162 S21 E54 15DA 1	73	600012	3998073	1952	883.76	887.00
162 S21 E54 15DA 1	73	600012	3998073	1953	883.91	887.00
162 S21 E54 15DA 1	73	600012	3998073	1954	883.36	887.00
162 S21 E54 15DA 1	73	600012	3998073	1955	883.25	887.00
162 S21 E54 15DA 1	73	600012	3998073	1956	883.08	887.00
162 S21 E54 15DA 1	73	600012	3998073	1957	883.00	887.00
162 S21 E54 15DA 1	73	600012	3998073	1958	882.77	887.00
162 S21 E54 15DA 1	73	600012	3998073	1959	882.79	887.00
162 S21 E54 15DA 1	73	600012	3998073	1960	882.42	887.00
162 S21 E54 15DA 1	73	600012	3998073	1972	884.85	887.00
162 S21 E54 15DA 1	73	600012	3998073	1974	884.33	887.00
162 S21 E54 15DA 1	73	600012	3998073	1975	884.19	887.00
162 S21 E54 15DA 1	73	600012	3998073	1976	883.94	887.00
162 S21 E54 15DA 1	73	600012	3998073	1977	883.87	887.00
162 S21 E54 17CA 1	74	596012	3998089	1966	818.24	823.00
162 S21 E54 17CA 1	74	596012	3998089	1967	818.22	823.00
162 S21 E54 17CA 1	74	596012	3998089	1972	818.44	823.00
162 S21 E54 17CA 1	74	596012	3998089	1974	818.15	823.00

Well Name	Well ID	UTM_E (NAD 83 Zone 11)	UTM_N (NAD 83 Zone 11)	Measure Date	Water Level Elevation (m)	Well Elevation (m)
162 S21 E54 18AA 1	75	595203	3998882	1966	815.26	820.00
162 S21 E54 18AA 1	75	595203	3998882	1967	816.28	820.00
162 S21 E54 18AA 1	75	595203	3998882	1968	816.28	820.00
162 S21 E54 18AA 1	75	595203	3998882	1971	816.17	820.00
162 S21 E54 18AA 1	75	595203	3998882	1972	816.83	820.00
162 S21 E54 18AA 1	75	595203	3998882	1973	816.61	820.00
162 S21 E54 18AA 1	75	595203	3998882	1974	816.85	820.00
162 S21 E54 18AA 1	75	595203	3998882	1975	816.52	820.00
162 S21 E54 18AA 1	75	595203	3998882	1976	816.31	820.00
162 S21 E54 18AA 1	75	595203	3998882	1977	816.39	820.00
162 S21 E54 19DD 1	76	595259	3996078	1946	813.74	817.00
162 S21 E54 19DD 1	76	595259	3996078	1949	813.43	817.00
162 S21 E54 19DD 1	76	595259	3996078	1954	813.59	817.00
162 S21 E54 19DD 1	76	595259	3996078	1955	813.64	817.00
162 S21 E54 19DD 1	76	595259	3996078	1956	813.63	817.00
162 S21 E54 19DD 1	76	595259	3996078	1957	813.60	817.00
162 S21 E54 19DD 1	76	595259	3996078	1963	813.15	817.00
162 S21 E54 19DD 1	76	595259	3996078	1964	813.01	817.00
162 S21 E54 19DD 1	76	595259	3996078	1965	813.06	817.00
162 S21 E54 19DD 1	76	595259	3996078	1966	813.05	817.00
162 S21 E54 19DD 1	76	595259	3996078	1967	813.05	817.00
162 S21 E54 19DD 1	76	595259	3996078	1968	813.00	817.00
162 S21 E54 19DD 1	76	595259	3996078	1969	813.04	817.00
162 S21 E54 19DD 1	76	595259	3996078	1970	813.10	817.00
162 S21 E54 19DD 1	76	595259	3996078	1971	813.17	817.00
162 S21 E54 19DD 1	76	595259	3996078	1972	813.17	817.00
162 S21 E54 19DD 1	76	595259	3996078	1973	813.15	817.00
162 S21 E54 20BA 1	77	596046	3997289	1966	818.18	823.00
162 S21 E54 20BA 1	77	596046	3997289	1967	818.35	823.00
162 S21 E54 20BA 1	77	596046	3997289	1971	818.00	823.00
162 S21 E54 20BA 1	77	596046	3997289	1972	818.72	823.00
162 S21 E54 20BA 1	77	596046	3997289	1974	818.44	823.00
162 S21 E54 20BA 1	77	596046	3997289	1975	818.37	823.00
162 S21 E54 20BA 1	77	596046	3997289	1976	818.23	823.00
162 S21 E54 20BA 1	77	596046	3997289	1977	818.19	823.00
162 S21 E54 28BD 1	78	597669	3995242	1955	837.97	840.00
162 S21 E54 28BD 1	78	597669	3995242	1958	838.01	840.00
162 S21 E54 28BD 1	78	597669	3995242	1959	837.99	840.00
162 S21 E54 28BD 1	78	597669	3995242	1960	838.00	840.00
162 S21 E54 28BD 1	78	597669	3995242	1961	838.00	840.00
162 S21 E54 28BD 1	78	597669	3995242	1962	837.99	840.00
162 S21 E54 28BD 1	78	597669	3995242	1963	837.96	840.00
162 S21 E54 28BD 1	78	597669	3995242	1964	837.96	840.00
162 S21 E54 28BD 1	78	597669	3995242	1965	837.98	840.00
162 S21 E54 28BD 1	78	597669	3995242	1966	837.95	840.00

Well Name	Well ID	UTM_E (NAD 83 Zone 11)	UTM_N (NAD 83 Zone 11)	Measure Date	Water Level Elevation (m)	Well Elevation (m)
162 S21 E54 28BD 1	78	597669	3995242	1967	837.94	840.00
162 S21 E54 28BD 1	78	597669	3995242	1968	837.95	840.00
162 S21 E54 28BD 1	78	597669	3995242	1969	837.94	840.00
162 S21 E54 28BD 1	78	597669	3995242	1970	837.93	840.00
162 S21 E54 28BD 1	78	597669	3995242	1971	837.96	840.00
162 S21 E54 28BD 1	78	597669	3995242	1972	837.96	840.00
162 S21 E54 28BD 1	78	597669	3995242	1973	837.98	840.00
162 S21 E54 28BD 1	78	597669	3995242	1974	837.96	840.00
162 S21 E54 28BD 1	78	597669	3995242	1975	837.94	840.00
162 S21 E54 28BD 1	78	597669	3995242	1976	837.95	840.00
162 S21 E54 28BD 1	78	597669	3995242	1977	837.85	840.00
162 S21 E54 28BD 1	78	597669	3995242	1978	837.45	840.00
162 S21 E54 31AC 1	79	594910	3993640	1966	793.51	801.00
162 S21 E54 31AC 1	79	594910	3993640	1967	793.33	801.00
162 S21 E54 31AC 1	79	594910	3993640	1975	793.69	801.00
162 S21 E54 31AC 1	79	594910	3993640	1976	793.64	801.00
162 S21 E54 31AC 1	79	594910	3993640	1977	793.45	801.00
162 S21 E54 31DD 1	80	595319	3992843	1966	801.36	804.00
162 S21 E54 31DD 1	80	595319	3992843	1967	801.25	804.00
162 S22 E53 01DA 1	81	593602	3991804	1966	781.36	785.00
162 S22 E53 01DA 1	81	593602	3991804	1967	780.88	785.00
162 S22 E53 01DA 1	81	593602	3991804	1968	781.17	785.00
162 S22 E53 01DA 1	81	593602	3991804	1969	781.21	785.00
162 S22 E53 01DA 1	81	593602	3991804	1970	780.88	785.00
162 S22 E53 01DA 1	81	593602	3991804	1971	780.73	785.00
162 S22 E53 01DA 1	81	593602	3991804	1972	780.73	785.00
162 S22 E53 01DA 1	81	593602	3991804	1973	780.80	785.00
162 S22 E53 01DA 1	81	593602	3991804	1974	780.75	785.00
162 S22 E53 01DA 1	81	593602	3991804	1975	780.70	785.00
162 S22 E53 01DA 1	81	593602	3991804	1976	780.66	785.00
162 S22 E53 01DA 1	81	593602	3991804	1977	780.49	785.00
162 S22 E53 01DA 1	81	593602	3991804	1978	780.14	785.00
162 S22 E53 01DA 1	81	593602	3991804	1979	779.66	785.00
162 S22 E53 01DA 1	81	593602	3991804	1980	779.92	785.00
162 S22 E53 01DA 1	81	593602	3991804	1981	779.77	785.00
162 S22 E53 01DA 1	81	593602	3991804	1982	779.57	785.00
162 S22 E53 01DA 1	81	593602	3991804	1983	779.43	785.00
162 S22 E53 01DA 1	81	593602	3991804	1984	779.23	785.00
162 S22 E53 01DA 1	81	593602	3991804	1985	779.01	785.00
162 S22 E53 01DA 1	81	593602	3991804	1986	779.05	785.00
162 S22 E53 01DA 1	81	593602	3991804	1987	778.93	785.00
162 S22 E53 01DA 1	81	593602	3991804	1988	778.95	785.00
162 S22 E53 01DA 1	81	593602	3991804	1989	778.87	785.00
162 S22 E53 01DA 1	81	593602	3991804	1990	778.80	785.00
162 S22 E53 01DA 1	81	593602	3991804	1991	778.86	785.00

Well Name	Well ID	UTM_E (NAD 83 Zone 11)	UTM_N (NAD 83 Zone 11)	Measure Date	Water Level Elevation (m)	Well Elevation (m)
162 S22 E53 01DA 1	81	593602	3991804	1992	778.81	785.00
162 S22 E53 01DA 1	81	593602	3991804	1993	778.75	785.00
162 S22 E53 01DA 1	81	593602	3991804	1994	778.63	785.00
162 S22 E53 01DA 1	81	593602	3991804	1995	778.50	785.00
162 S22 E53 01DA 1	81	593602	3991804	1996	778.44	785.00
162 S22 E53 01DA 1	81	593602	3991804	1997	778.15	785.00
162 S22 E53 01DA 1	81	593602	3991804	1998	778.10	785.00
162 S22 E53 01DA 1	81	593602	3991804	1999	778.06	785.00
162 S22 E53 01DA 1	81	593602	3991804	2000	777.97	785.00
162 S22 E53 01DA 1	81	593602	3991804	2001	777.50	785.00
162 S22 E53 01DA 1	81	593602	3991804	2002	777.12	785.00
162 S22 E53 01DA 1	81	593602	3991804	2003	777.07	785.00
162 S22 E54 06AD 1	82	595328	3992011	1966	791.56	798.00
162 S22 E54 06AD 1	82	595328	3992011	1967	791.68	798.00
162 S22 E54 06AD 1	82	595328	3992011	1970	791.31	798.00
162 S22 E54 06AD 1	82	595328	3992011	1971	791.18	798.00
162 S22 E54 06AD 1	82	595328	3992011	1972	791.13	798.00
162 S22 E54 06AD 1	82	595328	3992011	1974	790.97	798.00
162 S22 E54 06AD 1	82	595328	3992011	1975	790.94	798.00
162 S22 E54 06AD 1	82	595328	3992011	1976	790.82	798.00
162 S22 E54 06AD 1	82	595328	3992011	1977	790.76	798.00
6161	83	593836	3998837	2000	795.81	812.79
6161	83	593836	3998837	2002	795.65	812.79
6161	83	593836	3998837	2003	795.87	812.79
Allstar1	84	591749	3999970	2002	780.32	802.72
AW01	85	590563	4001662	2000	781.93	799.44
AW01	85	590563	4001662	2002	780.71	799.44
AW01	85	590563	4001662	2003	780.24	799.44
AW02	86	594131	3997372	2000	794.56	812.35
AW02	86	594131	3997372	2002	793.94	812.35
AW02	86	594131	3997372	2003	793.77	812.35
AW07	87	585112	4015982	2000	768.13	786.61
AW07	87	585112	4015982	2002	767.31	786.61
AW07	87	585112	4015982	2003	767.01	786.61
AW10	88	587683	4015248	2002	772.56	795.40
AW10	88	587683	4015248	2003	772.36	795.40
AW11	89	589091	4014470	2002	777.35	800.01
AW11	89	589091	4014470	2003	777.32	800.01
AW24	90	586805	4007127	2002	767.91	784.60
AW24	90	586805	4007127	2003	767.24	784.60
AW26	91	585289	4010109	2002	763.00	779.74
AW26	91	585289	4010109	2003	762.64	779.74
AW28	92	583891	4010398	2002	763.36	778.33
AW28	92	583891	4010398	2003	762.92	778.33
AW29	93	582413	4012009	2002	768.00	781.88

Well Name	Well ID	UTM_E (NAD 83 Zone 11)	UTM_N (NAD 83 Zone 11)	Measure Date	Water Level Elevation (m)	Well Elevation (m)
AW29	93	582413	4012009	2003	767.82	781.88
AW33	94	591218	4013466	2003	790.06	854.80
AW34	95	593028	4013648	2003	793.24	934.90
AW35	96	593410	4012471	2003	797.81	941.29
AW37	97	590283	4010493	2002	792.90	808.27
AW37	97	590283	4010493	2003	793.49	808.27
AW39	98	590394	4011277	2002	792.35	821.67
AW39	98	590394	4011277	2003	793.03	821.67
AW40	99	588636	4003432	2002	773.48	790.06
AW46	100	590996	3999021	2003	773.21	796.37
AW47	101	583070	4007618	2000	756.78	773.01
AW47	101	583070	4007618	2002	755.88	773.01
AW48	102	584223	4006122	2002	756.61	774.41
AW53	103	589883	4007799	2002	792.90	801.84
AW53	103	589883	4007799	2003	792.96	801.84
AW57	104	590426	4002398	2002	781.20	798.04
AW57	104	590426	4002398	2003	780.72	798.04
AW59	105	592101	4001375	2002	785.84	804.86
AW60	106	592314	4001960	2002	788.47	807.11
AW62	107	592811	4002025	2002	790.36	809.14
AW62	107	592811	4002025	2003	790.33	809.14
AW63	108	592404	4000652	2002	784.35	804.85
AW63	108	592404	4000652	2003	784.06	804.85
AW64	109	590986	4000623	2000	777.90	797.49
AW64	109	590986	4000623	2002	776.47	797.49
AW64	109	590986	4000623	2003	775.87	797.49
AW65	110	591834	4000549	2000	783.94	802.88
AW65	110	591834	4000549	2002	782.70	802.88
AW65	110	591834	4000549	2003	782.32	802.88
AW66	111	592604	3999844	2000	786.55	805.76
AW66	111	592604	3999844	2002	785.73	805.76
AW66	111	592604	3999844	2003	785.71	805.76
AW69	112	575583	4010224	2003	741.59	750.62
AW70	113	587705	4019612	2003	772.87	810.74
AW74	114	589404	4013721	2002	787.93	802.16
AW74	114	589404	4013721	2003	789.17	802.16
Boosel	115	591774	3999968	2002	780.21	802.55
Boosel	115	591774	3999968	2003	779.79	802.55
CC1	116	585252	4010248	2002	762.25	778.61
CC1	116	585252	4010248	2003	761.91	778.61
Cline	117	593262	4001077	2002	787.94	806.70
Cline	117	593262	4001077	2003	787.82	806.70
Collins	118	591598	3998829	2000	776.82	798.30
Collins	118	591598	3998829	2003	774.21	798.30
Courtney	119	582506	4014725	2002	767.62	785.02

Well Name	Well ID	UTM_E (NAD 83 Zone 11)	UTM_N (NAD 83 Zone 11)	Measure Date	Water Level Elevation (m)	Well Elevation (m)
Courtney	119	582506	4014725	2003	767.53	785.02
Dan	120	595982	3996551	2000	799.73	821.00
Dan	120	595982	3996551	2002	798.76	821.00
Dan	120	595982	3996551	2003	798.52	821.00
Debbie	121	581933	4007769	2002	753.47	770.92
Debbie	121	581933	4007769	2003	753.11	770.92
Deserae	122	593721	4002322	2000	794.48	814.22
Deserae	122	593721	4002322	2002	793.72	814.22
Flipper	123	588570	4017956	2002	772.84	805.61
Flipper	123	588570	4017956	2003	773.18	805.61
Foster	124	591937	3999763	2000	780.15	800.56
Foster	124	591937	3999763	2002	779.22	800.56
Foster	124	591937	3999763	2003	778.72	800.56
Garcia1	125	592361	3997545	2002	781.45	801.45
Garcia1	125	592361	3997545	2003	780.87	801.45
Garcia2	126	592309	3997513	2002	782.67	801.73
Garcia2	126	592309	3997513	2003	782.23	801.73
Hall2	127	585817	4012728	2003	766.90	783.75
Harley	128	586843	4023134	2002	771.50	884.27
Harley	128	586843	4023134	2003	771.44	884.27
Hidden Hills	129	602337	3986187	2003	814.89	850.85
Koeller	130	584178	4007158	2002	760.32	775.32
Koeller	130	584178	4007158	2003	759.75	775.32
LaComb Irrigation Well	131	584563	4007920	2002	757.07	775.47
Lamm	132	591136	3999722	2003	778.26	801.50
Marris	133	592336	4002255	2000	789.19	807.48
Marris	133	592336	4002255	2002	788.28	807.48
Marris	133	592336	4002255	2003	787.94	807.48
NSM	134	588493	4013232	2003	776.02	793.70
Nursery1	135	586622	4007998	2000	766.28	782.88
Nursery1	135	586622	4007998	2002	765.26	782.88
Nursery1	135	586622	4007998	2003	764.82	782.88
Our Bar	136	582581	4013639	2002	765.83	781.71
Our Bar	136	582581	4013639	2003	765.94	781.71
Raetz	137	591828	3998643	2000	778.50	800.79
Raetz	137	591828	3998643	2002	778.17	800.79
Slaughterhouse	138	590823	4000334	2002	777.68	799.60
Soffa	139	586826	4008339	2000	766.42	782.31
Soffa	139	586826	4008339	2002	765.28	782.31
Soffa	139	586826	4008339	2003	764.81	782.31
Stateline	140	603003	3981491	2003	765.84	817.73
Stewart Valley Vacant	141	575728	4010007	2003	746.96	752.64
Tony	142	583008	4015678	2000	768.43	783.67
Tony	142	583008	4015678	2002	767.54	783.67
Tony	142	583008	4015678	2003	767.23	783.67

Well Name	Well ID	UTM_E (NAD 83 Zone 11)	UTM_N (NAD 83 Zone 11)	Measure Date	Water Level Elevation (m)	Well Elevation (m)
Wright	143	583003	4010704	2002	763.16	777.21
Wright	143	583003	4010704	2003	762.74	777.21

APPENDIX C: Inputs and outputs of the model for each stress period. Note that the storage is not included.

Year	Stress Period	Recharge (m^3/d)	Wells (m^3/d)	Evapotranspiration (m3/d)	Flux at Southwest Boundary (m^3/d) Constant Head Out
1913	1	87864.40	-11270.30	-42242.75	-34457.65
1914	2	87864.40	-11270.30	-42242.75	-34457.65
1915	3	87864.40	-11270.30	-42242.75	-34457.64
1916	4	87864.40	-11270.30	-42242.75	-34457.65
1917	5	87864.40	-11270.30	-42242.75	-34457.64
1918	6	87864.40	-11270.30	-42242.75	-34457.64
1919	7	87864.40	-11270.30	-42242.75	-34457.64
1920	8	87864.40	-11270.30	-42242.75	-34457.64
1921	9	87864.40	-11270.30	-42242.75	-34457.64
1922	10	87864.40	-11270.30	-42242.75	-34457.64
1923	11	87864.40	-11270.30	-42242.75	-34457.64
1924	12	87864.40	-11270.30	-42242.75	-34457.64
1925	13	87864.40	-11270.30	-42242.75	-34457.64
1926	14	87864.40	-11270.30	-42242.75	-34457.64
1927	15	87864.40	-11270.30	-42242.75	-34457.64
1928	16	87864.40	-11270.30	-42242.75	-34457.64
1929	17	87864.40	-11270.30	-42242.75	-34457.64
1930	18	87864.40	-11270.30	-42242.75	-34457.64
1931	19	87864.40	-11270.30	-42242.75	-34457.64
1932	20	87864.40	-11270.30	-42242.75	-34457.64
1933	21	87864.40	-11270.30	-42242.75	-34457.64
1934	22	87864.40	-11270.30	-42242.75	-34457.64
1935	23	87864.40	-11270.30	-42242.75	-34457.64
1936	24	87864.40	-11270.30	-42242.75	-34457.64
1937	25	87864.40	-11270.30	-42242.75	-34457.64
1938	26	87864.40	-11270.30	-42242.75	-34457.64
1939	27	87864.40	-11270.30	-42242.75	-34457.64
1940	28	87864.40	-11270.30	-42242.75	-34457.64
1941	29	87864.40	-11270.30	-42242.75	-34457.64
1942	30	87864.40	-11270.30	-42242.75	-34457.64
1943	31	87864.40	-11270.30	-42242.75	-34457.64
1944	32	87864.40	-11270.30	-42242.75	-34457.64
1945	33	87864.40	-54923.70	-42242.75	-34457.64
1946	34	87864.40	-54923.70	-42242.75	-34457.64
1947	35	87864.40	-54923.70	-42242.75	-34457.64
1948	36	87864.40	-54923.70	-42242.75	-34457.64
1949	37	87864.40	-54923.70	-42242.75	-34457.64
1950	38	87864.40	-54923.70	-42242.75	-34457.64

1951	39	87864.40	-54925.39	-42242.75	-34457.64
1952	40	87864.40	-70838.98	-42242.75	-34457.64
1953	41	87864.40	-83719.56	-42242.75	-34457.64
1954	42	87864.40	-83721.25	-42242.75	-34457.64
1955	43	87864.40	-83724.63	-42242.75	-34457.64
1956	44	87864.40	-83724.63	-42242.75	-34457.64
1957	45	87864.40	-83724.63	-42242.75	-34457.64
1958	46	87864.40	-83726.32	-42242.75	-34457.64
1959	47	87864.40	-86766.09	-42242.75	-34457.64
1960	48	87864.40	-88596.04	-42242.75	-34457.64
1961	49	87864.40	-104531.60	-42242.75	-34457.64
1962	50	87864.40	-99314.66	-42242.75	-34457.64
1963	51	87864.40	-103713.79	-42242.75	-34457.64
1964	52	87864.40	-122785.42	-42242.75	-34457.64
1965	53	87864.40	-121779.38	-42242.75	-34457.64
1966	54	87864.40	-121653.34	-42242.75	-34457.64
1967	55	87864.40	-133776.94	-42242.75	-34457.64
1968	56	87864.40	-158452.47	-42242.75	-34457.64
1969	57	87864.40	-134107.44	-42242.75	-34457.64
1970	58	87864.40	-144470.02	-42242.75	-34457.64
1971	59	87864.40	-126453.77	-42242.75	-34457.64
1972	60	87864.40	-122054.14	-42242.75	-34457.64
1973	61	87864.40	-132322.09	-42242.75	-34457.64
1974	62	87864.40	-136807.23	-42242.75	-34457.64
1975	63	87864.40	-133847.91	-42242.75	-34457.64
1976	64	87864.40	-152670.48	-42242.75	-34457.64
1977	65	87864.40	-141339.34	-42242.75	-34457.64
1978	66	87864.40	-112381.27	-42242.75	-34457.64
1979	67	87864.40	-114111.20	-42242.75	-34457.64
1980	68	87864.40	-83201.16	-42242.75	-34457.64
1981	69	87864.40	-81621.80	-42242.75	-34457.64
1982	70	87864.40	-76364.30	-42242.75	-34457.64
1983	71	87864.40	-76002.70	-42242.75	-34457.64
1984	72	87864.40	-79582.34	-42242.75	-34457.64
1985	73	87864.40	-74775.98	-42242.75	-34457.64
1986	74	87864.40	-61916.52	-42242.75	-34457.64
1987	75	87864.40	-61208.53	-42242.75	-34457.64
1988	76	87864.40	-62420.89	-42242.75	-34457.64
1989	77	87864.40	-65558.67	-42242.75	-34457.64
1990	78	87864.40	-69358.80	-42242.75	-34457.64
1991	79	87864.40	-79579.80	-42242.75	-34457.64
1992	80	87864.40	-72707.79	-42242.75	-34457.64
1993	81	87864.40	-63743.93	-42242.75	-34457.64
1994	82	87864.40	-77774.87	-42242.75	-34457.64
1995	83	87864.40	-71670.66	-42242.75	-34457.64
1996	84	87864.40	-82082.59	-42242.75	-34457.64
1997	85	87864.40	-85413.66	-42242.75	-34457.64

1998	86	87864.40	-80421.95	-42242.75	-34457.64
1999	87	87864.40	-70898.80	-42242.75	-34457.64
2000	88	87864.40	-61774.59	-42242.75	-34457.64
2001	89	87864.40	-70332.92	-42242.75	-34457.64
2002	90	87864.40	-61088.57	-42242.75	-34457.64
2003	91	87864.40	-59884.66	-42242.75	-34457.64